3.2.2 Number of books and chapters in edited volumes/books published and papers published in national/ international conference proceedings per teacher during last five years (10)

SUMMARY SHEET

Academic Years	2019-20	2018-19	2017-18	2016-17	2015-16	TOTAL
TOTAL	19	5	2	3	8	37

PRINCIPAL
Sri Indu Institute of Engineering & Tech
Sheriguda(V), Ibrahimpatnam(M)
R.R. Dist. Telangana.-501 510

Academic Year 2019-2020

Research Publications – Book & Book Chapters

Sl. No	Name of the Faculty Author	Title of the Book Chapter	Name of the Publisher	ISBN Number	URL
1	Dr.B.Gangadhara Bula Reddy	A Brevity & Descriptive View On Big Data And Data Science	Shashwat	978-93-90290-55-0	https://shashwatpublication.com/books/A%20Brevity%20&%20Descriptive%20View%20On%20Big%20Data%20And%20Data%20Science
2	Gaddam Rahul Paul	Fundamentals of Management	Walnut Publication	978-9389744 39-2	https://www.walnutpublication.com/book/9789389744392/
3	U.Fanidara Baradwaja Sharma	Fundamentals of Management	Walnut Publication	978-9389744 39-2	https://www.walnutpublication.com/book/9789389744392/
4	Dr. Dayaydi Lakshmaiah	Analog And Pulse Circuits	BS Publications / BSP Books	97893893 54096	https://www.bspublications.net/book_detail.php?bid=1546
5	Dr. Dayaydi Lakshmaiah	Minimization Of Dynamic Power Through Structural Changes And Threshold Voltage Techniques	LAP Lambert Academic Publishing	978-620-2-67229-0	https://www.lap-publishing.com/catalog/details/store/gb/book/978-620-2-67229-0/minimization-of-dynamic-power-through-structural-changes-amp;vt-techniques

Academic Year 2015-2016

Research Publications – Book & Book Chapters

Sl. No	Name of the Faculty Author	Title of the Book Chapter	Name of the Publisher	ISBN Number	URL
1	Dr. D. Premalatha	Advances in Bioprocess Technology /Starter Culture Technology: Fermented Foods	Springer	978-3-319-1794-8	https://books.google.co.in/books?id=Y4RgCgAAQBAJ&printsec=frontcover&source=gbs_ge_summary_r&cad=0#v=onepage&q&f=true

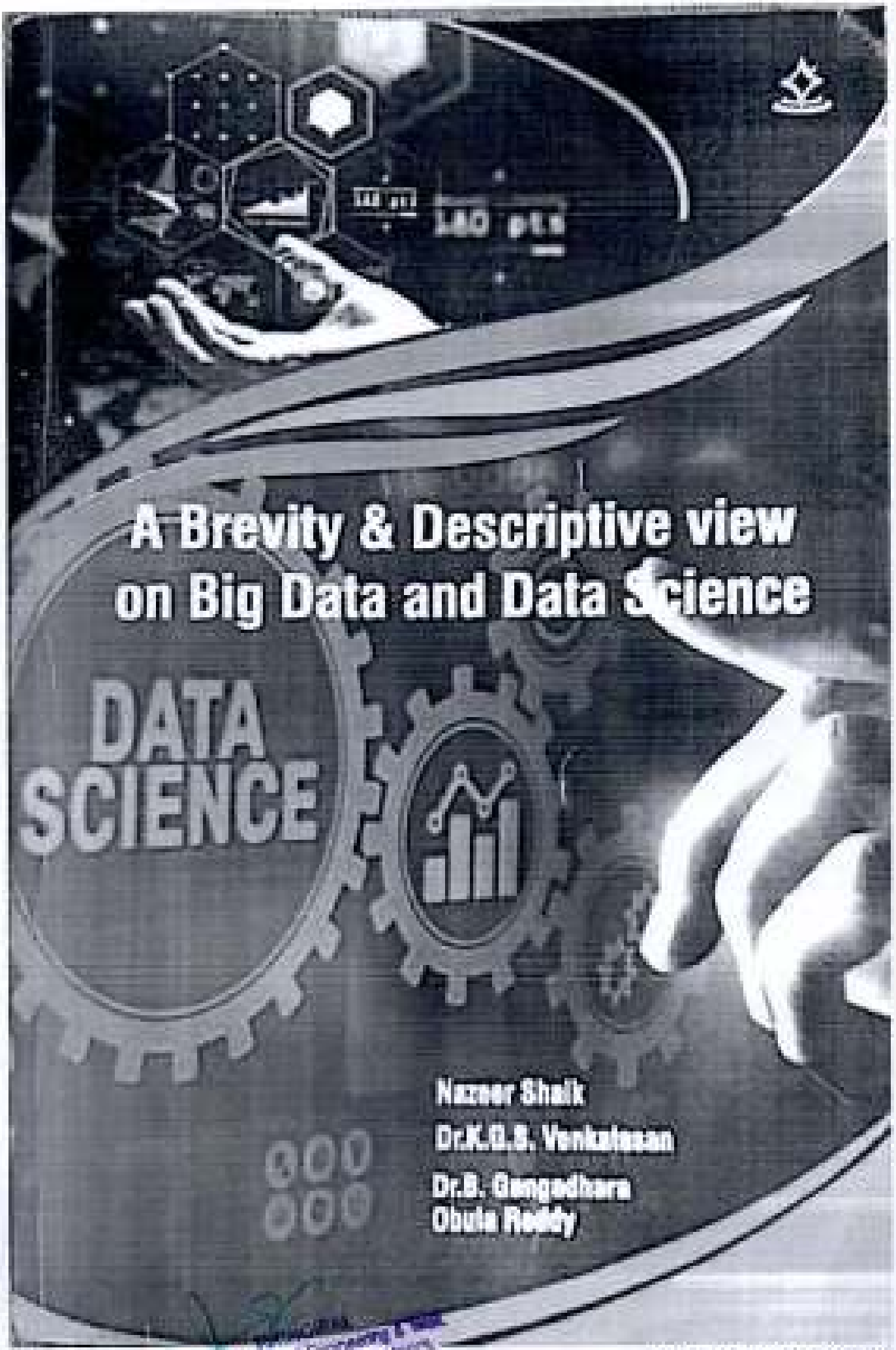

About the Book

Big Data approach cannot be easily obtained from traditional data analysis methods. Instead, [illegible] requires and needs specialized data modelling techniques. This book will help you to make a career in Data Science and Big Data. Data Science has been a trending approach that applies mathematical and statistical methods and computer tools for making processed Big data. Data science is a specialized and focused field that combines various fields such as statistics, mathematics, intelligent data capture techniques, data discovery, training and programming to prepare and align big data. Learn all you need to extract insights and information.

Data Science and BIG Data are rapidly growing fields that find applications in many areas like health care, business, advertising, marketing and sales. This book focuses on how the data science and Big Data are being processed and applied to various areas/domains served by other technologies like making a good impact on the users. Actually, we are so anxious to make the things land on the users/people who are having such revolutions to make aid by the book.

Key Features:

1. It provides a concise and a trivial coverage on Big Data and Data Science in a descriptive manner.
2. Some of the contemporary technologies empowered along with them in a limited way and it gives you a value information in more about such contemporaries as well, which are being interacted with these technologies such as Big Data and Data Science.
3. It describes the differences among Data Science with other core technologies and Big Data differences with other technologies as well.
4. It allows to explain every topic on a new way and will also be explained and described and [illegible] manner.
5. This book will surely make a glance over these technologies for the students and learners and industry people who wants [illegible] in [illegible].
6. This book implies that how usually technologies are being [illegible] by an expert as well as being reader a one of the job market.

ISBN: 978-93-90298-55-8

Price: 599.00

Publishing Year 2020

Published and Printed by
Shashwat Publication
Office Address: Ram Das Nagar,
Bilaspur, Chhattisgarh – 495001
Phone: +91 9993605164, +91 9993603491
Email: contact.shashwatpublication@gmail.com
Website: www.shashwatpublication.com

Printed in India

A Brevity
&
Descriptive View on Data Science
and
Big Data

Authors

Nazeer Shaik
Dr.K.G.S. Venkatesan
Dr.B. Gangadhara Obula Reddy.

SHASHWAT PUBLICATION

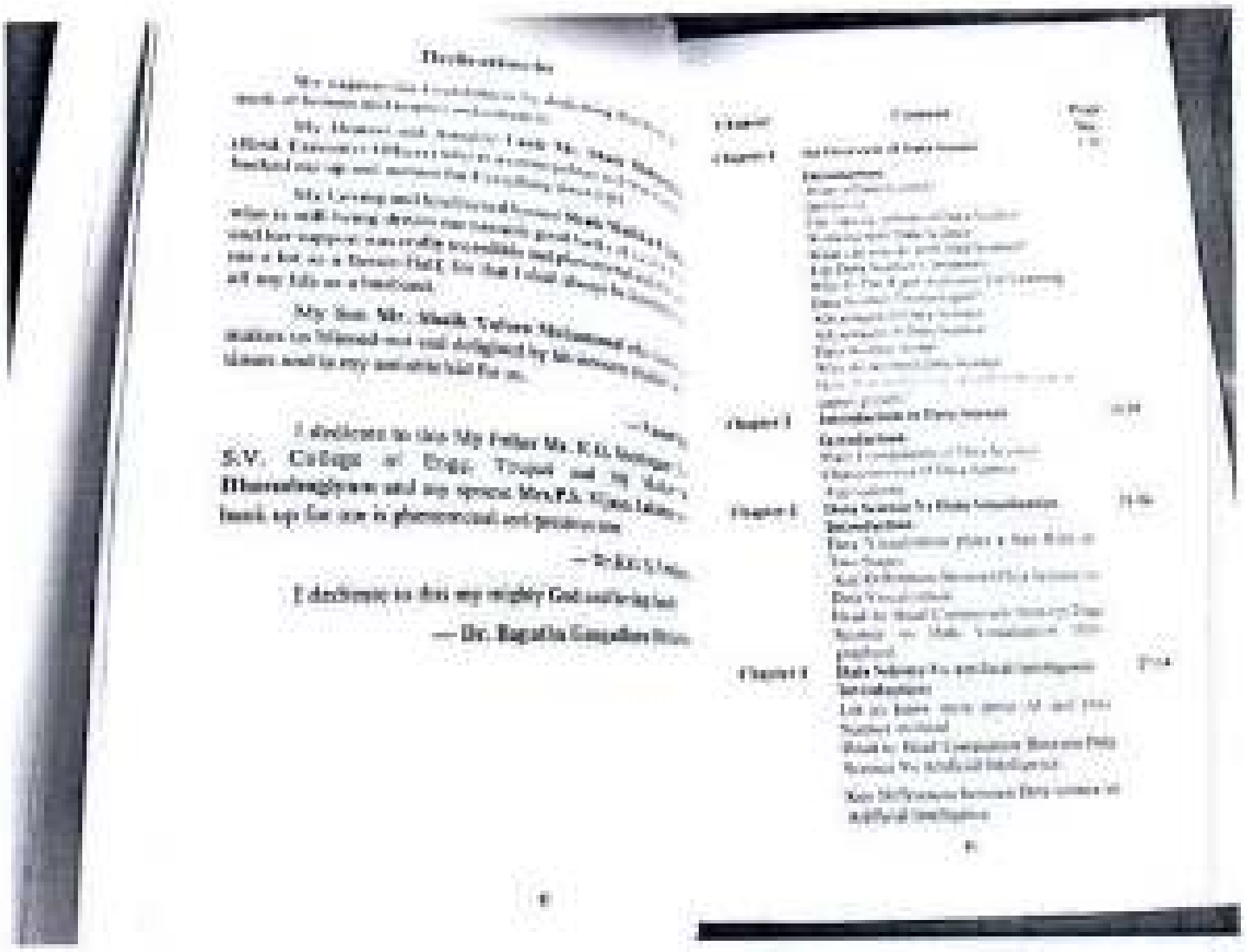

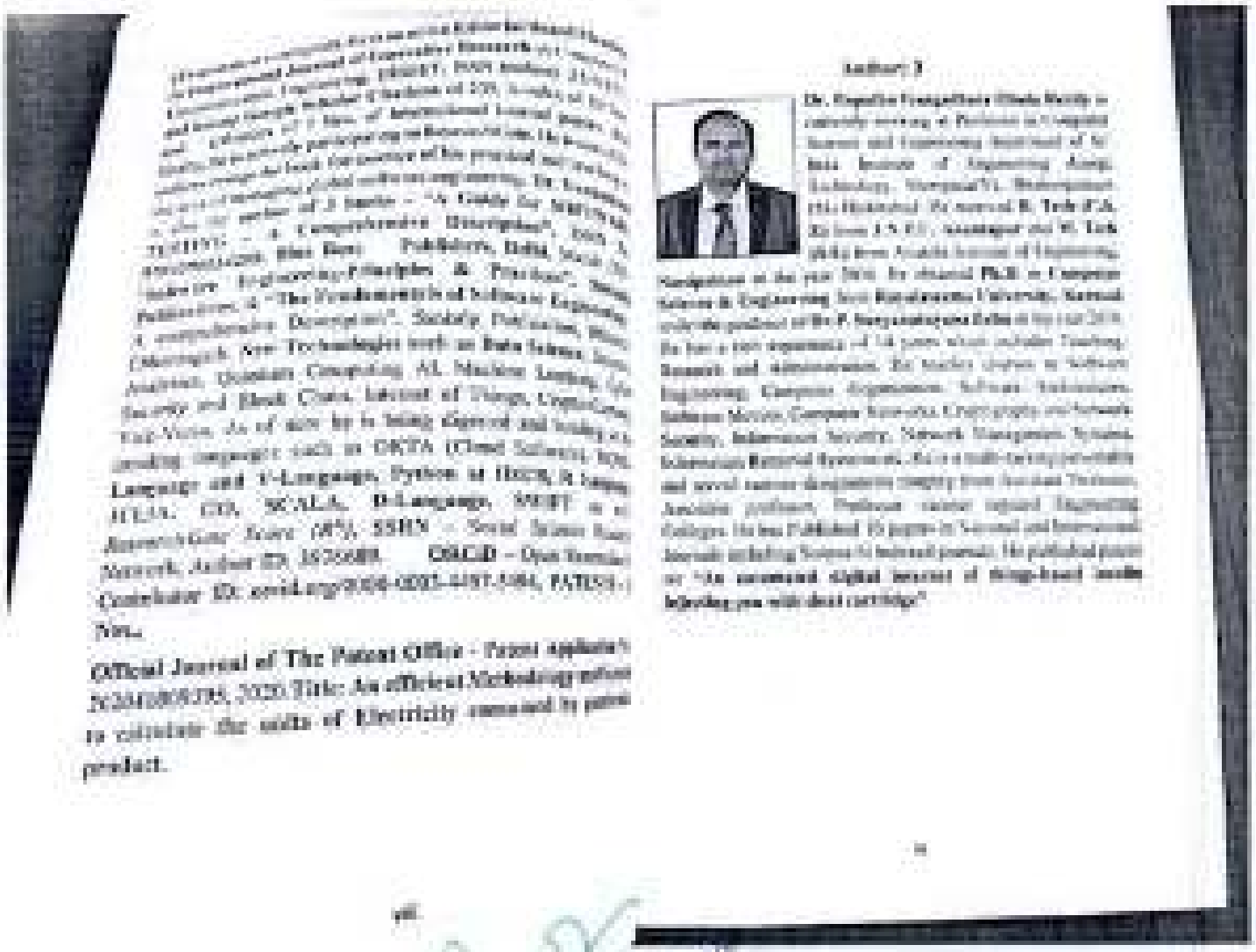

Official Journal of The Patent Office - Patent application number 202041005395, 2020. Title: An efficient Methodology method to calculate the units of Electricity consumed by patent product.

Author: 3

Dr. Rupatha Pranganthara Hindu Reddy is currently working as Professor in Computer Science and Engineering Department of Sri Indu Institute of Engineering & Technology, Hyderabad,TS, Hyderabad. He received B. Tech (C.S. E) from J.N.T.U., Anantapur and M. Tech (I&C) from Acharya Institute of Engineering, Bangalore in the year 2010. He obtained Ph.D. in Computer Science & Engineering from Rayalaseema University, Kurnool under the guidance of Dr. P. Sreenivasulu Reddy in the year 2019. He has a rich experience of 14 years which includes Teaching, Research and Administration. His teaching courses in Software Engineering, Computer Organization, Software Architecture, Software Metrics, Computer Networks, Cryptography and Network Security, Information Security, Network Management Systems, Information Retrieval Systems etc. He is a life time member of ISTE and several various professional societies. He is working presently as Associate professor, Professor cum Head, Engineering Colleges. He has Published 10 papers in National and International Journals including Scopus & Indexed journals. He published patent on "An automated digital bracelet of things-based insulin injecting pen with dose cartridge"

Fundamentals of Management

Gaddam Rahul Paul
U.Fanidara Baradwaja Sharma

Fundamentals of

Management is a process of planning, decision making, organizing, leading, motivation and controlling the human resources, financial, physical, and information resources of an organization to reach its goals in an efficient and effective manner. Every course has to examine from the management perspective to absorb more insights into its relevance and public utility. When Engineering students learn management concepts and practices and apply these to their core engineering curriculum, they explore the fullness of their subject in terms of value proposition, value creation, and value capture. This is the very purpose of teaching Fundamentals of Management as a core subject to all engineering branches.The book is written considering the academic requirements of B.Tech (all branches) course of JNTUH. Considering the previous examination pattern and in the context of the future examinations, this book can be referred to as the guide, consisting of a brief of the topics for the preparation of the students.

Gaddam Rahul Paul

Mr. Gaddam Rahul Paul is a young and dynamic faculty at Sri Indu Institute of Engineering and Technology, Affiliated to JNTUH. He is also designated as the Editorial Board Member for the DKRF Journals. He is qualified in 15-Set – 2019 and done his dual masters in MBA (Human Resources and Marketing) and MSc (Psychology).

He has to his credit, several research papers published in reputed Journals and in National and International Conferences. Mr.Gaddam Rahul Paul was conferred Best Young Faculty Award for the year 2019 by DK International Research Foundation.

U.Ravindara Baradwaja Sharma

Mr. U.Ravindara Baradwaja Sharma is a young and dynamic faculty at Sri Indu Institute of Engineering and Technology, Affiliated to JNTUH. He has completed his B.Tech in Mechanical Engineering and MBA in Finance and Marketing. He has to his credit, several research papers published in reputed Journals and in National and International Conferences.

₹249

VarietyPublication

Analog and Pulse Circuits by D. Lakshmaiah, C. B. Rama Rao and K. Kishan Rao

Published by:

BSP BS Publications
A unit of BSP Books Pvt. Ltd.
4-4-309/316, Giriraj Lane, Sultan Bazar,
Hyderabad - 500 095
Phone: 040 - 23445688
e-mail: info@bspbooks.net
www.bspbooks.net

Printed and Bound in India by Bharath Print Solutions Pvt. Ltd.

ISBN: 978-93-8915-[illegible] (Hardbound)

Published by Walnut Publications
#722, Esplanade One, Rasulgarh
Bhubaneswar - 751010, India
www.walnutpublication.com

This book has been published with all reasonable efforts taken to make the material error-free after the consent of the author. The author of this book is solely responsible and liable for its content including but not limited to the views, representations, descriptions, statements, information, opinions and references ["Content"]. The publication does not endorse or approve the Content of this book or guarantee the reliability, accuracy or completeness of the Content published herein. The publisher and the author make no representations or warranties of any kind with respect to this book or its contents. The author and the publisher disclaim all such representations and warranties, including for example warranties of merchantability and educational or medical advice for a particular purpose. In addition, the author and the publisher do not represent or warrant that the information accessible via this book is accurate, complete or current.

ISBN: 9789389744392
Price ₹249
Published in January 2020

Acknowledgements

We express our heartiest thanks and gratitude as well as indebtedness to the authors, publishers and other researchers of those books, blogs and journals from which we have taken the idea, opinion, data, etc., in order to provide ample information to the students.

We would like to thank the portfolio and production teams at Walnut Publications who have performed a tremendous job in completing the book. My sincere thanks to Head of Walnut Publications for his support, encouragement and motivation in our academic endeavour.

We would also like to thank our honourable chairman Sri.R.Venkat Rao, M.A, I.A.S for his immense support and Dr. I. Satyanarayana, M.TECH(IIT-KGP), Ph.D., FIE, MIE, MISHMT, Principal of Sri Indu Institute of Engineering and Technology and R.Yadagiri Rao, M.Sc, B.Ed, M.Tech, (Ph.D), for validating the content and suggesting improvements at different stages.

The unstinted support we received from our family members in general, from Vedha Prof. Uma Srinivasa Sharma, Padma Latha, Sridhar Sharma, Santhoshi Kiranmayi, Sneha who stood behind us in all odd situations to convert any distress into delight, deserves unconditional recognition.

Thanks are also due to K.P.Shoeon, MA, D.Ed., who edited the manuscript and also to N.S.C.Sidhu, MHA, PGDCA, PGDMM, (Ph.D.), B.Swathy, MBA, and Asra Khatoon, MBA, who took time to provide their valuable feedback.

Gaddam Rahul Paul
U.Fanidara Baradwaja Sharma

Syllabus

Fundamentals of management

B.Tech III Year I Sem.
Course Code: SM504MS

L T P C
3 0 0 3

Course Objective: To understand the Management Concepts, applications of Concepts in Practical aspects of business and development of Managerial Skills.

Course Outcome: The students understand the significance of Management in their Profession. The various Management Functions like Planning, Organizing, Staffing, Leading, Motivation and Control aspects are learnt in this course. The students can explore the Management Practices in their domain area.

Unit - I

Introduction to Management: Definition, Nature and Scope, Functions, Managerial Roles, Levels of Management, Managerial Skills, Challenges of Management, Evolution of Management- Classical Approach- Scientific and Administrative Management; The Behavioral approach; The Quantitative approach; The Systems Approach; Contingency Approach; IT Approach.

Unit - II

Planning and Decision Making: General Framework for Planning - Planning Process, Types of Plans, Management by Objectives; Development of Business Strategy. Decision making And Problem Solving - Programmed and Non-Programmed Decisions, Steps in Problem Solving and Decision Making; Bounded Rationality and Influences on Decision Making; Group Problem Solving and Decision Making; Creativity and Innovation in Managerial Work.

PRINCIPAL
Sri Vidya Institute of Engineering & Tech.
Kanuru, Vijayawada-520 007
A.P. (INDIA)

Unit - III

Organization and HRM: Principles of Organization; Organizational Design & Organizational Structures; Departmentalization; Delegation; Empowerment; Centralization, Decentralization, Recentralization; Organizational Culture; Organizational Climate and Organizational Change. Human Resource Management & Business Strategy; Talent Management, Talent Management Models and Strategic Human Resource Planning; Recruitment and Selection; Training and Development; Performance Appraisal.

Unit - IV

Leading and Motivation: Leadership, Power and Authority, Leadership Styles; Behavioral Leadership, Situational Leadership; Leadership Skills, Leader as Mentor and Coach; Leadership during adversity and Crisis; Handling Employee and Customer Complaints; Team Leadership. Motivation – Types of Motivation; Relationship between Motivation, Performance and Engagement; Content Motivational Theories - Needs Hierarchy Theory, Two Factor Theory, Theory X and Theory Y.

Unit - V

Controlling: Control, Types and Strategies for Control; Steps in Control Process; Budgetary and Non- Budgetary Controls, Characteristics of Effective Controls, Establishing control Systems; Control frequency and Methods.

PRINCIPAL
Indira Institute of Engineering & Tech.

Table of Contents

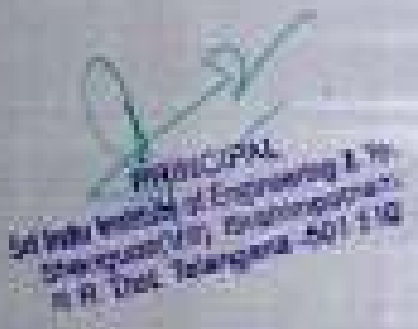

Analog and Pulse Circuits

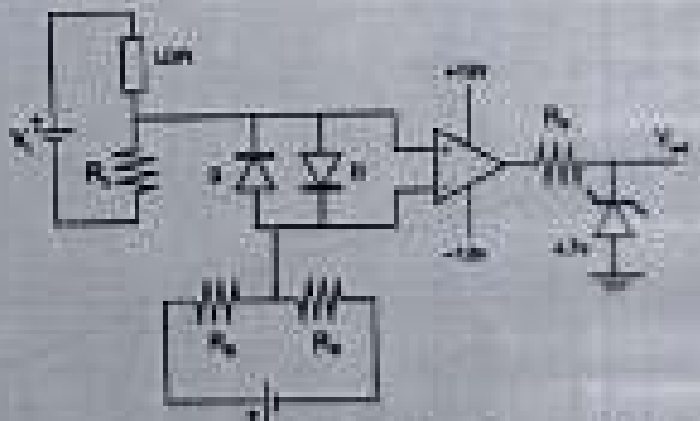

Dayadi Lakshmaiah
C. B. Rama Rao
K. Kishan Rao

BS Publications

Analog and Pulse Circuits

Dr. Dayyadi Lakshmaiah
Professor
Department of ECE
SIET, Hyderabad

Dr. C. B. Ramarao
Professor
Department of ECE
NIT, Warangal

Dr. K. Kishan Rao
Professor
Department of ECE & Ex Director
NIT, Warangal

BSP BS Publications
A unit of BSP Books Pvt. Ltd.
4-4-309/316, Giriraj Lane, Sultan Bazar
Hyderabad - 500 095

Analog and Pulse Circuits

This book has been designed as per the revised syllabus of analog and pulse circuits offered to the second year students of ECE in all JNTU, NTU, various universities. The mathematical derivations are done completely and in easy to understand manner. Typical examples and problems have been included to help the student grasp the subject better and to build their confidence.

SALIENT FEATURES

- Complete coverage of topics as per the syllabus of various universities like all JNTU, NTU
- Clear analysis and design of all Analog and Pulse Circuits in easy to understand manner
- Numerous solved examples which gives a clear understanding of the subject
- Well illustrated with worked out examples
- Simple Language aimed to benefit average students
- An exclusive chapter on solving Analog and Pulse Circuits problems using Arrays

About the Authors

Daryoli Lakshmaiah, professor of Electronics and Communication Engineering, is presently with Sri Indu Institute of Engineering and Technology, Hyderabad, India. He obtained his Doctoral degree from JNTUK, Kakinada. He has M.Tech JNTU Anantapur (campus), He received his B.Tech from National Institute of Technology, Warangal (REC-W). He has 18 year of experience as a teacher and industry. He has published about 45 technical research paper in national and international journals and conferences, interesting areas and subjects are low power VLSI, Digital electronics, Electronics and Devices circuits, analog electronics, Linear IC applications, analog CMOS circuits, Digital system design.

C. B. Rama Rao professor of Electronics and Communication Engineering is presently with National Institute of Technology, Warangal, India. He obtained his Doctoral degree from IIT Kharagpur. He received his M.Tech and B.Tech degrees from JNTU Kakinada, Andhra Pradesh (campus). He has 38 years of experience as a teacher and worked at NITW at different positions. He has guided successfully three Ph.D scholars. He has published about 40 technical research papers in national and international journals and conferences. Interesting areas and subjects are adaptive signal processing, Bio Medical Signal Processing, Acoustical Signal Processing, Analog Electronics, Linear IC Applications, Digital Signal Processing, Signals and Systems.

K. Kishan Rao professor of Electronics and Communication Engineering, is presently with Sreenidhi Institute of Science & Technology, Hyderabad and former principal of Regional Engineering college, Warangal (NITW), India. He obtained his Doctoral degree from IIT Kanpur. He received his M.Tech and B.Tech degree from Osmania University, Hyderabad, Telangana (campus). He received his B.Tech from National Institute of Technology Warangal (NITW). He has 40 year of experience as a teacher and worked at NITW at different positions. He has guided successfully 10 Ph.D scholars are completed. He has published about 110 technical research papers in National and International Journals and Conferences. Interesting areas and subjects are Electronics and Devices Circuits, Pulse and Digital Circuits, Bio Medical Signal Processing, Analog Electronics, Linear IC applications, Digital Image processing, communications. He received Two Gold Medals from Osmania University for standing 1st in B.E. Examinations – 1966, Distinguished Alumni Award of ECE Dept. O.U. – 1994, Best Teacher Award of A.P. Govt. – 1995, AP Scientist Award of APSCOT – 2001, Engineers A Scientist Award of BBH, Hyderabad – 2001. He has visited U.K. Universities – Leeds Metropolitan University, Huddersfield University and UMIST as a part of UK-REC DGAP project in November 1997 for two weeks. Visited Singapore and Malaysia during 12-20th July 1999, to present two technical papers at IPCH, Malaysia and chaired one technical session at the International Conference on 'Robotics, Vision and Parallel Processing for Automation' (ROVPIA'99), 16-17th July 1999, IPCH, Malaysia.

BSP BS Publications
A Unit of BSP Books Pvt. Ltd.

Lakshmaiah Dayadi
Subramanyam M. V.
Satya Prasad Kodati

Minimization of Dynamic Power Through Structural Changes &Vt Techniques

low power cmos circuits

LAMBERT Academic Publishing

Advances in Bioprocess Technology

Pugalenthi Ravindra *Editor*

Springer

Starter Culture Technology: Fermented Foods

B. Prema Latha, S.M. Reddy, K.S. Yoon, and Pogaku Ravindra

Introduction

Since the ancient time's fermentation technology have been in common practice of man for the production of different products such as curd, wine, alcohol, idly, dosa etc. In the initial stages these food products were produced without the knowledge of scientific principles involved in the process of product formation. It was due to spontaneous microorganisms present in the environment or container. Traditional fermentations were captured to store the food products (Holzapfel 2002). This concept was originated after later half of nineteenth century when the fermented products developed after pasteurization (Klaenhammer and Fitzgerald 1994). The role of microorganisms in food fermentations were realized (Caplice and Fitzerald 1999; Baldino et al. 2003) with passing of time the clear picture of the fermentation and role played by starter cultures or microorganisms.

In the past fermentation process was utilized to enhance the quality of product (Holzapfel 1997, 2002). Final Product was the result of interaction of flora of the raw material and the environmental conditions prevailing such as temperature, oxygen, water activity, pH etc. the microorganisms beside selecting necessary enzymes they also produce beneficial substances which are needed for production of fermented products (Klaenhammer and Fitzgerald 1998) such as lactic acid, alcohol, organic acid etc. (Ranum 2002). These products act as preservatives, enhance flavor and increase shelf life of product (Noan 1991). Preservation of food is man's struggle for survival since prehistoric times was to ensure required food for all the time. Microbial fermentation not only preserves the food but also contributes the taste, aroma, flavor, stability etc. (Hammes 1990).

D.P. Latha • S.M. Reddy • K.S. Yoon • P. Ravindra (✉)
Faculty of Engineering, Chemical Engineering Program, University Malaysia Sabah, Sabah, Malaysia
e-mail: dr_ravindra@hotmail.com

P. Ravindra (ed.), *Advances in Biochemical Technology*,
DOI 10.1007/978-3-319-17915-5_21

Sri Indu Institute of Engineering & Technology

Academic Year 2019-2020

Research Publications – Papers Published in National/ International Conference

Sl. No	Name of the Faculty Author	Title of the paper	Name of the Publisher	ISBN Number	URL
1	DR. S.SURESH SUBRAMANAIAN	COMPACT MICRO STRIP FED KOCH FRACTAL MONOPOLE LOOP ANTENNA FOR MULTIBAND PERFORMANCE	IEEE	978-1-7281-5198-4	https://ieeexplore.ieee.org/document/9074354
2	DR. S.SURESH SUBRAMANAIAN	DESIGN AND DEVELOPMENT OF RF ENERGY HARVESTING LOOP ANTENNA	IEEE	978-1-7281-5198-4	https://ieeexplore.ieee.org/abstract/document/9074402
3	DR. S.SURESH SUBRAMANAIAN	A DETAILED INVESTIGATION ON REDUCTION OF FALSE POSITIVE RATE IN BREAST CANCER DETECTION	IEEE	978-1-7281-5198-4	https://ieeexplore.ieee.org/document/9074382
4	Dr.PANDU KURRE	EVALUATION OF PULLOUT RESISTANCE OF REINFORCING STRIPS EMBEDDED IN CEMENT MODIFIED MARGINAL BACKFILL OF MECHANICALLY STABILIZED EARTH (MSE)WALLS	SPRINGER	978-3-030-24314-2	https://link.springer.com/chapter/10.1007/978-3-030-24314-2_30

5	Dr.PANDU KURRE	EFFECT OF ECCENTRIC LOAD ON FOOTING RESTING ON PLANAR GEOSYNTHETIC REINFORCEMENT	SPRINGER	978-3-030-24314-2	https://link.springer.com/chapter/10.1007/978-3-030-24314-2_20#:~:text=Results%20from%20laboratory%20load%20test,there%20is%20no%20much%20improvement.
6	Dr.PANDU KURRE	STUDY ON INTERACTION OF REINFORCING STRIPS EMBEDDED IN CEMENT MODIFIED MARGINAL BACKFILL	SPRINGER	978-3-030-24314-2	https://link.springer.com/chapter/10.1007/978-3-030-24314-2_17
7	Dr.PANDU KURRE	RESILIENT MODULUS OF UNSSATURATED SOIL -A COMPREHENSIVE REVIEW	SPRINGER	978-3-030-24314-2	https://link.springer.com/chapter/10.1007%2F978-3-030-24314-2_19
8	DR. I.SATYANARAYANA	EVALUATION OF MATERIAL PROPERTIES AND ABRASIVE RESISTANCE OF TANTALUM CARBIDE BASED HARDOX STEEL FOR CONSTRUCTION PURPOSE	SPRINGER	978-981-15-4739-3	https://link.springer.com/chapter/10.1007/978-981-15-4739-3_6
9	DR. C.SIVAKANDHAN	EVALUATION OF MATERIAL PROPERTIES AND ABRASIVE RESISTANCE OF TANTALUM CARBIDE BASED HARDOX STEEL FOR CONSTRUCTION PURPOSE	SPRINGER	978-981-15-4739-3	https://link.springer.com/chapter/10.1007/978-981-15-4739-3_6

10	DR. C.SIVAKANDHAN	EEFFECT OF DIETHYL ETHER ON LHR ENGINE CHARACTREISTICS USING PAPAYA METHYL ESTER - EUCALYPTUS OIL BLEND	THE INSTITUTION OF ENGINEERS HOSUR	978-81-942561-6-8	
11	DR. I.SATYANARAYANA	EEFFECT OF DIETHYL ETHER ON LHR ENGINE CHARACTREISTICS USING PAPAYA METHYL ESTER - EUCALYPTUS OIL BLEND	THE INSTITUTION OF ENGINEERS HOSUR	978-81-942561-6-8	
12	P.VIJAY KUMAR	EEFFECT OF DIETHYL ETHER ON LHR ENGINE CHARACTREISTICS USING PAPAYA METHYL ESTER - EUCALYPTUS OIL BLEND	THE INSTITUTION OF ENGINEERS HOSUR	978-81-942561-6-8	
13	M.V.B. KALYAN	EEFFECT OF DIETHYL ETHER ON LHR ENGINE CHARACTREISTICS USING PAPAYA METHYL ESTER - EUCALYPTUS OIL BLEND	THE INSTITUTION OF ENGINEERS HOSUR	978-81-942561-6-8	
14	DR. C.SIVAKANDHAN	TAGUCHI'S OPTIMIZATION OF AWJM PROCESS PARAMETER ON ALUMINIUM HYBRID COMPOSITE	SPRINGER	978-981-15-4739-3	https://link.springer.com/chapter/10.1007%2F978-981-15-4739-3_28

Academic Year 2018-2019

Research Publications – Papers Published in National /International Conference

Sl. No	Name of the Faculty Author	Title of the paper	Name of the Publisher	ISBN Number	URL
1	DR.S.SURESH	TESTING AND IMPLEMENTATION OF SMART BRAKE PEDAL SYSTEM WITH SIDNAL DIAGNOSTIC AND FALIURE DETECTION	IEEE	978-1-5386-9354-4	https://ieeexplore.ieee.org/document/8899361
2	DR.S.SURESH	FACE DETECTION BASED AUTOMATION OF ELECTRICAL	SPRINGER	978-3-030-37218-7	https://link.springer.com/chapter/10.1007/978-3-030-37218-7_23#:~:text=The%20proposed%20method%20uses%20Viola,our%20day%20to%20day%20life.&text=Based%20on%20the%20position%20of,particular%20region%20can%20be%20controlled.
3	MRS.A.SWETHA	ANTENNA BEAMFORMING AND BEAM CONTROLLING FOR IMPROVING THE WI-FI SIGNAL	MRECW	978-93-83038-75-6	

4	MR.S.NARESH	ANTENNA BEAMFORMING AND BEAM CONTROLLING FOR IMPROVING THE WI-FI SIGNAL	MRECW	978-93-83038-75-6	
5	DR. C.SIVAKANDHAN	STUDIES ON MECHANICAL PROPERTIES OF SISAL AND JUTE FIBER HYBRID SANDWICH COMPOSITE	SVCE	978-93-86638-87-8	

Academic Year 2017-2018

Research Publications – Papers Published in National /International Conference

Sl. No	Name of the Faculty Author	Title of the paper	Name of the Publisher	ISBN Number	URL
1	DR.I.SATYANARAYANA	NANO COMPOSITE PROPERTIES AND ITS APPLICATIONS: A REVIEW	INTERNATIONAL CONFERENCE ON INNOVATIONS IN MECHANICAL ENGINEERING	978-93-85100-86-4	
2	DR. C.SIVAKANDHAN	INFLUENCE AND EFFECT ON MECHANICAL PROPERTIES OF STITCHED AND UN-STITCHED WOVEN GLASS FIBER / EPOXY COMPOSITE LAMINATES	NATIONAL CONFERENCEON RECENT TRENDS &DEVELOPMENTS IN MECHANICAL ENGINEERING		

Academic Year 2016-2017

Research Publications – Papers Published in National /International Conference

Sl. No	Name of the Faculty Author	Title of the paper	Name of the Publisher	ISBN Number	URL
1	DR. K.S.SADASIVA RAO	A STEGANOGRAPHIC TECHNIQUE FOR TRANSFERRING SOURCE IMAGE FILE WITHOUT STEGO FILE WITH HIGH LEVEL OF ROBUSTNESS	ICISC	978-1-5090-4716-1	https://ieeexplore.ieee.org/document/8068740
2	DR. K.S.SADASIVA RAO	A NOVEL STEGANOGRAPHIC TECHNIQUE FOR TRANSFERRING IMAGE FILE WITHOUT STEGO FILE BY USING SHUFFLED ABSOLUTE DIFFERENTIAL VECTORS OF IMAGE	WISPNET	978-1-5090-4443-6	https://ieeexplore.ieee.org/document/8299948
3	DR. K.S.SADASIVA RAO	AN EFFICIENT AND ROBUST IMAGE STEGANOGRAPHIC TECHNIQUE WITHOUT STUFFING DATA BITS	ICETCS	978-981-10-2750-5	https://link.springer.com/chapter/10.1007/978-981-10-2750-5_43#:~:text=So%20this%20algorithm%20is%20named,bit%20positions%20of%20the%20pixel.

Academic Year 2015-2016

Research Publications – Papers Published in National /International Conference

Sl. No	Name of the Faculty Author	Title of the paper	Name of the Publisher	ISBN Number	URL
1	DR. I.SATYANARAYANA	COOLING AND HEATING OF A SUBSTANCE USING VAPOUR COMPRESSION REFRIGERATION CYCLE	MREC		
2	DR .I.SATYANARAYANA	THERMAL ANALYSIS COMPARISIONS ON NATURAL VENTILATED OPEN POLY GREENHOUSE TO CLOSED POLY GREENHOUSE	MREC		
3	DR. I.SATYANARAYANA	DESIGN AND ANALYSIS OF TORSEN DIFFERENTIAL	MREC		
4	DR. I.SATYANARAYANA	CFD ANALYSIS ON TURBULENT CONVECTION HEAT TRANSFER WITH FE3O4 NANOPARTICLES IN WATER	MREC		

5	DR.I.SATYANARAYANA	ADVANCED FUEL OPERATED INTERNAL COMBUSTION ENGINES	MREC		
6	DR.I.SATYANARAYANA	PERFORMANCE TEST ON SINGLE CYLINDER FOUR STROKE DIESEL ENGINES BY USING CONVERGENT DIVERGENT INLET MANIFOLD	MREC		
7	DR.I.SATYANARAYANA	DESIGN AND THERMAL ANALYSIS OF WARM (COLD) FORGING PROCESS AND DIES	MREC		

Compact Micro Strip Fed Koch Fractal Monopole Loop Antenna For Multiband Performance

Suresh Subramanian
Department of ECE
Sri Indu Institute of Engineering and Technology
Hyderabad, India
sureshsaranathi@gmail.com

R.Sundaramurthy
Department of CSE
Chennai Institute of Technology
Chennai, India
sundaiperthu@gmail.com

Abstract— *A compact Koch fractal monopole loop antenna with 50Ω micro strip feed for multiband application is presented. The proposed antenna is designed on Arlon 1849 substrate with the dimensions of Lsub 37 mm x Wsub x 49 mm x h 1.6 mm with the ground plane dimensions 11 X 9.5 mm x 10 X 8.92 mm and 1.5 GHz - 2.37 GHz (WiMAX), 4.72 GHz - 6GHz (UNII/ISM), and 8.4 GHz -10.45 GHz (WLAN) suitable for BLUETOOTH/ZIGBEE, WiMAX 802.16, Radar navigation respectively. The proposed antennas exhibits good return loss in the simulation and the symmetrical geometric structure of the antenna provides Omni directional radiation patterns.*

Keywords—Micro strip feed, Koch fractal, monopole antenna, multiband characteristics.

I. INTRODUCTION

Fractals describe galaxies and some other natural phenomena. Fractal geometry and its concepts have become central tools in most of the natural sciences such as physics, chemistry, biology, geology and even in material science. The rapid development in the wireless communication field requires design of small antennas that can be used in more than one frequency band. The self-similarity and space filling property of fractals makes them especially suitable for multi frequency antenna design [2-3]. Monopole antennas [4]. In this paper, a micro-strip feed Koch fractal monopole loop antenna for multiband application is designed and analyzed. This antenna consists a fractal monopole of the second iteration of Koch geometry. The radiation pattern, which is omnidirectional, adds additional value for the proposed antenna design.

II. KOCH FRACTAL ANTENNA DESIGN

Initially the creation of Koch curve is obtained by dividing a line of any given length into 3 equal parts. Figure 1 shows the achievement of Koch curve which clearly shows the transformation of a line into equilateral triangles. Then the triangles which are identical to each other are placed one above the other in such a way that all their centroids coincides with each other [5]. The same procedure is replicated for the entire triangle in all of its sides. This results in the formation of new triangles and the same procedure is applied to the newly formed triangles too which end up with the generation of Koch loop of higher order. The formation of various Koch fractal loop is as shown in Figure 2 and Figure 3 (a). The antenna is in the x-y plane and the normal direction is parallel to the z axis. Duroid 5880 is used as the dielectric material with $\varepsilon_r = 2.2$ and the dimension of the substrate is 37 mm x 49mm x 1.6 mm.

Figure 1 Koch curve Formation

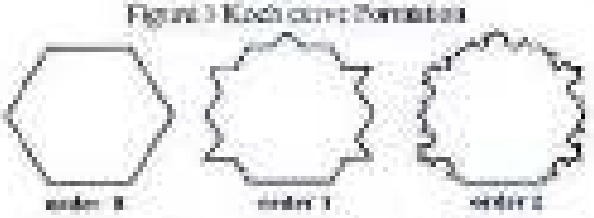

Figure 2 Koch loop generation with higher order

The radiation element is a hexagonal [6] loop with the size of each side is 16.6mm. A 50 Ω micro strip line with feed length (L_f) = 17 mm and width (W_f) = 4.92 mm is used to excite the antenna. A gap of 0.5 mm is maintained between antenna and ground plane for achieving required impedance bandwidth. The ground plane dimension is 10.2mm*9.9 mm. The design and simulation results are analyzed using HFSS [8] (High Frequency Structure Simulator) for various configuration of Koch fractal geometry (Zeroth order to Second order). The basic structure could not achieve the impedance bandwidth properly. So, iterations are carried out. During the simulation, it has been observed that, in the second iteration the multiband frequency is obtained with required band width and return loss. In order to improve the return loss of each band [7], a slit with the dimension of [L] 5.5 mm x [W] 4.92 mm is removed from the ground plane. The structure of the slit in the ground plane is shown in the Figure 3(b).

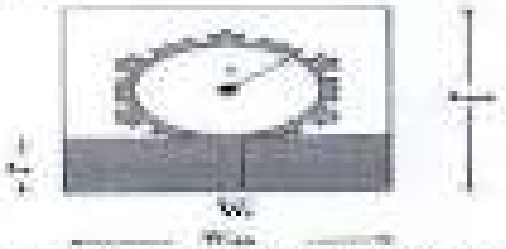

Figure 3 (a) Structure of Micro strip fed Koch fractal monopole antenna

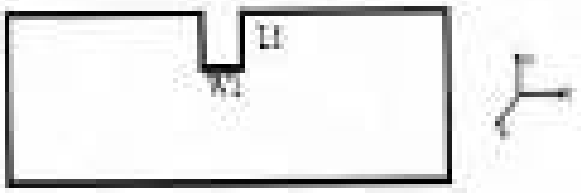

Figure.3 (b) Ground structure of proposed antenna

III. RESULTS AND DISCUSSION

The first band Fig 4 and Fig 5 has a impedance bandwidth as large as 510MHz and covers PCS (1850-1990 MHz) band with center frequency of 1.9GHz.

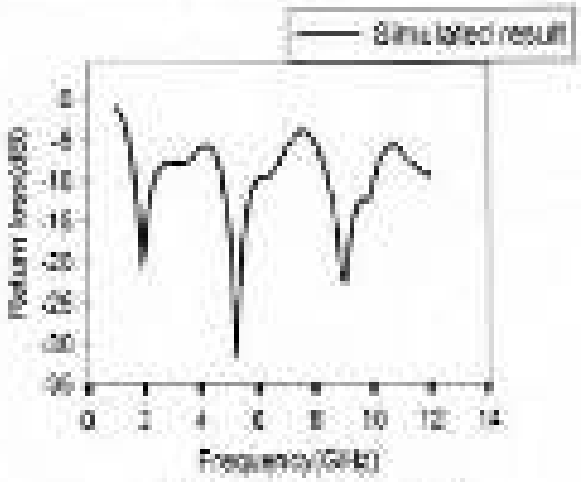

Figure.4 Simulated antenna

The upper band has the impedance bandwidth of 2051 and covers the RADIO NAVIGATION band (4500MHz-5000MHz) with center frequency of 9GHz. In all the frequency band range, we can see that the VSWR is maintained less than 2.

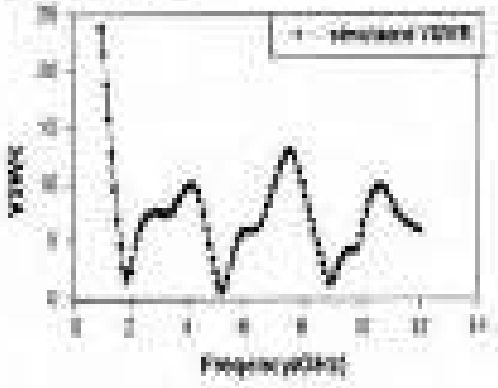

Figure.5 Simulated proposed antenna

The figure 6 (a) shows the nature of H and E Plane radiation pattern are nearly Omni-directional and dumbbell shaped respectively. Here, the simulated radiation pattern in H Plane and E plane is more Eddy monopole radiation pattern for all bands.

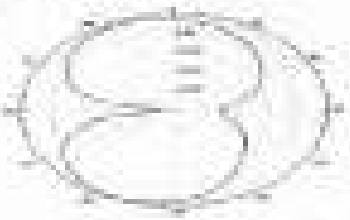

Figure.6 (a) Simulated radiation pattern of y-z plane

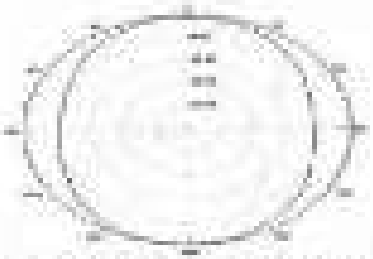

Figure.6 (b) Simulated radiation pattern of x-y plane

IV. CONCLUSION

The Koch fractal monopole loop antenna with ground slit for multi band characteristics for the second iteration has been designed and results are analyzed. The triple band covers 1.9GHz, 5.2GHz, and 9GHz which is useful for the application of DCS/PCS/UMTS, IEEE 802.11, and RADIONAVIGATION respectively with impedance bandwidths of 510MHz, 1280MHz and 2050MHz respectively. The radiation pattern for azimuth and elevation angle for the designed structure is more likely monopole radiation pattern. The proposed modified micro strip fed Koch fractal monopole antenna is simple to design and easy to fabricate.

References

[1] [illegible]

[2] [illegible]

[3] [illegible]

[4] [illegible]

[5] [illegible]

[6] [illegible]

[7] [illegible]

[8] [illegible]

[9] [illegible]

2020 4th International Conference on Advanced Computing & Communication Systems (ICACCS)

Design and Development of RF Energy Harvesting Loop Antenna

Sumit Subramanian
Department of Electronics and Communication Engineering, Sri Sai Ram Institute of Engineering and Technology, Thirumazhisai, India.
sai.subramanian@gmail.com

P.N.Parameswari
Department of Electronics and Communication Engineering, Rajalakshmi Institute of Technology, Kuthambakkam, India.
parameswari.p@gmail.com

B. Sankaranarayanan
Department of Computer Science and Engineering, Chennai Institute of Technology, Chennai, India.
sankaranarayanan@gmail.com

Abstract— Indian urban areas are encompassed by Radio Frequency (RF) signals and communicated by different remote systems.To improve the usage of wireless energy effectively, RF Energy Harvesting System is designed for the applications of sensor devices, battery chargers, and compact devices. The fundamental components of the RF power harvesting scheme are the antennas. High-Impedance Surfaces (HIS) have been widely considered in order to upgrade the field of the antenna. Exhibition of such meta-surfaces is the in-phase basis of an incident wave, which is based on a limited frequency dimension to mention as the Artificial Magnetic Conductor (AMC). The research proposes a loop antenna realized on an AMC for RF energy harvesting to operate at ISM frequency of 868MHz.

Keywords— *Radio Frequency,High-Impedance Surfaces, Artificial Magnetic Conductor*

I. INTRODUCTION

The power harvesting scheme is utilized to capture and collect the ambient power that should be converted into electrical energy. It is also called energy scavenging. Typically, there are adequate energy resources available around as like wind, solar, thermal and mechanical but these energies are not used in electrical load as a power supply. The different form of energy is available in our surroundings,the main challenge will be to differentiate them and analyse what form that would be most beneficial for the Radio Frequency [1].The suppliers and stable RF sources are available like broadcasting digital TV signals in the band of 500-698Hz and downlink mobile phone services in the band of 925MHz.

Loop antenna is used to design the band of 900-MHz and 835-MHz because of its high input impedance, it may be used in transmitter section and added advantage to convert RF signal to Direct current [2]. To enhance the efficiency of the receiving section of the antenna, a reflector also required because of the sensitivity in both the broadside directions of the loop antenna. Each type of reflectors made up of an electromagnetic band gap (EBG) for the purpose of achieving high gain antenna and low profile.

Nowadays researchers are showing too much interest on doing research in electromagnetic artificial materials [3], for example Double Negative metamaterials, EBG [5], twofold/double positive photonic previous stones [7]. These types of structures are called as metamaterials and characteristically understood that periodic dielectric substrates and many modification patterns. These Metamaterials shows the novel features in electromagnetics that cannot take place in nature, and have conclusions a wide range uses in application of propagated antenna and fields.

To enhance the performance of patch antenna because of the band-gap of surface waves and suppression, EBG structure is integrated with patch antennas. In order to achieve low profile structure, they additionally utilized as the ground plane of rod and spiral antennas.

Metamaterial having the interesting properties is that special interesting feature is the reflection phase. The electric field is reflected at the reflecting surface with phase is called the reflection phase. At reflecting surface, the reflection phase is correlated with respect to the phases of the incident electric segment. The both magnetic and electric conductors pose a reflection stage of 180^0 for a normal case plane wave that affirm the magnetic conductors, which do not exist.

Mainly-distributed HIS have been presented [4], the artificial magnetic conductor (AMC) is equivalent to the illumination from the incident plane wave. This type of structure is reflected with a reflection phase of 0^0 for the incident plane wave and it is complementary for the electric conductor which introduces 180^0 phase shift for the incident wave.

II. FUNCTIONING OF ARTIFICIAL MAGNETIC CONDUCTOR

The 2-D artificial ground plane EBG surface consists of the top surface which is aligned with metal patches periodically and bottom surface is metal ground plane [3]. Here all the metal patches are connected with the ground plane via the metallic post known as the mushroom structure. Because of the periodic condition in the EBG, surface waves have been stopped to transmit frequency in the band gaps.

A significant feature of metamaterial property is the incident radio waves are reflected without changing the phase in the band gap at the frequencies, as if the surface was considered a magnetic conductor. In that case, it is known as the AMC surface and shown in Fig.1. In general, the distance between the antenna and metal reflectors must have the quarter-wavelength to eliminate any forms of destructive interference between the direct and reflected waves because of phase reversal of 180^0 immediately after the reflection. In the meantime, AMC surfaces are very close to the antenna because of the reflected wave phase does not change for the incident plane wave.Hence the high radiation efficiency is

A Detailed Investigation on Reduction of False Positive Rate in Breast Cancer Detection

B.Sandyarani
Professor
Chennai Institute of Technology
Chennai – 600 069
sandyarani@citchennai.com

J.M.Mirnalinee
Professor
Chennai Institute of Technology
Chennai – 600 069

Suresh Subramanian
Professor
Sri Venkateswara Institute of Engineering and Technology
Thiruvallur – TN 631 203

R.Sandesh
Student
Chennai Institute of Technology
Chennai – 600 069

G.Durgadevi
Student
Chennai Institute of Technology
Chennai – 600 069

Abstract— Breast cancer is known as the most common form of cancer in Indian women and is about 14% of women cancer. Thus a detailed investigation is done to improve the level of screening mechanism and accuracy of breast cancer detection in Computer Aided Diagnosis system. The initial level of screening of breast can be performed using thermography and then the suggestions can be provided for necessity of further screening using mammography for cancer detection. If the presence of breast cancer is confirmed using mammograms, to address the high false positive rate with mammograms, the cancer patients can be examined again with biopsy images for further confirmation of the presence of breast cancer. Thus a detailed investigation on applicability of various modalities for the breast cancer screening is conducted to minimize the false positive rate in breast cancer detection.

Keywords—Breast Cancer Detection, Thermography, Mammography, Biopsy.

I. INTRODUCTION

According to World Health organization, breast cancer is feared predominantly which affects the lives of 2.1 million women each year[1]. The survey shows that one third of women have been subjected to the mortality rate and the breast cancer rate because the cancer is also increased to 1796[2]. It is obvious that early detection of presence of any type of breast cancer can save lives of many women across different countries.

Globally breast cancer also increases everywhere in the world. The instances of breast cancer are diagnosed each 19 seconds, which makes it risky for women to die from this disease one minute. In the next 20 years, about 40 million novel instances are proposed to be there globally and other 15 million individuals will perish due to the disease [3].

Figure 1 shows that the disease is a most predominant type of cancer in India [4]. Confederation of Indian Industry (CII) report says that young Indian women are more vulnerable to breast cancer[5]. Indian council of medical research says that out of 100,000 women, 25.8 women are having cancer in the year 2016 and there is an expectation that the number will rise to 36 in the year 2026[6].

Breast cancer is developed when the cells grow in an uncontrolled manner[7]. This extraordinary growth of cells can be visualized in x-ray as shades. If the growth of cells extended to nearby regions, then the tumor is malignant and on the other hand, if restricted to a specific portion, the tumor is benign. No doubt, an identification of malignant or benign helps the clinicians to proceed with further treatment. Thus the challenge lies in building an intelligent system to detect whether the patient suffers from breast cancer.

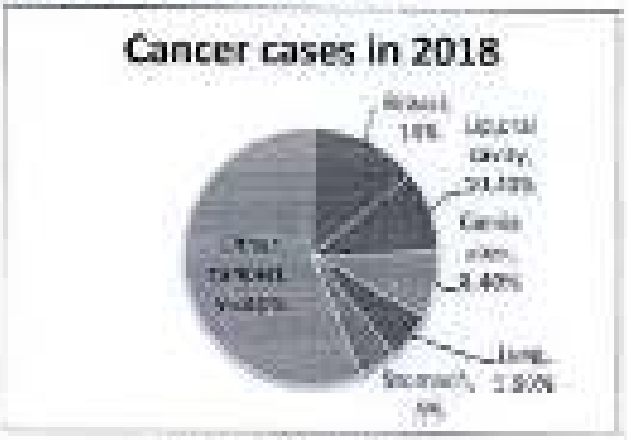

Fig. 1 Cancer cases in year 2018

The doctors recommended that women with age more than 40 years should undergo periodical breast cancer screening to confirm the availability of breast cancer at its initial stages [8]. Initial detection is possible before the women realize physical symptoms using below screening methodologies. This early detection of cancer enables physicians to provide less invasive treatments and save the lives of patients.

This research is arranged as follows. Part II explains the literature review presented in some modality methods that are applicable in the process of detecting breast cancer. Part III

presents the methodology that can be adopted to reduce the false positive rate in breast cancer detection. Section IV concludes the paper.

II. Breast Cancer Detection Techniques

The survey shows that the most widely used screening mechanism for breast cancer is mammography. The abnormality in breast is visualized easily with mammography images that have low cancer detection levels with mammography screening such as improper to replaced radiation patients and more limitations for breast is compressed while screening[9].

Hence to address the drawbacks of mammography, the diagnosis mechanism can be integrated with initial screening using thermography which is non-invasive and non-ionizing[10-11]. Thus the pain and uncomfortness due to compressing the breast is removed. Also it is not exposed to any radiation. Moreover, clinicians avoid mammography screening for women just to have their menstrual cycle including that period. Breasts become more soft and tender data about several days[12]. But thermography can be applicable at any time. The thermal sensors using infrared recordings, takes the photo of the breast with different temperature levels and puts them in a heat map[13]. The higher level of temperature infer the chance of presence of cancer. Thus the thermography can be used as an initial screening mechanism which alerts the medical workers using mammography for further tests.

Though the drawbacks of mammography are addressed with thermography, the other major drawback is identified. The survey shows that 10% of mammography screenings gives false positive results[14]. Many researchers are going on nowadays to reduce the false positive rate in breast cancer detection. Thus it can be preferred to integrate breast biopsy after mammography screening to confirm the presence of cancer further. Breast biopsy is considered as the best method to determine whether the suspected area is subjected to cancer.

III. Mechanisms To Reduce False Positive Rate in Breast Cancer Detection

The advantages of Deep Learning in Computer Aided Diagnosis systems, namely, the best accuracy in prediction even surpassing human performance and less computation time spread its popularity throughout the world and many researcher from their education to applying the different deep learning architectures in interested tasks.

Yassir Khaled et al used deep learning with convolutional neural networks tool to diagnosing the tissues using Mammographic MIAS database. They applied preprocessing techniques such as Watershed segmentation, Adaptive Mean Filter and Circular based segmentation and achieved 98% accuracy[15]. Abdullah-Al Nahid used back propagation for classification of breast cancer with histography images[16].

Mohammad Mahmood Al Rahhal got accuracy of 86.8% in classification and used deep learning with convolutional neural network[17]. Mei Hwai Yap applied Le-Net, FCN-Alex-Net and U-Net and got 90% accuracy[18]. Tanzila Araujo used images, images and achieved 83.3% accuracy with convolutional neural network[19]. The classifiers proposed by R. C. Gonzalez are RF implemented and RF-ELM that is concluded to be 98% accurate [20]. Main research done by Nayak achieved 100 percent and achieved 98% accuracy based on SVM classification[21].

Kevin A.Schulter et al validated the breast cancer prediction results with 4 publicly available datasets, namely, Ramella, ICIAR, Nuclei analysis and Histopathology datasets and attained 98.13%, 97.50%, 94.64% and 87.10% respectively[22]. They adopted an ensemble of DenseNet, MobileNet and VGG19 for feature extraction and used multi-layer perceptron classifier.

Eun Mi Yi et al used breast density dataset and applied CNN with boosting tree classifier for detecting breast cancer[23]. An ensemble of histological learning was performed on BreakHis dataset by Sawsan Bardou et al[24]. Kanadath Rayed et al worked with histopathology images in ICIAR dataset and used pre-trained classifier [25]. Zhongyi Han et al used GoogLeNet architecture[26] and Babak Ehteshami Bejnordi et al used ensemble CNN for classification[27]. Fabio Alexander Spanhol classified breast cancer histological images with the help of AlexNet architecture[28].

Since many researchers are focused in suggesting solutions for breast cancer, the survey is done extensively for breast cancer screening mechanisms and various findings are given in the following table.

Table I: Comparison of Breast Cancer Screening Mechanisms

Technique	Sensitivity	Specificity	Method	Remarks if Any
Mammography	90%	94%	Compressed the Breast	Breast not suitable for small age
MRI	90%	94%	Contrast substance injection, and expensive, longer duration	Screening of women at high risk for breast cancer
PET	90%	94%	Small amount of radioactive tracer	Detection of tumors can spread to other part of body
Ultrasound	87%	77%	Portable, Cheaper device	Sensitivity is more
Thermography	90%	97%	Compressed the Breast	Appropriate and Economic
Biomarker Molecular Imaging (BMI)	94%	82%	Needed to examine tissue sample	Performing after abnormal findings
Elastography	90%	>90%	Independent technique, attached to the main system	Successful
Thermal Infrared Tomography	87%	87%	Observation attached to the main system	Screening

The table clearly depicts that MRI imaging is the best current imaging tool for breast cancer. But the survey shows not research activities towards affordable radiologists available for breast cancer using mammograms with incorporating their findings at the earliest stages and biopsy at the later stage. It is illustrated in figure 2.

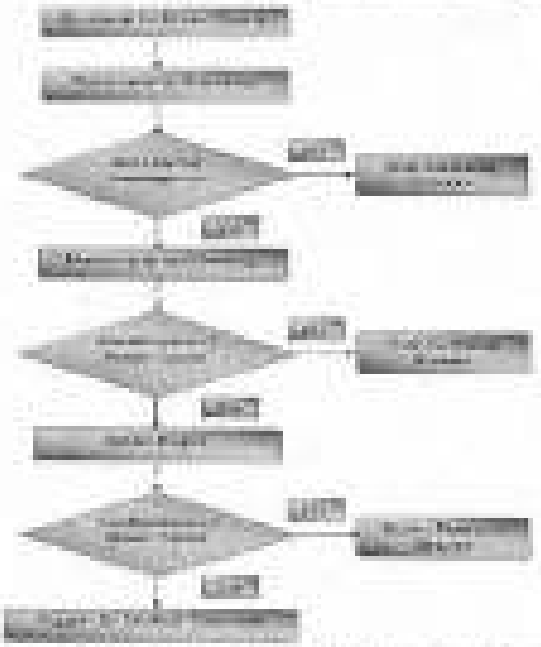

Fig. 2. Methodology to reduce false positive rate in breast cancer detection

IV. Conclusion

Initial detection of the disease shall drastically reduce the rate of mortality in women. Though the incidence rate is expected to increase every year, we have taken initiatives to reduce the mortality rate. Since periodical screening detects breast cancer at an early stage, processing with mammography is our investigation aims to undergo cost effective and painless screening. This facilitates the suspicious patients to undergo further diagnosis only when required thereby preventing unnecessary costly and painful invasive procedures in the initial stage itself. Though mammography is accepted as a standard procedure for breast cancer screening, the survey shows that the false positive rate is also high. In order to minimize the reported false positive rate, additional screening using biopsy is done for further confirmation of presence of cancer. Thus our findings suggest the inclusion of the preprocessing and post screening of detailed mammography to improve the health outcomes of women. Since the increase in incidence rate of breast cancer is beyond our control, at least we can take some initiatives to reduce the mortality rate in the initial level.

References

[1] http://www.who.int/cancer/prevention/diagnosis-screening/breast-cancer/en/

[2] https://www.cancer.org/cancer/breast-cancer/screening-tests-and-early-detection/breast-cancer-screening-guidelines-for-average-risk-women.html#:~:text=The%20American%20Cancer%20Society%20recommends,to%20have%20a%20mammogram%20every

[3] https://www.breastcancer.org/symptoms/understand_bc/statistics

[4] http://www.cancer.org/cancer/breast-cancer/index

[5] https://www.researchgate.net/figure/Architecture-of-the-proposed-system-for-breast-cancer-detection-and-classification_fig1_320172774

[6] https://www.researchgate.net/figure/Flowchart-of-the-methodology-used-in-this-study_fig1_320172774

[7] https://www.ncbi.nlm.nih.gov/books/NBK9962/

[8] DMIA 2016 Secondary IEEE Int Symp Biomed Imaging. doi: 10.1109/isbi.2016.7493240.

[9] Sickles EA, Wolverton DE, Dee KE. Performance parameters for screening and diagnostic mammography: specialist and general radiologists. Radiology. 2002 Mar;224(3):861-9. doi: 10.1148/radiol.2243011390. PMID: 12202726.

[10] Mahesh Pattabiraman, Nitin VR, Raj. Breast mammography as a potential non-invasive method in the early detection of cancer. A review. June 2015. Journal of Medicine in Medicine and Biology 15(02). DOI: 10.1142/S0219519415500049

[11] R.Y. Ng, A review of mammography in assessing non-palpable abnormalities in the breast before. International Journal of Thermal Sciences Volume 48, Issue 5, May 2009, Pages 849-859

[12] https://www.cancer.org/content/dam/cancer-org/research/cancer-facts-and-statistics/breast-cancer-facts-and-figures/breast-cancer-facts-and-figures-2019-2020.pdf

[13] Segundo L, Nichols A, Bhatia Sen RK, Rodrigo K, Castaneda N, Zavaleta M, Sobrevilla P, Quispe A, Beltran B, Martinez-Tineo JA. Detection of breast cancer from thermographs images. International Journal of Engineering and Advanced Technology. 2019; 2161 - 8305. Volume 8 Issue 6, August 2019

[14] Tsochatzidis L, Costaridou L, Pratikakis I. Deep learning for breast cancer diagnosis from mammograms—a comparative study. J Imaging. 2019 Nov 22;5(12):37. doi: 10.3390/jimaging5120037. PMID: 34460448; PMCID: PMC8321080.

[15] Mahdi Abunasr, Nidhi Mishra, Ahmed Elaksa, Debarun Bhattacharjee, Anupam Dutta Deep Learning for Mammogram Breast Cancer Detection and Classification. International Conference on Innovative Computing and Communications Lecture Notes in Networks and Systems, vol 56. Springer, Singapore. https://doi.org/10.1007/978-981-10-3332-4_41

[16] Ahmed Al Rahal, Ayman Mohamed and Tarek Kang, Mammography: breast cancer risk assessment and clinical decision making with mammographers. Biomedical Research (2018) Volume 29, Issue 20

[17] Mohamed Meselhy Eltoukhy, Ibrahima Faye, Brahim Belhaouari Samir, A statistical based feature extraction method for breast cancer diagnosis in digital mammogram using multiscale decomposition, Computers in Biology and Medicine, Volume 42, Issue 1, 2012, Pages 123-128, ISSN 0010-4825, https://doi.org/10.1016/j.compbiomed.2011.11.004.

[18] M. H. Yap et al., "Automated Breast Ultrasound Lesions Detection Using Convolutional Neural Networks," in IEEE Journal of Biomedical and Health Informatics, vol. 22, no. 4, pp. 1218-1226, July 2018.

[19] Arevalo J, González FA, Ramos-Pollán R, Oliveira JL, Lopez MA. Representation learning for mammography mass lesion classification with convolutional neural networks. Comput Methods Programs Biomed. 2016 Jan;127:248-57. doi: 10.1016/j.cmpb.2015.12.014. Epub 2016 Jan 6. PMID: 26775139.

[20] S. D. Olabarriaga and J. C. Wolbers, "Estimation and classification of breast cancer tissue digital mammograms using RF and RF-ECOC algorithms," 2017 Computing and Electrical Engineering (ICCEE), Dhaka, 2017, pp. 1-6.

[21] S. Hayes and D. Gross, "Comparison of supervised learning algorithms for 3D breast cancer detection," 2017 Computing and Communication Workshop and III Conference (CCWC), Las Vegas, NV, 2017, pp. 1-6.

[22] Kumpala, Nida Rahmani-Hakkh, et al. "Breast Cancer Diagnosis with Transfer Learning and Global Pooling." 2019 International Conference on Information and Communication Technology Convergence (ICTC), 2019, 819-824.

[23] Wei-Min Yin, Guang Ruyang, Classification of Breast Cancer Histology Images Based on Adaptive Sparse Self-Coding Neural Network, American Journal of Science, November 2018.

[24] Steven Eschrich and Nicholas Chrisman, Breast Deep Learning with Discriminative Ensemble of Histological Scoring & Classification, Stanford University for Biomedical Imaging & Computational Neuroscience, ICASSP 2014-2014 IEEE

[25] Arnaldo Rec, Rebecca Hornik, DeVon Middleton, Mia Morgan, Radiologist system for Computer-aided Power Planning using deep learning, Computerized Medical Imaging and Graphics, Volume 71, January 2019, Pages 90-115

[26] Jiaxuan Wu, Chengyi Hao, Tony Learning model based deep learning Hospital Medical Image classification, 2017 IEEE 2nd International Conference on Cloud Computing and Big Data Analysis

[27] Rajesh KS, Dornfeld D, Beckwith JC, et al. Concordance between surgeon and pathologist assessment of breast carcinoma in-situ in the National Surgical Breast and Bowel Project. J Med Imaging (Bellingham). 2017;4(1):015501. doi:10.1117/1.JMI.4.1.015501

[28] Nizar A. Ayoub, Luai S. Alzoubi, Caroline Peterson, Jun Luyang Wang, Ercan Gucer, Data Sociological Cluster Classification using Computational Intelligence (IC-ICCI'11)

Evaluation of Pullout Resistance of Reinforcing Strips Embedded in Cement Modified Marginal Backfill of Mechanically Stabilized Earth (MSE) Walls

Pradip Kore[1(✉)] and Gunavanthi Venkata Prasad[2]

[1] Civil Engineering, Jain Vishwa Bharati Institute of Engineering and Technology, Hyderabad, India
pradip.kore@gmail.com
[2] Civil Engineering, S. R. Engineering College, Warangal, India
prasadmanchikatla@yahoo.co.in

Abstract. Pull-out resistance of reinforcing materials is one of the internal stability criteria in Mechanically Stabilized Earth (MSE) construction. The pull-out resistance is normally ratio and taking the friction coefficient equal to unity. Finding the capacity of internal reinforcement or of rigid reinforcing materials. For flexible reinforcing strips, the friction coefficient cannot be directly measured in the laboratory, several empirical functions made by various researchers to evaluate suitable pull-out parameters. However, the complexity increases while the use of marginal backfill soils. However, suitable soils are not available. The present work is an effort to determine the pull-out parameters of different types of reinforcing materials embedded in marginal backfill and without and with cement modifications. The testing was carried out in laboratory using a test tank and in the field by constructing model embankments. The pull-out factors F^* and α as suggested by FHWA were evaluated using the test data and compared them with those obtained using conventional sand backfill.

Keywords: Mechanically Stabilized Earth · Marginal soil · Cement modification · Geotextile reinforcement · Pull-out resistance

1 Introduction

Mechanically Stabilized Earth walls gained prominence in place of conventional retaining walls in view of the inherent advantages of soil systems. These walls consist of free draining frictional backfills reinforced with suitable materials having connected to facing units. Though the criterion for standard backfill is specified, at several work sites, such materials are not available in accordance and hence, the use of locally available marginal backfills is reported by various investigators (Saran 2006; Long et al. 2007). With this soils from standard backfills, few failures of reinforced soil structures were reported (Farag 2004; Abu-Zeineh et al. 2007). It is reported that majority of failures were attributed to the use of poor quality backfills with high plasticity and low permeability (Bergado et al. 2001; Hayashi et al. 1999; Gandhisiri

© Springer Nature Switzerland AG 2020
S. C. Satapathy et al. (Eds.): ICETE 2019, LNLS 2, pp. 234–247, 2020.
https://doi.org/10.1007/978-3-030-03348-3_20

Effect of Eccentric Load on Footing Resting on Planar Geosynthetic Reinforcement

Pratik Kute[1(✉)], M. Hanifa[2], and T. S. D. Venkatesh[2]

[1] Department of Civil Engineering, Sri Indu Institute of Engineering and Technology, Hyderabad, India
pratik.kute@gmail.com
[2] Department of Civil Engineering, NIT Warangal, Hanamkonda, India

Abstract. A structural foundation transmits all the loads from the superstructure to the soil underneath safely. But in earthquake or wind loading, the line of action of total load from the superstructure does not pass through the center of gravity of the footing resulting in eccentric loading. The compensation for reduction of the bearing capacity by increasing the size of footing is uneconomical. Geosynthetics can be used to improve the bearing capacity of the footing. In the present study a series of tests were conducted and comparative study is made when Geotextile (Bonar G-120) is used as planar reinforcement to improve the bearing capacity of sand. Also the improvement of bearing capacity in accordance to eccentricity was studied. The test results indicate that there is significant improvement in the bearing capacity and reduction in the settlement by providing planar reinforcement until the eccentricity is 0.1 times the width of footing.

Keywords: Planar reinforcement · Eccentric loading · Bearing Capacity Ratio

1 Introduction

Earth provides the ultimate bearing support for all the civil engineering structures like buildings, bridges, reinforced fills, earthen embankments and concrete dams. Hence the behaviour of the bearing ground defines the stability of whole structure. Hence the structural foundation should be able to transfer the load from superstructure such that the overstressing of soil underneath is avoided besides preventing the excessive settlement of structure. If line of action of the load does not pass through the center of loaded area, the contact area decreases. The reduction in contact area results in the reduction of effective width of footing resulting in decrease in bearing capacity of supporting soil [3]. Eccentric loading of footing can occur in exterior column footing or due to earthquake or wind loading.

Several studies conducted on eccentrically loaded footing and bearing capacity improvement using geosynthetics and found that significant bearing capacity improvement can be achieved using geosynthetics so that the reduction of load carrying capacity due to the eccentricity of the footing can be compensated [1, 3, 4]. Geosynthetics can be used to improve the load carrying capacity [5, 6]. Though there are many types of geosynthetics, a non-woven geotextile is used in this study to find the effect of

S. C. Satapathy et al. (Eds.): ICETE 2019, LAIS 3, pp. 181–192, 2020.
https://doi.org/10.1007/978-3-030-24322-7_23

Study on Interaction of Reinforcing Strips Embedded in Cement Modified Marginal Backfill

Pavan Kumar[1(✉)], Vinoth Reddy Kamal[2], and Sheershal Mudavath[2]

[1] Department of Civil Engineering, Sri Indu Institute of Engineering and Technology, Hyderabad, India
[2] Department of Civil Engineering, NIT Warangal, Hanamkonda, India

Abstract. Pullout resistance of reinforcing materials is one of the keenest stability considerations in Mechanically Stabilized Earth (MSE) construction which is normally constructed using the locally available granular soils. Owing the angle of internal friction in case of rigid reinforcing materials like flexible/extensible reinforcing strips, the friction coefficient cannot be directly taken and in this direction, several attempts have been made by various researchers to evaluate suitable pullout parameters. Further, the complexity increases within the use of marginal backfill soils whose suitable uses are not available. The present work aims at determining the pullout parameters of different types of reinforcing materials embedded in marginal backfill soil with/without cement modification. The testing was carried out in laboratory using a steel box. The pullout factors F and α as suggested by FHWA were determined using the test data.

Keywords: Mechanically Stabilized Earth · Marginal soil · Cement modification · Geotextile reinforcement · Pullout resistance

1 Introduction

MSE walls gained prominence in place of conventional retaining walls in view of the inherent advantages of such systems. These walls consist of free draining frictional backfills reinforced with suitable materials connected to facing units. Though the criterion for standard backfill is specified, at several work sites, such materials are not available in abundance and hence, the use of locally available marginal backfills is resorted by various investigators [1, 12]. With this shift from standard backfills, few failures of reinforced soil structures were reported [1, 14]. It is reported that majority of failures were attributed to the use of poor quality backfills with high plasticity and low permeability [2, 3]. Few attempts were also made by investigators to overcome the ill-effects of marginal backfills by the use of electro-kinetic dewatering [5], preloading and unloading and the use of nonconventional materials [15]. The researchers have also studied the efficacy of cement modification of marginal soils for their use in reinforced soil structures [13] by conducting load tests on model embankments. In order to evaluate the design parameters for internal stability in case of cement modified backfills, an

K. C. Narasimhaiah et al. (Eds.): ICGTE 2019, LNCE 2, pp. 423–430, 2020.
https://doi.org/10.1007/978-3-030-27194-0_37

Resilient Modulus of Unsaturated Soil – A Comprehensive Review

A. G. Shivaraj[1(✉)], M. Hanu Lal[1], and Pandu Kore[2]

[1] Department of Civil Engineering, National Institute of Technology, Warangal, India
[2] Department of Civil Engineering, Sri Indu Institute of Engineering and Technology, Hyderabad, India

Abstract. Unsaturated soil is a three-phase system which has the property to show significant changes in its strength and stiffness with varying moisture content. Compacted pavement soil is in the unsaturated state thus exhibiting the tendency to weaken or strengthen with varying moisture contents. With ever changing vehicular loading conditions, the necessity to study the dynamic behavior of pavement materials in the design of pavements have been validated in numerous research works. Thus the elastic modulus of pavement material have been incorporated as a key parameter in MEPDG. In-service condition of the compacted soil presents the ability to exhibit changes in strength with seasonal moisture variation. This paper is intended to summarize the findings and the necessity to understand the pore-compaction-moisture variation and their influence on the mechanical property of pavement materials. Furthermore, the investigations on granular subbase and subgrade material have been provided by briefly describing some of the findings and information. However, the present work aims at the comprehensive information to be updated as available correlations in this.

Keywords: Unsaturated soils · Soil suction · Degree of saturation · Compacted subgrade · Resilient modulus · Repeated load triaxial test

1 Introduction

With the rapid progress of cities, the areas farther inland is developed to accommodate the increasing population. The behavior of soil in areas of low or moderate rainfall fall in the category of unsaturated or partially saturated soils. The soil is represented as a two-phase system with solid and liquid, whereas the unsaturated soil mechanics considers the soil as a four-phase system in most of the cases with air and air-water interface in count [1]. The geotechnical engineering practice dealing with these soils is still ingrained in conventional soil mechanics [1]. Pavement infrastructure is predominantly located on unsaturated soils and the compacted subgrade soil also resembles that of unsaturated soil. Thus the stability of soil to shrink or deteriorate with varying moisture content leads to alter the property of the pavement material which in turn influences their mechanical behavior.

S. C. Satapathy et al. (Eds.): ICETE 2019, LNNS 2, pp. 141–148, 2020
https://doi.org/10.1007/978-3-030-01143-5_19

Advances in Industrial Automation and Smart Manufacturing pp 69-78 | Cite as

Evaluation of Material Properties and Abrasive Resistance of Tantalum Carbide-Based Hardox Steel for Construction Purpose

Authors Author and affiliations

P. S. Senthil Kumar, S. Harichurn, C. Shalarathan, [illegible] V. Dhinakaran, I. Satyanarayana

Conference paper
First Online: 31 October 2020

Part of the Lecture Notes in Mechanical Engineering book series (LNME)

Abstract

In recent days, the demand of high strength and wear resistant steel has been increased. The

Evaluation of Material Properties and Abrasive Resistance of Tantalum-Carbide-Based Hardox Steel for Construction Purpose

[redacted]

[redacted]

Abstract

In recent days, the demand of high strength and wear resistant steel has been increased. The

Effect of Diethyl Ether on LHR Engine Characteristics using Papaya Methyl Ester-Eucalyptus Oil Blend

C.Sivakandhan[1], R. Silambarasan[1], I.Satyanarayana[2], P.Vijay Kumar[3], M.V.B.Kalyan[3].
[1]Department of Mechanical Engineering, Sri Indu Institute of Engineering and Technology, Hyderabad.
[2]Department of Mechanical Engineering, J.K.K.Nattraja College of Engineering and Technology, Kumarapalayam.

The present experiment deals the study of addition of diethyl ether on the performance and emission characteristics of LHR engine using papaya methyl ester-eucalyptus oil blends. The test blends are CPME30Eu70 (Carica papaya methyl ester 30% and Eucalyptus oil 70%), CPME30Eu70+10%DEE and diesel. The optimum results we get with presence of DEE in CPME30Eu70 in LHR engine. The presence of DEE creates a lean mixture and its low viscosity, high cetane number and volatility improves performance for a large degree. The graph depicts that addition of 10% diethyl ether gives the best performance in BSEC, BSFC, BTE and emission wise when coupled with LHR engine. Most notably NOx emission rate is decreased by the presence of the DEE and BSFC is brought under acceptable limit. BSEC decreases in CPME30Eu70+10%DEE and betters the performance of diesel in conventional engine. It also said to improve the cold flow properties of the CPME-eucalyptus oil blend.

****

The Institution of Engineers

Hosur Local Centre

Certificate of Participation

This is to certify that Mr/Ms C. Sivaramakrishnan, SJBIT has participated in the 35th National Convention of Mechanical Engineers & National Conference on Trends & Developments in Automotive Industry during 4th & 5th September 2019.

Dr. V. MANIVASAGAR, MIE
HONORARY SECRETARY

Dr. J. ARIVUDAI NAMBI, FIE
CHAIRMAN

The Institution of Engineers

Hosur Local Centre

Certificate of Participation

This is to certify that Mr/Ms T. SATYANARAYANA, SITE has participated in the 35th National Convention of Mechanical Engineers & National Conference on Trends & Developments in Automotive Industry during 4th & 5th September 2019.

Dr.V.MANIVANNAN,MIE
HONORARY SECRETARY

Dr.J.ARUNDAI NAMBI,FIE
CHAIRMAN

PRINCIPAL
Sri Vidyanikethan Institute of Engineering & Tech.
Sriramapuram, Tirupati-517502
A.P. (Dist.) Telangana State

The Institution of Engineers

Hosur Local Centre

Certificate of Participation

This is to certify that Mr/Ms P. VIJAY KUMAR, S1187

has participated in the 35th National Convention of Mechanical Engineers & National Conference on Trends & Developments in Automotive Industry during 4th & 5th September 2019.

Dr. V. MANIVASAGAM, MIE
HONORARY SECRETARY

Dr. J. ARIVUDAI NAMBI, FIE
CHAIRMAN

PRINCIPAL
Sri Indu Institute of Engineering & Tech.
Sheriguda (V), Ibrahimpatnam (M),
R.R. Dist. Telangana-501 510

The Institution of Engineers (India)

Hosur Local Centre

Certificate of Participation

This is to certify that Mr/Ms [redacted] has participated in the 35th National Convention of Mechanical Engineers & National Conference on Trends & Developments in Automotive Industry during 4th & 5th September 2019.

Dr. V. MARIVARADAN, MIE
HONORARY SECRETARY

Dr. J. ARIVUDAI NAMBI, FIE
CHAIRMAN

PRINCIPAL
[illegible] Institute of Engineering & Tech
Sheriguda(V), Ibrahimpatnam(M)
R.R. Dist. Telangana -501 510

SANTHIRAM ENGINEERING COLLEGE

Springer

(Approved by AICTE, New Delhi, Permanently Affiliated to JNTUA, Anantapuramu)
(An ISO 9001 - 2015 certified Institution, 2(f) & 12(B) recognition by UGC ACT 1956)
NH-40, NANDYAL – 518501 :: Kurnool Dist. A.P.

2nd International Conference on
Advances in Industrial Automation & Smart Manufacturing

ICAIASM 2019

Certificate of Recognition

This is to certify that Prof./Dr./Mr./Ms. _____

from Dept of Mech, SNIST- Hyd has presented / participated in the ICAIASM 2019 with his/her research paper titled Taguchi's optimization of ASDM process parameters on Aluminium hybrid Composite and/or Santhiram Engineering College, Nandyal, Andhra Pradesh, India during 26th & 27th July 2019.

Dr. Ramesh Raju
Organizing Secretary

Dr. M.V. Subramanyam
Convener & Principal

2019 International Conference on Vision Towards Emerging Trends in Communication and Networking (ViTECoN)

Testing and Implementation of Smart Brake Pedal System with Signal Diagnostic and Failure Detection

Anmol Tiwari
M. Tech Embedded Systems
Vellore Institute of Technology
Vellore, India

Prof. B. Karthikeyan
School of Electronics Engineering
Vellore Institute of Technology
Vellore, India

Dr. S. Suresh
Dept. of Electronics Engineering
Sri Indu Institute of Engineering and Technology
Hyderabad, India

Abstract— Brake pedal signal diagnostic is an important feature in driver assistance system. The primary aim of implementing this feature is to avoid any false detection of brake pedal signal. It also provides information to the driver regarding brake switch failure. Along with proper implementation it is necessary that the feature is tested thoroughly in order to make it full proof before it's usage in vehicle. The code for this feature is written in embedded C language. National Test Real Time (RTRT) and Polyspace tools are used for testing of this feature. The project focuses on implementation and testing of Brake Pedal Signal Diagnostic in vehicle.

Keywords— Brake pedal signal diagnostic, Brake switch signal, Fault block, Brake light switch diagnostic, Low fault condition, High fault condition, switch.

I. INTRODUCTION

Brake pedal signal has to be correctly diagnosed in vehicles. It assists the driver in case of situations where the brake switches have failed or wrong signals are being generated. It is an important safety aspect in each vehicle. Accurate detection of brake signals as well as any failure in brake switches can avoid any kind of casualty (Jo Hwan et al., 2011). This feature aims at detecting brake pedal signals under high fault and low fault conditions. Requirements are given by the customer, depending on which the apse author will develop the specification document. Once the specification document has been developed the code to implement the same has to be developed. In the next phase the developed code has to be tested. In the testing phase any flaws in the code will be caught. The test reports will be generated at the end. These reports will be analyzed in order to confirm the errors are valid issues or not. In case of valid errors, the code needs to corrected and again testing of the same is carried out. Once the testing reports are without any Defects the code will be sent for validation phase. After the validation of the code it will be sent to the production phase. The software development follows V model. This model defines the different stages of development. The name is given because of the typical process that is being followed during the software development phase. This model shows how each stage in the development has been related to each other thus giving a clear picture of software development.

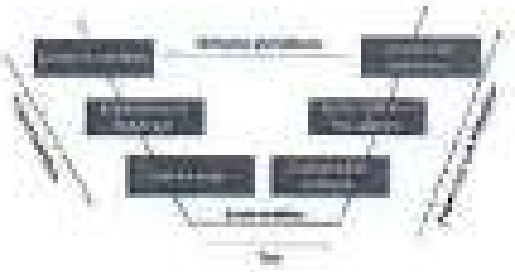

Fig. 1 V-model of System Engineering Process

II. V-MODEL

"Fig. 1", shows the V-model that is being followed in an automotive industry. As said earlier it shows the different stages of software development (i.e, Ramesh et al., 2016). The different stages are shown in the figure and the explanation is given below.

A. Verification Phase

1. Requirement analysis

In this phase the customer requirement for brake pedal feature were collected. This was done by examining the needs of client. This document contains the features expected feature, functionality, data, performance etc. (Liu and Peng, 2008)

2. System design

In this phase the requirement document is studied and ideas are proposed to implement the same. If any of the requirements can't be implemented then it has to be informed to the customer at this phase.

3. Module design

This phase is said to be low level design. Here the design of the system is split into smaller units. This will help in making the programmer aware about the requirement of each smaller unit. The code idea after understanding the requirement can start programming.

B. Validation phase

1. Unit testing

The same code that has been developed is divided into many small modules or programs that can work individually. These are tested to find any bugs. These bugs can be rectified at the unit level and later the smaller

978-1-5386-8353-7/19/$31.00 ©2019 IEEE

tested module or can be integrated (Alexander Schaefermeier et al., 2017).

2. Integration testing

This test will give confirmation that the individual codes can be integrated and are able to communicate without any issues (Johannes et al., 2017).

3. System testing

This testing plan will be developed by the client. The test is made to make sure that the developed functionality meets all the requirements of client. This test confirms that both functional and non-functional requirements have been met (Nidd J. et al., 2007).

4. User acceptance testing

This test plan will confirm that the functionality that has been developed and validated meets client requirements and is ready to be used in real time (Ahmad et al., 2008).

III. IMPLEMENTATION

Fig. 2 Process flow of the system

The code for this feature has been developed in three stages and its flow is depicted in "Fig. 3"

A. Brake switch operational

In the first stage a check is done to make sure that the brake switches have been powered. This check forms the base of this functionality (Mitra Jo et al. 2017). Only when the brake switches are powered signals can be generated and can be used for further analysis. Basically two switches are used, the second switch is used as a backup. In case the brake switch is not working properly or has failed due to some reasons and the driver is unaware except the sensor then the backup switch will detect this. The logic is that both the switches should give the same signal in one instance. If this doesn't happen then the switch needs to be checked. Both the switches are given recovery time. Recovery time is the time given to the sensors to detect and send the signals. If the signals are not received even after the recovery time, then a check on the brake switches needs to be performed.

B. Brake switch diagnostic

The second stage that is brake switch diagnostic can be further sub divided in three more stages as shown in "Fig. 3". Namely brake diagnostic condition, brake light switch diagnostic and brake safety switch diagnostic.

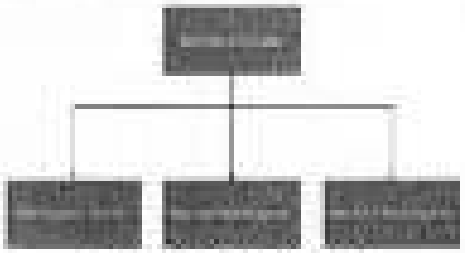

Fig. 3 Brake Switch Diagnostics

1. Brake diagnostic condition

Several signals are built depending on vehicle speed and pedal position thresholds in order to perform pedal diagnostics. Sensors will sense the speed of the vehicle and the angle of accelerator pedal. Based on both these parameters signals are generated which are further used for diagnosis of the fault signal. If the automatic brakes or the ESP fluid pressure control are activated by the Vehicle Stability Assistance, then brake diagnostics could be frozen to avoid misdetection.

2. Brake light switch diagnostic

The brake light diagnostic fault condition is set if the brake light switch operational is stuck or fails during the following conditions:

- Vehicle speed is decreasing from 45km/hr to 0km/hr.
- No automatic brake activation.
- Previous conditions to prevent the counter for diagnostics is enabled when this counter becomes higher or equal to specified value.

3. Brake safety switch diagnostic

The fault brake light during high fault condition is set if brake light switch operational is stuck to true during specific conditions:

- Vehicle speed is higher than 20 km/hr
- Accelerator pedal is pressed (1 to 5 percentage)
- Previous conditions to prevent the issue.

The diagnostic is enabled when this issue becomes higher or equal to specified value.

If brake light switch operational is detected to false during more than the maximum brake light off time in the driving cycle the result of the diagnostic is considered to be okay, and the flag is enabled to set the readiness flag. As soon as the readiness flag is set, the fault is frozen until the next key off/on. Brake safety switch acts as back up for the brake light switch. Its implementation is similar to brake light switch (Richard et al., 2017).

IV. RESULTS

Code implementation of some blocks and verification results are as shown below:

A. Brake switch operational

Code implementation of brake switch operational was implemented as shown in "Fig. 4". In the below part

of the code a check is done to make sure that the brake status of the vehicle is working perfectly.

Fig. 4 Logic of Brake Switch Operation

8. Chronometer (Low fault condition)

Chronometer is used to measure time. The chronometer will have two conditions (e.enable and reset based on which the output will be produced. The output produced will be in the units of time. Initially the reset condition will be checked. If reset is true the chronometer output will be zero. The chronometer will start giving the output in units of time when the enable condition is true. Chronometer macro will be having three parameters one for the timer, second is enable condition and the third parameter is previous value of outside conditions. When the previous enable is true then only chronometer will produce the output irrespective of the current enable conditions. "Fig. 5" shows the code snippet of chronometer under low fault condition.

Fig. 5 Code snippet of Chronometer (Low fault condition)

C. Verification Results

Verification results are as shown below in "Fig. 6".

Fig. 6 Verification results of RTRT

V. Conclusion

The competition in automotive industry has increased recently with the increase of electronics in vehicles. This has made it important that proper testing and validation is being done. The electronic system in vehicles is critical because of the passenger's safety. This emphasizes the importance of testing along with the correct feature implementation. In this project the implementation of code based on the feature requirement has been done. After implementation of the code it was moved to testing phase. here RTRT and polyspace tools were used for testing purpose. The polyspace tool was used for static analysis of the code. It gave information regarding potential problems in the code which would have occurred during run time. Division by zero, range overflow, underflow in some of the real time problems examples. The IBM's RTRT tool is a dynamic testing and where the code was tested by writing different test strategies and varying the inputs accordingly. The testing ensured that the code is error free will be sent for validation phase.

VI. Future Work

Time is the main constraint across different organizations. A developer and tester lacks the time to implement and test any feature from the client side. On time deliver is the top priority because of the intense competition from other organizations and the dynamic market requirements. Implementation of the feature i.e. writing codes and testing can be automated. Scripts can be written to automate this process in such a way that minimal human intervention is needed. This will help in delivering the feature on time to the customers. It will also save the cost.

REFERENCES

[1] de Groot, S., de Wilde, J.C., Mulder, N. and Wieringa, P.A., 2011. On racing in a simulator: Validation and assessment of three point airborne Reserve Teleoperators and Virtual Environments, 2011, pp.17-61.2 Klark Maxwell, A Treatise on Electricity and Magnetism, 3rd ed., vol. 2. Oxford: Clarendon, 1892, pp.68-73.

[2] Liu, H., Zhang, H. and Zhu, S., 2011, December. An incremental V-model process for automotive development. In Software Engineering Conference (APSEC), 2011 18th Asia Pacific (pp. 225-232). IEEE. Elsa, "Title of paper if known," unpublished.

[3] Schoemaker, A., Rauh, A., Hinterseer, S., Hecke, T., Rauhala, R. and Bohl, J., 2012. New validation of vehicle components in virtual models for intelligent Vehicles Symposium (IV), 2012 IEEE (pp. 409-414). IEEE.

[4] Jia, M., Rauh, V., Lau, S. and Xia, X.H., 2007, March. Performance Analysis of Hybrid Fusion Models for Brake Pedal in a Brake-by-Wire System. In Advanced Information Networking and Applications (AINA), 2011 IEEE 21st International Conference on (pp. 177-183). IEEE.

[5] Jingying, L. and Ling, F., 2008, August. The research of V model in testing embedded software. In Computer Science and Information Technology, 2008. ICCSIT'08. International Conference on (pp. 461-464). IEEE.

[6] Abdulkadeem, A., Jiguang, H. and Youssef, N., 2010. A New Platform for Rapid Prototyping of Brake-By-Wire Systems: Experimental Validation Using Real-Time Hardware-in-the-Loop. SAE International Journal of Passenger Cars-Electronic and Electrical Systems, 3(2010-01-2294), pp.1-8. A Case Study of ISO Chevrolet Volt 2nd Generation. IEEE Transactions on Vehicular Electronics.

[7] Li, N., Hyde, D.W., Zhang, M., Fidler, S., Rabinovitch, I. and Strand, S.R., 2013. Considerations in modeling of driver and vehicle characteristics for validation and calibration of autonomous vehicle control systems. IEEE Transactions on control systems technology.

Face Detection Based Automation of Electrical Appliances

S. V. Lokesh[1(✉)], B. Karthikeyan[1], R. Kanna[2], and S. Sarol[3]

[1] School of Electronics Engineering, Vellore Institute of Technology, Vellore, India
lokeshsangam@gmail.com, bkarthikeyan@vit.ac.in
[2] Electronics and Instrumentation Engineering, NIT Nagaland, Dimapur, India
ee.rajagopal.kanna@nitnagaland.ac.in
[3] Electronics and Communication Engineering, Sri Indu Institute of Engineering and Technology Sheriguda, Hyderabad, India
sri.ts2sarma@gmail.com

Abstract. This paper addresses the problem of automation of electrical appliances with the use of sensors. The proposed method uses Viola-Jones method a real time face detection algorithm for controlling the electrical appliances which are part of our day to day life. A detector is initialized by Viola-Jones based face detection algorithm automatically without the need for any manual intervention. After initializing the detector, the position where the face detected is compared. The region captured by the camera is split into four different regions. Based on the position of the detected face the electrical appliances subjected to that particular region can be controlled.

Keywords: Face detection · Viola Jones · Split to four regions visually

1 Introduction

With the growth in the field of electronics, constant efforts have been made to automate various day-to-day tasks. One of these tasks is the automation of electrical appliances. This can be accomplished using GSM which requires the users to check the status of the appliances through mobile phones when they step out, or it can also be done through voice commands [12]. However this is still subjected to errors as it requires human effort and is not completely automated. Another way of controlling electrical devices is through the use of sensors [13] which provides complete automation, however the poor responsiveness of the sensors and complexity of network troubleshooting brings down the efficiency of the entire system.

Due to the drawbacks posed by the already existing methods, this paper proposes automation of electrical appliances by using face detection. The simplicity of the circuit involved, the wide coverage range and a fully automated setup ensures power efficient control of appliances. Face detection is used to compute the size and identify the position of the face in a given input image. The background information are ignored and only the facial feature from the image are detected. From the detected face we can able to predict the age of the person, gender, facial expression etc. in general terms face

S. Smys et al. (Eds.): ICCVBIC 2019, AISC 1108, pp. 204–212, 2020.
https://doi.org/10.1007/978-3-030-37218-7_23

detection is to localize the face in the given input image. Localization helps to know the amount of faces and where the faces are detected in the image.

2 Related Work

This section addresses few techniques which are used for computer vision face detection.

Detection based on skin colour segmentation aims at analysing the visuals in different colour spaces and identifying the face with certain threshold values [14]. The different colour spaces that have been widely used are YCbCr, HIS and binary and some works have proposed the combination of different spaces to threshold the facial features. However this method can be efficient for stationary images but not for real time video streams.

The second section involves feature extraction for object detection using features from SMQT. In order to increase the computation of SNOW classifier, the classifier is divided into multiple stages on which a single classifier is trained to form a weak classifier and these weak classifiers are combined to form a strong classifier in cascade which help in face detection [1].

Neural network consists of perceptron which are artificial neurons are available in multiple layers and are connected to each other. Perceptron network are under semi-supervised learning and no kind of programming is required [2]. Perceptron network composes of a threshold function or summation function. Face detection using neural network is determined by checking whether the detected region is face or not at a small window level. It is not necessary to train with non-face images and thus computational speed is also reduced [3]. Face detection using neural network composes of two steps. A part of image of 20 * 20 size is fed to the neural network as input in the first step. The output of the filter determines whether the detected region is face or not a face. In the second step the efficiency of the overall neural network is increased by fusing all the single neural network to find the overlapping detections and this reduces the false detections.

Maximum hyperplane or set of hyper planes in an infinite dimensional space is constructed using a supervised learning model which groups the information in two classes and separation is from two categories is through the hyperplane [4]. The area between hyper plane and closest data points is called the margin. Data points that exists on the margin boundary of the hyper plane are called as support vectors. This method can be applied for object detection then the object can be assumed from positive samples and non-object classes are from the negative samples.

The kernels can be of type polynomial kernels or radial kernels. The main difficulty lies is finding the appropriate kernel for the given problem. The selected kernel is used for the classification of problems and the results produced by them may not be good when compared to the result produced from sample set. They are used in application like detection of pedestrians. Haar wavelets are applied on samples which are positive as well as negative to extract features and they are helpful in discrimination of classes [5].

3 Proposed Method

3.1 Face Detection

The face detection was carried out through Viola Jones Algorithm. Paul viola and Michael jones proposed the algorithm in 2001 [6, 7]. Since this many works have been done using this algorithm [8–11]. It is mainly used for detecting faces in real time rather than object detection. The algorithm is very robust and also the computation speed is less. The main goal of face detection is to distinguish face from non faces. It is the first step in face recognition. The algorithm comprises of four steps which are:

(1) **Haar Feature Selection:** Haar-like features are used in object recognition. Computation of image intensity (i.e. calculation of RGB pixel values from every pixel made the computation to be very slower and expensive. In a human face the nose bridge region is lighter than the eye region etc. Using Haar basis function the properties of face are computed using Haar features. They are rectangular pixels of dark and white regions and the resultant of each haar feature is calculated by subtracting the black pixel count from the white pixel count (Fig. 1).

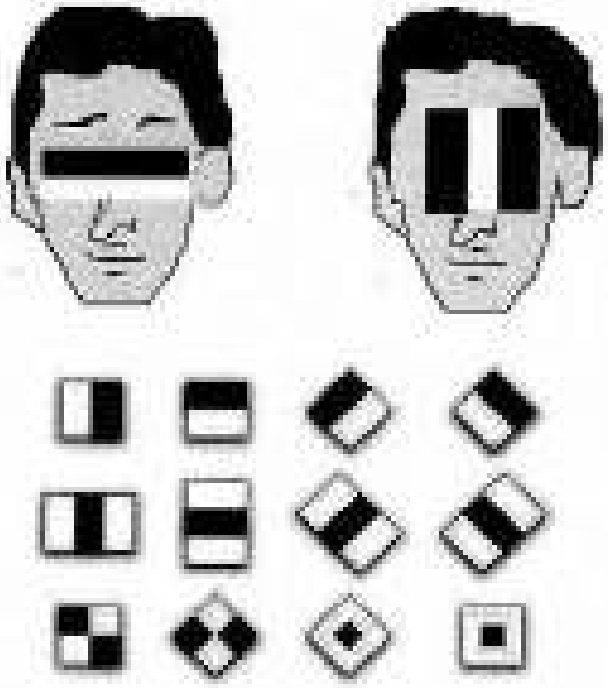

Fig. 1. Haar features

(2) **Creating an Integral Image:** For a faster and effective way for calculating the pixel values we go for integral image. If we have to use integral image we go for the conversion of original image into gray scale image. Computation of adjacent pixel values with respect to the pixel value at (x, y) forms the integral image which helps in speeding up the computation. Integral image is the summation of values

pixels above, left and its own pixel value at (x, y). This is done to make the Haar feature compute efficiently (Fig. 2).

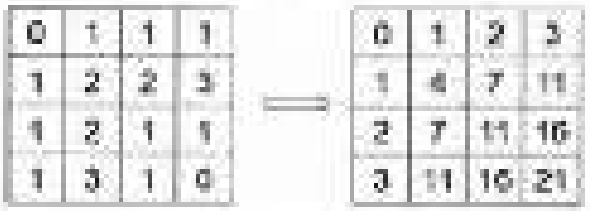

Fig. 2. Integral image

(3) **Adaboost Training:** In order to separate relevant and irrelevant haar like features we go for Adaboost training. Irrelevant features doesn't give any information about the detected image whether it is face not. Relevant features are the features which provide information about face. Relevant features are provided with weights to form a weak classifiers. Adaboost training gives a strong classifiers which we able to say whether the detected image is a face or not a face. These strong classifiers are nothing but a linear combination of all the weighted weak classifiers.

$$f(x) = \alpha_1 f_1(x) + \alpha_2 f_2(x) + \ldots\ldots + \alpha_n f_n(x) \tag{1}$$

(4) **Cascading Classifiers:** Adaboost gives information about the classifiers which will be able say whether the detected image is face or not. Cascade classifiers are used to integrate many classifiers which are useful in neglecting background windows so that more operation are performed on regions where the face is present. Each stage in the classifier consists of distinct sets of face features which is checked step by step for the input video to detect the presence of a face. The strongest classifiers are kept in set 1, so a when the detected image is not a face no need to check for all the classifiers. From the first set of features itself we can be able to predict whether the detected image is face or not a face (Fig. 3).

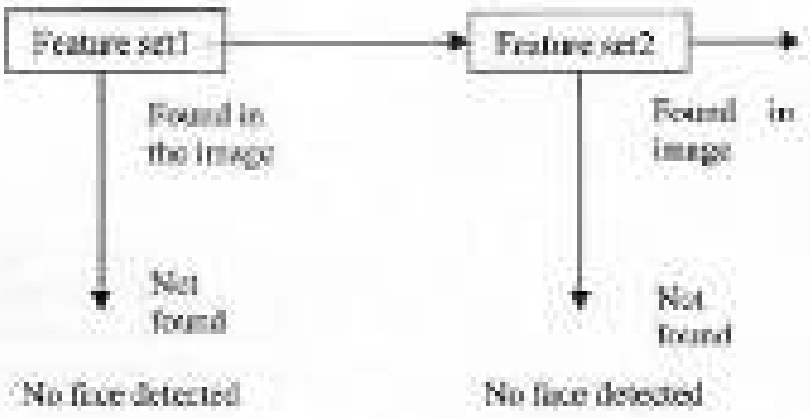

Fig. 3. Cascade classifiers

3.2 Automation of Appliances

Raspberry pi is a microprocessor which is a small size CPU which runs on Raspian OS. It supports cameras as peripherals and hence it is the best choice for this application. Up to three cameras can be connected to a raspberry pi board at a time (Fig. 4).

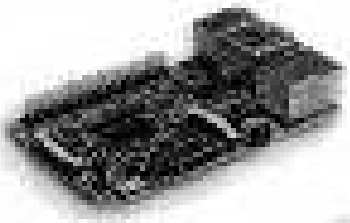

Fig. 4. Raspberry Pi model 3B

The automation of appliances happens by controlling them using a programmed Raspberry pi microcontroller to which a web camera is connected to record the real time video (Figs. 5, 6 and 7).

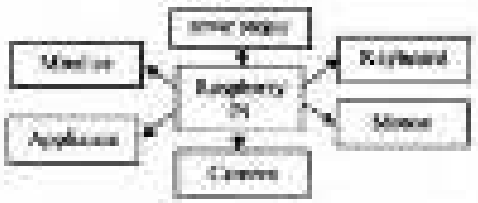

Fig. 5. Block scheme of hardware

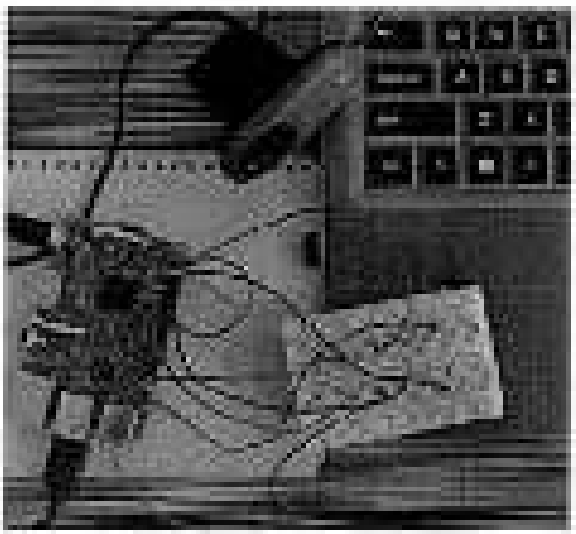

Fig. 6. Proposed system hardware

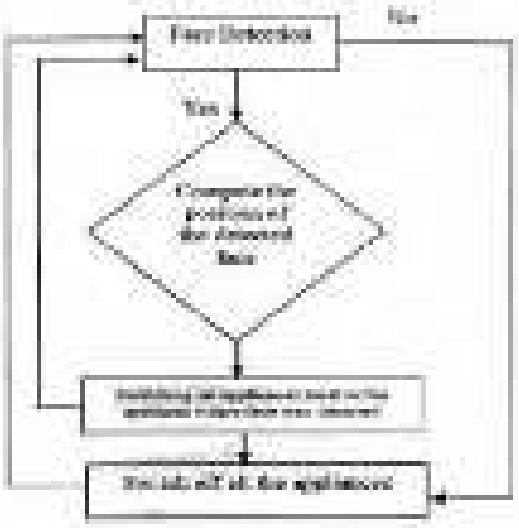

Fig. 7. Design flow of hardware

4 Results and Discussion

OpenCV is an open source computer vision library. The library is written in Python and runs under Raspbian Operating System. The proposed method with Viola-Jones detection was simulated in Python Idle using OpenCV Python library. The simulations were done on Raspberry Pi 3 Model B which has RAM of 1 GB. This system was tested on real time videos captured in laboratory. Video is captured at a resolution of 640 * 480 using a web camera. The video is split virtually into four regions. Each region has specific appliance which will be automated only if faces are detected in that region (Fig. 8).

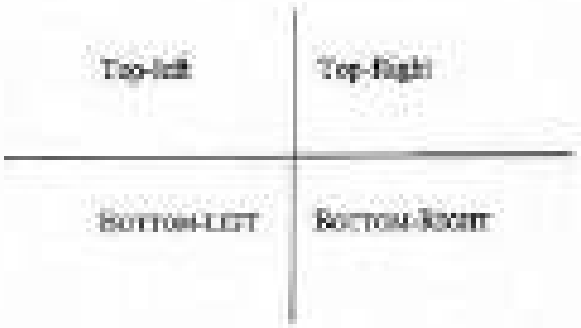

Fig. 8. Region split of a video

Based on the region where the face got detected we can be able to say whether is very close or far to the camera. When camera placed at a certain height from the ground, if face gets detected at the top region we can say that the person is far from the camera since the scale factor of the image will be less. If the image gets detected in the bottom region we can say that the person will be closer to the camera since the scale factor will be high when face gets detected in this region (Figs. 9, 10, 11, 12 and 13).

Fig. 9. Shows the face detected in top left and corresponding led is turned on and rest of the led is turned off.

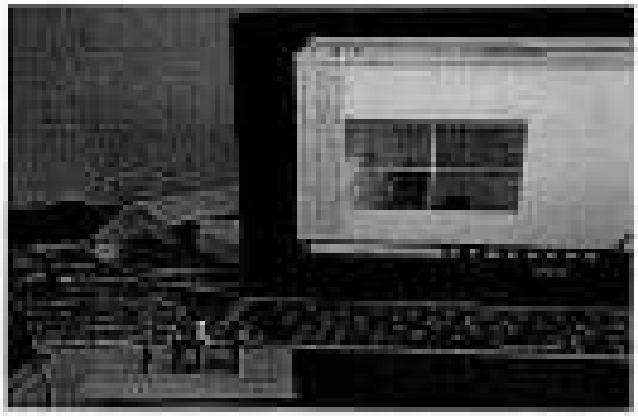

Fig. 10. Shows the face detected in bottom left and corresponding led is turned on and rest of the led is turned off.

Fig. 11. Shows the face detected in bottom right and corresponding led is turned on and rest of the led is turned off.

Fig. 12. Shows the face detected in top right and corresponding led is turned on and rest of the led is turned off.

Fig. 13. Shows all the led turned off when there is no face detected.

The proposed method will help in efficient use of power. The system on the whole covers the drawbacks like human fatigue in conventional manual control of appliances, small coverage area of sensors. The system will have a disadvantage when there is no sufficient light to detect face. The above discussed idea was prototyped using led s. The work will be extended to controlling the device based on face recognition and also integrating the appliances to the system.

Compliance with Ethical Standards

✓ All authors declare that there is no conflict of interest

✓ No human/animals involved in this research work.

✓ We have used our own data.

References

1. Chesnais, L: Face detection using local SMQT features and split up snow classifier. In: 2007 IEEE International Conference on Acoustics Speech and Signal Processing - ICASSP 2007 (2007)
2. Rowley, H.A., Baluja, S., Kanade, T.: Neural network-based face detection. IEEE Trans. Pattern Anal. Mach. Intell. 20(1), 22–38 (1998)
3. Sung, K.K., Poggio, T.: Example-based learning for view-based human face detection. IEEE Trans. Pattern Anal. Mach. Intell. 20(1), 39–51 (1998)
4. Boser, B., Guyon, I.M., Vapnik, V.: A training algorithm for optimal margin classifiers. In: ACM Workshop on Conference on Computational Learning Theory (COLT), pp. 142–152 (1992)
5. Yilmaz, A., Javed, O., Shah, M.: Object tracking: a survey. ACM Comput. Surv. 38(4), 45 (2006)
6. Paul, V., Jones, M.J.: Rapid object detection using a boosted cascade of simple features. In: Proceedings of the 2001 IEEE Computer Society Conference on Computer Vision and Pattern Recognition, vol. 1, pp. 511–518 (2001)
7. Allen, J.G., Xu, R.Y.D., Jin, J.S.: Object tracking using CamShift algorithm and multiple quantized feature spaces. In: Proceedings of the Pan-Sydney Area Workshop on Visual Information Processing. In: ACM International Conference Proceeding Series, vol. 103, pp. 3–7. Australian Computer Society, Inc., Darlinghurst (2004)
8. Jain, V., Patel, D.: A GPU based implementation of robust face detection system. Procedia Comput. Sci. 57, 155–163 (2015)
9. Chaturah, J., Gupta, P., Ahuja, P., Goel, A., Arora, S.M.: Real time human face detection and tracking. In: International Conference on Signal Processing and Integrated Networks (SPIN), pp. 705–710 (2014)
10. Tao, Q.-Q., Zhan, S., Li, X.-H., Kurihara, T.: Robust face detection using local CNN and SVM based on kernel combination. Neurocomputing 211, 98–105 (2016)
11. Di'aze, M., Algaldi, A., Debeir, O.: Face detection using Viola and Jones method and neural networks. In: International Conference on Information and Communication Technology Research, pp. 40–43 (2015)
12. Singh, P., Chandra, K., Pingale, S., Kadam, S.: Smart GSM based home automation system. Int. Res. J. Eng. Technol. (IRJET) 03(04), 1583–1585 (2016)
13. D'mello, A., Deshmukh, G., Motwalkar, M., Tripathi, G.: Home automation using Raspberry Pi 2. Int. J. Curr. Eng. Technol. 6(3), 730–734 (2016)
14. Kong, S., Chen, B., Ju, D.: Faces detection method based on skin color modeling. J. Syst. Archit. 64, 100–109 (2016)

ANTENNA BEAMFORMING AND BEAM CONTROLLING FOR IMPROVING THE WI-FI SIGNAL

K Raghavendra[1], A Swetha[2], S. Naresh[3]
[1]Asst. Professor, Dept. of ECE, Malla Reddy Engineering College for Women(Autonomous), Secunderabad-TS
[2][3]Asst. Professor, Sri Indu Institute of Engineering & Technology, Ranga Reddy-TS
Email: raghu.ster@gmail.com[1], swetha.vidit@gmail.com[2], sreebhanaresh2012@gmail.com[3]

Abstract:

Antenna design plays a prominent role when we consider the far-field patterns when compared with near field patterns. By using a PIN diode (which has a wide intrinsic region when compared with normal diode) as a switch and a capacitor as a filter we are proposing an antenna design that able to radiate far field regions. The reason behind choosing capacitor as a filter means that we are designing antenna to transfer high frequency signals. For antenna design simulations we have different software's (like FEKO, ZELAND IE 3D etc.,) but the preferred software for this antenna design is Computer Simulation Technology Microwave Studio (CST MWS) as we are operating in a frequency band of 2 to 2.54GHz and the diameter of the antenna 30X30cm. Based on the distance chosen the antenna is able to switch direction of signalling by using a switch with four different angles. The material used for antenna design FR-4 which is a Composite material composed of fibre glass cloth with an epoxy resin Binder i.e. flame resistance and SMB connectors with 75Ω impedance.

Keywords —— Antenna Directivity, Strip antenna array, Wi-Fi.

Introduction:

If we want to increase the gain of the antenna as well as to reduce the unwanted source we must be able to control the beam of radiation pattern and this can be achieved by using the Beam Control antenna which is designed by using PIN diode as a switch and capacitor as filter. Beam antenna must work on the principle of directional antenna which has the ability to concentrate to a single direction with high gain and to reduce the energy that gets wasted in different areas (example Yagi antenna). The material used for antenna design FR-4 which is a Composite material composed of fibre glass cloth with an epoxy resin Binder i.e. flame resistance and SMB connectors with 75Ω impedance.

Antenna Design

In this method we are using four PIN diodes as switches with four different angles to allow the specific radiation pattern. Each diode need two capacitors to act as filter in order to prevent the dc current not to enter the antenna[1] [3]. If any one of the diode is supplied with energy of 3V DC then each angle is able to radiate 90 degrees. This antenna design is done by using FR-4 material whose dielectric substrate is assumed to be 0.17mm and the thickness of copper wire is assumed to be 0.035mm. Here the pin diode which is acting as a switch restricts the DC current and allows the AC current to pass through the antenna. The Capacitor filter acts as a high pass circuit which allows only high frequency signals and avoids the low frequency signals [3].

Fig 1: Antenna Front View

The front view of the antenna is represented in fig 1and the middle patch is simulate as 2.54 GHz frequency with the diameter 75mm X 75mm while the outside four patches is to generate the far-field

and diode switching and filtering is used for antenna functioning.

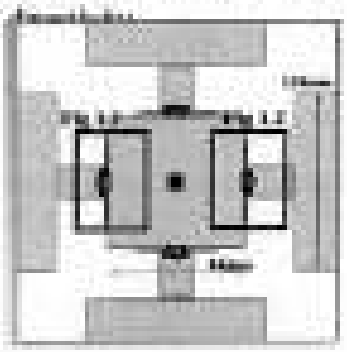

Fig: 2 Antenna Back view

The red square at the middle of the part in fig 1 indicates SMB connection with 75Ω impedance. This region shows the antenna connection from main section to ground. The mid region of the antenna is of diameter 86mm X 86mm. In the design point of view the PIN diode is connected between the ground and the small patch of the antenna as shown below

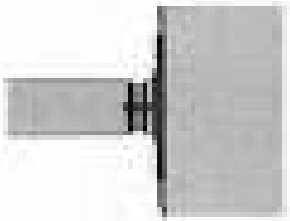

Fig: 3 Antenna Design with Switch as Short Circuit

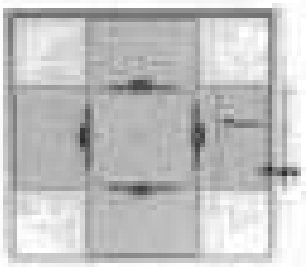

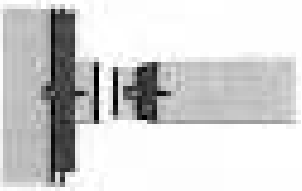

Fig: 4 Antenna Design with Switch as Open circuit

In fig 3 we can observe that the connection between the ground of the antenna and the small patch did not connect which shows that PIN diode is not connected to switch is working as open circuit logic. Fig 2 and Fig 3 are the zoom versions of Fig 1.

In fig 1 we observe three capacitors are represented as three triangles with blue colour dots and the middle one is the PIN diode acts as switch whereas remaining three as filters. When we apply the DC current of 5V then PIN diode gets activated and it will drain the AC signal from antenna to other side and both the filters restrict the dc current.

From Fig 3 we can observe that if PIN diode is not connected then the signal from antenna enable to pass through the other side of antenna then it cannot generate the far field on the other side.

Result Analysis

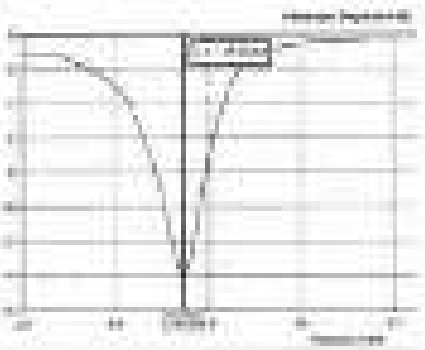

Fig: 4 S11 Parameter

From fig 4 we observe a frequency drop at 2.47GHz and S11 magnitude at -14.00 and after simulation with and without diode the frequency

and S11 magnitude remained same. The desire frequency range is dropped to below -10 while the frequency 2.47 GHz is under ISM band and in the range of WI-FI band range i.e. 2.4 GHz to 2.5GHz [4].

Conclusion:

The antenna is able to radiate far field signal by using diode and capacitor and by using CST MWS software we are able to simulate the antenna to get desired frequency, fs field and gain. As diode rotates it represents far-field with different angles.

References

[1] J.L.Lawson, Yagi-antenna Design, American Radio Relay League, 1986

[2] W. K. Chen, The Electrical Engineering Handbook, vol. 16, Academic Press, 2004

[3] David M. Pozar, D. Schubert, Microstrip Antenna, IEEE Antenna and propagation Society, 1995

[4] Stephen C. Thierauf, High Speed Circuit Board Signal Integration , Artech House , 2004

Authors Profile:

1.

K.Raghavendra, Asst. Professor Received B.Tech degree in Electronics and Communication Engineering from the University of JNTU Hyderabad and M.Tech degree in Electronics & Communication Engineering from the University of JNTU Hyderabad. He is currently working as an Asst. Professor in ECE Department at Malla Reddy Engineering College for women, Dhulapally (V), Secunderabad, Hyd.
He is working as advisory member in WATT (World Association of Technical Teachers). He is having membership in IAENG (International Association of Engineers),IRED (Institute of Engineers & Doctors), IJACSIT &SDIWC (Society of Digital Information & Wireless Communication).Up to now he attended many Workshops Conducted by different organizations also attended Virtual conference conducted by IEEE. His currently research interests include Microwave Antennas, Communications, Digital Electronics, VLSI.

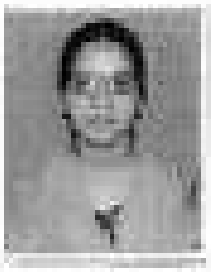

2.

A.Swetha, Asst. Professor Received B.Tech degree in Electronics and Communication Engineering from Venkateshwara College of Engineering, Mahaboobnagar affiliated to the University of JNTU Hyderabad and M.Tech degree in VLSID from SSJ Engineering College affiliated to University of JNTU-Hyderabad. She is having memberships in IAENG (International Association of Engineers)and IRED (Institute of Engineers and Doctors). She is currently working as an Asst. Professor in ECE Department at Sri Indu Institute of Engineering &Technology, Hyderabad. Her Currently research interests include Signal Processing, VLSI, Embedded Systems.

3.

S.Naresh, Asst. Professor Received B.Tech degree in Electronics and Communication Engineering from Gitanjali Engineering College Warangal affiliated to JNTUHyd. M.Tech degree in Digital Systems and Computer Electronics from Malreddy Engineering College affiliated to JNTUH. He is currently working as an Asst. Professor in ECE Department at Sri Indu Institute of Engineering &Technology, Hyderabad. Up to now he attended many Workshops Conducted by different organizations. His Currently research interests include Signal Processing, VLSI.

ANTENNA BEAMFORMING AND BEAM CONTROLLING FOR IMPROVING THE WI-FI SIGNAL

K Raghavendra[1], A. Swetha[2], S. Naresh[3]
[1]Asst. Professor, Dept. of ECE, Malla Reddy Engineering College for Women(Autonomous), Secunderabad TS
[2][3]Asst. Professor, Sri Indu Institute of Engineering & Technology, Ranga Reddy-TS
Email: raghu.ciet@gmail.com[1], swetha.vit@gmail.com[2], sureshnaresh031209@gmail.com[3]

Abstract:

Antenna design plays a prominent role when we consider the far-field patterns when compared with near field patterns. By using a PIN diode (which has a wide intrinsic region when compared with normal diode) as a switch and a capacitor as a filter we are proposing an antenna design that able to radiate far field regions. The reason behind choosing capacitor as a filter means that we are designing antenna to transfer high frequency signals. For antenna design simulations we have different software's (like FEKO, ZELAND IE 3D etc.,) but the preferred software for this antenna design is Computer Simulation Technology Microwave Studio (CST MWS) as we are operating in a frequency band of 2 to 2.5GHz and the diameter of the antenna 200x200mm. Based on the diameter chosen the antenna is able to cover each direction of signalling by using a switch with four different angles. The material used for antenna design FR-4 which is a Composite material composed of fibre glass cloth with an epoxy resin binder ie. flame resistance and SMB connectors with 75Ω impedance.

Keywords —— Antenna Directivity, Strip antenna array, Wi-Fi.

Introduction:

If we want to increase the gain of the antenna as well as to reduce the unwanted source we must be able to control the beam of radiation pattern and this can be achieved by using the Beam Control antenna which is designed by using PIN diode as a switch and capacitor as filter. Beam antenna must work on the principle of directional antenna which has the ability to concentrate in a single direction with high gain and to reduce the energy that gets wasted in different areas (example Yagi antenna). The material used for antenna design FR-4 which is a Composite material composed of fibre glass cloth with an epoxy resin binder ie. flame resistance and SMB connectors with 75Ω impedance.

Antenna Design

In this method we are using four PIN diodes as switches with four different angles to allow the specific radiation pattern. Each diode need two capacitors to act as filter in order to prevent the dc current not to enter the antenna[1] [3] If any one of the diode is supplied with energy of 5V DC then each angle is able to radiate 90 degrees. This antenna design is done by using FR-4 material whose dielectric substrate is assumed to be 0.17mm and the thickness of copper wire is assumed to be 0.035mm. Here the pin diode which is acting as a switch restricts the DC current and allows the AC current to pass through the antenna. The Capacitor filter acts as a high pass circuit which allows only high frequency signals and avoids the low frequency signals [2].

Fig 1: Antenna Front View

The front view of the antenna is represented in fig 1 and the middle patch is simulate as 2.54 GHz frequency with the dimension 78mm X 56mm while the outside four patches is to generate the far-field

and diode switching and filtering is used for antenna

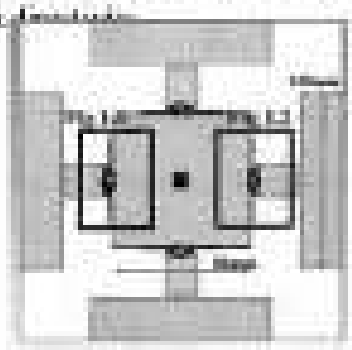

Fig: 2 Antenna Back view

The red square at the middle of the part in fig 1 indicates SMB connection with 75Ω impedance. This region shows the antenna connection from main section to ground. The mid region of the antenna is of diameter 35mm X 98mm. In the design point of view the PIN diode is connected between the ground and the small patch of the antenna as shown below

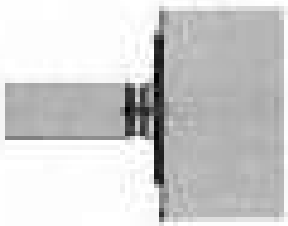

Fig: 3 Antenna Design with Switch as Short Circuit

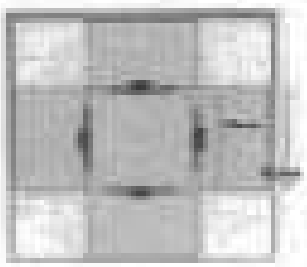

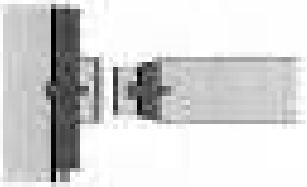

Fig: 4 Antenna Design with Switch as Open circuit

In fig 3 we can observe that the connection between the ground of the antenna and the small patch did not connect which shows that PIN diode is not connected i.e; switch is working as open circuit logic. Fig 2 and Fig 3 are the zoom versions of Fig 1.

In fig 1 we observe three capacitors are represented as three triangles with blue colour dots and the middle one is the PIN diode acts as switch whereas remaining three as 56nh. When we apply the DC current of 5V then PIN diode gets activated and it will drain the AC signal from antenna to other side and both the filters restrict the dc current.

From Fig 3 we can observe that if PIN diode is not connected then the signal from antenna unable to pass through the other side of antenna then it cannot generate the far field on the other side.

Result Analysis:

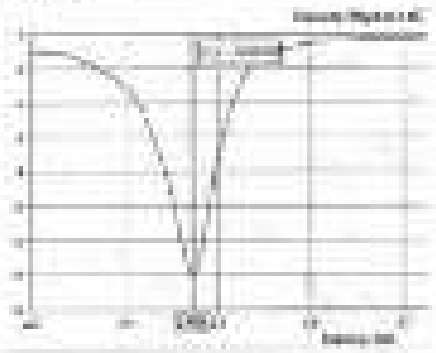

Fig: 5 S11 Parameter

From fig 4 we observe a frequency drop at 2.45GHz and S11 magnitude at -14.60 and after simulation with and without diode the frequency

and S11 magnitude remained same. The desire frequency range is dropped to below -10 while the frequency 2.47 GHz is under ISM band and in the range of WI-FI band range i.e. 2.4 GHz to 2.5GHz [4].

Conclusion:

The antenna is able to radiate far field signal by using diode and capacitor and by using CST MWS software we are able to simulate the antenna to get desired frequency, far field and gain. As diode rotates it represents far-field with different angles.

References

[1] J.L.Lawson, Yagi-antenna Design, American Radio Relay League, 1986.

[2] W. K. Chen, The Electrical Engineering Handbook, vol. 16, Academic Press, 2004

[3] David M. Pozar, D. Schaubert, Microstrip Antenna,"IEEE Antenna and propogation Society, 1995

[4] Stephen C. Thierauf, High Speed Circuit Board Signal Integration , Artech House , 2004

Authors Profile:

1. **K.Raghavendra, Asst. Professor** Received B.Tech degree in Electronics and Communication Engineering from the University of JNTU Hyderabad and M.Tech degree in Electronics & Communication Engineering from the University of JNTU Hyderabad. He is currently working as an Asst. Professor in ECE Department at Malla Reddy Engineering College for women, Dhulapally (V), Secunderabad, Tel.

He is working as advisory member in WATT (World Association of Technical Teachers). He is having membership in IAENG (International Association of Engineers),IRED (Institute of Engineers & Doctors), IACSIT &SDIWC (Society of Digital Information & Wireless Communication)He is/are he attended many Workshops Conducted by different organizations also attended Virtual conference conducted by IEEE. His currently research interests include Microwave-Antennas, Communications, Digital Electronics, VLSI.

2.

A.Swetha, Asst. Professor Received B.Tech degree in Electronics and Communication Engineering from Venkateshwara College of Engineering, Mahaboobnagar affiliated to the University of JNTU Hyderabad and M.Tech degree in VLSID from SSI Engineering College affiliated to University of JNTU-Hyderabad. She is having memberships in IAENG (International Association of Engineers)and IRED (Institute of Engineers and Doctors). She is currently working as an Asst. Professor in ECE Department at Sri Indu Institute of Engineering &Technology, Hyderabad. Her Currently research interests include Signal Processing, VLSI, Embedded Systems.

3.

S.Naresh, Asst. Professor Received B.Tech degree in Electronics and Communication Engineering from Ganapathi Engineering College Warangal affiliated to JNTUHand M.Tech degree in Digital Systems and Computer Electronics from Mallareddy Engineering College affiliated to JNTUH. He is currently working as an Asst. Professor in ECE Department at Sri Indu Institute of Engineering &Technology, Hyderabad. He is/are he attended many Workshops Conducted by different organizations. His Currently research interests include Signal Processing, VLSI.

5TH INTERNATIONAL CONFERENCE ON AUTOMOBILE, MARINE AND PRODUCTION ENGINEERING – 2018
4th & 5th May 2018

STUDIES ON MECHANICAL PROPERTIES OF SISAL AND JUTE FIBER HYBRID SANDWICH COMPOSITE

C.Sivakandhan[1], G.Murali[2], N.Tamiloli[2], L.Ravikumar[3]

[1] Department of Mechanical Engineering, Sri Indu Institute of Engineering and Technology, Hyderabad, Telangana-501510, India,kandhansiva69@gmail.com

[2]Department of Mechanical Engineering, Koneru Lakshmaiah Education Foundation, Guntur, Andhra Pradesh-522502, muralimit@gmail.com

[3]Department of Mechanical Engineering, Sri Sairam Engineering College, West Tambaram, Tamilnadu-600044, ravikumar.mech@sairam.edu.in

Abstract

The present study deals with the fabrication of hybrid composites and mechanical properties are tensile, flexural, compression strength and impact of sisal fiber and jute fiber combinations. Epoxy resin (LY556 grade) and hardener (HY951) is taken as the matrix and binder for the sisal and jute fiber combination. The five different kinds of samples of jute/epoxy and sisal fiber/epoxy composite were made with the fiber-matrix weight ratio of 35 %. After fabrication, the test specimens were prepared as per in the ASTM standards. The result shows the co-axial tensile strength of jute/epoxy and sisal fiber /epoxy composite the result was increased 35% than sisal epoxy. The tensile, flexural, compression strength and impact of jute fiber/epoxy composites are higher than those of sisal fiber/epoxy composites at the same fiber loading. Additionally, the SEM images are studied in the different combinations.

Keywords: Hybrid composite, jute/sisal, epoxy, hardener

1. INTRODUCTION

The composite material can be defined as the material which is composed of two or more distinct material on a macro scale with different properties to form a new material with a property that is entirely different from the individual constituents. The cost of natural fiber Composites is low and light in weight but strength is not lower than synthetic fibers [1]. The primary phase of a composite materials called a matrix having a continuous character. In other words, the matrix is a material which acts as a binder and holds the fibers in the desired position there by transferring the external load to reinforcement. These matrices are considered to be less hard and more ductile. The composite material consists of a matrix along with a fiber with some filler material. The reinforced material can be either synthetic or natural fibers. In the demand of increasing environmental security, several natural fibers reinforced polymer composites (NFPCs) are brought into the competitive market. NFPCs provide a wide range of advantages over synthetic fiber based composites. Due to the superior properties of Natural fiber composites it become so popular and attractive. [2]. These advantages include high strength to weight ratio, high strength at elevated temperatures, high creep resistance and high toughness [3]. These advantage may also be in the form of high durability and design flexibility.M.Boopalan,et.al investigated the mechanical properties of new jute and sisal fiber reinforced epoxy composites treated with sodium hydroxide and the results found better for treated composites [4].

Hybrid composites are more advanced composites as compared to conventional FRP composites. Hybrids can have more than one reinforcing phase and a single matrix phase or single reinforcing phase with multiple matrix phases or multiple reinforcing and multiple matrix phases. They have better flexibility as compared to other fiber reinforced composites. It usually contains a high modulus fiber with low modulus fiber. The high-modulus fiber provides the stiffness and load bearing qualities, whereas the low-modulus fiber makes the composite more damage tolerant and keeps the material cost low. M.K.Gupta,et.al studied about the dynamic mechanical properties and water absorption characteristics of hybrid sisal and jute fiber reinforced epoxy composites. From their work they concluded that natural fibers are a better replacement of synthetic fibers due to its acceptable mechanical properties [5]. Srivastava,et.al carried out an experimental work to study the wear and frictional properties of the hybrid composite with different operating parameters; their study reveals that the alkali treatment of fibers is used to increase the percentage reduction of wear rate and friction coefficient [6]. Hariom Maurya et al [7] studied about the jute fiber reinforced with both polyester and epoxy resins; the results show that the jute reinforced epoxy composite exhibits better mechanical properties than jute polyester composites.Alvi,et al [8] investigated the properties of sisal reinforced epoxy composites using varying the fiber lengths(5,10,15,20cm) with constant 30% of sisal fiber. The results of their work reveal that 15cm and 20cm sisal fiber reinforced composite shows significant improvement in the flexural and impact property.Leninet.al [9] studied through a case study design about the possibilities for the replacement of glass fibers by natural jute fibers to produce a structural hatches of an off-road vehicle(Buggy motorcycle). Chandrasekar,et.al [10] discussed the optimum mixing of fiber and resin of sisal banana & nettle hybrid composites in dry and wet conditions. The mechanical properties of a hybrid composite can be varied by changing volume ratio and stacking sequence of different plies.

1.2 Problem Identification

Based on the Literature presented in the chapter 1, it is found that some researchers are carried out on fractional fiber reinforced composites; they have found the Co-axial tensile properties and other mechanical properties of these composites. There is no research to characterize of Tri-axial properties of Jute and Sisal fiber reinforced composites. So it is decided to carry out research the topic of Co axial and Tri axial Tensile Properties of composite material and analysis the mechanical properties of flexural behaviour, impact behaviour, compression behaviour.

2. Materials and Methods

Since the present study deals with the manufacturing of hybrid composites, the material for reinforcement is chosen as sisal fiber and jute fiber tape to get suitable mechanical properties and epoxy resin (LY556 grade) and hardener (HY951) is taken as the matrix and binder for the composite. This process carried out with the help of compressive moulding. Work piece prepared in the dimension 300x300x3 mm was used for casting the composite sheet. The sample specimen is shown in Figure 1. There are five different kinds of samples were made with the fiber-matrix weight ratio of 35 %.The sample is tabulated below the Table 1.

Table 1 Composite Sample Details

Sample Number	Wt % of jute fiber	Wt % of Steel fiber	Wt % of Epoxy and Hardener
Sample 1	0	35	65
Sample 2	10	25	65
Sample 3	20	15	65
Sample 4	25	10	65
Sample 5	35	0	65

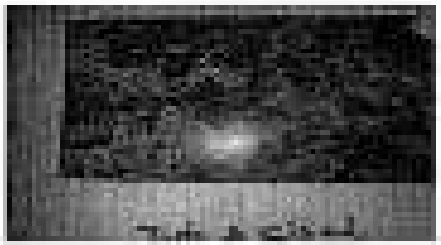

Figure 1 Compression molding process

3. Mechanical Testing

The test specimens were prepared and undergone different mechanical testings namely Tensile test, flexural test and impact test as per the ASTM standards. The specimen size and shape for corresponding tests are as follows.

3.1 Tensile Test

A composite specimen is subjected to Tensile testing to measure the force required to break the test specimen and the extent to which the specimen stretches or elongates to that breaking point. The physical properties of materials at a temperature that reasonably intended end user environment. The most common specimen for ASTM D3039 has a constant rectangular cross section, 25mm wide and 250mm long is used to study.

3.2 Flexural Test

Flexural strength is carried out to find the ability of the material to resist the deformation under the load. This is a three point bend test is used to promote failure by inter laminar shear. This test is conducted as per ASTM D790 standard by UTM. The specimen dimension is 12x125x3 mm. The flexural strength is expressed as modulus of rupture (MR) in psi (MPa).The flexural strength is calculated using the Equation 1.

$$\sigma_f = 3P_{max}L/2bh^2 \text{ ---------- (1)}$$

where,

P_{max} = maximum load at failure

b = specimen width,h = specimen thickness

L = specimen length between the two support points

3.3 Impact Test

The impact is a single point test that measures the resistance of a material to impact from a swinging pendulum. The impact is defined as the kinetic energy needed to initiate fracture and continue the fracture until the specimen is broken. The ASTM D256 (13x60x3) mm) size is taken for the test.

3.4 Compression Test

The main aim of a compression test is to determine the ability of the material to withstand the compressive force under the compressive load during a period of time to measure the parameters such as strain, stress, and deformation. The specimens prepared by ASTM D 3410.

3.5 Scanning Electron Microscope(SEM)

SEM is a type of electron microscope that produces images of a sample by scanning it with a focused beam of electrons. The morphological characterization of the composite surface is observed in scanning electron microscope of Model TESCAN VEGA 3.The composite samples are adequately cleaned, air dried and are coated with 100A^0 thick platinum in IB3L sputter ion coater and observed SEM at 10 KV. The fracture surface morphology of the composite specimens is observed with SEM.

4 Results and Discussion

The mechanical properties of the Jute / Sisal Fiberhybrid epoxy composites prepared for this present investigation is presented in this discussion. The results of various characterization tests are reported here. These include evaluation of tensile strength, flexural strength, impact strength and compression values are tabulated in Table 3 and the properties are discussed.

4.1 Tensile Test

Random directional tensile specimens were cut in the longitudinal and transverse direction for tensile test according to ASTM D 3039 type IV sample the tensile test specimens were carried out, using a tensile testing machine with crosshead speed of 2mm/min and a gauge length of 150 mm. Three specimens were tested for each set of samples and mean values were tabulated in Table 2.

4.1.1 Co-axial Tensile Test.

The co-axial tensile strength of hybrid composite at 30:0at % Jute and Sisal fiber were 22.33 N/mm^2. As can be seen figure 2, increasing weight fraction of jutefiber resulted in the positive effect on tensile properties of hybrid composites.The maximum tensile stress value of the composites was 22.33 N/mm^2.This is probably due to the loss of the integrity of the matrix and insufficient wetting between fiber and matrix as a result of high fiber loading.

Table 3 Mechanical Properties values

S.No	Co-axial Tensile strength	Tran-sverse Tensile strength	Flexural Strength	Impact Strength
	N/mm^2	N/mm^2	N/mm^2	J
30/0/0	15.28	17.89	32.17	0.82
20/0/20	14.21	14.84	43.50	0.4
20/0/0	13.91	8.72	29.68	0.55
0/25/0	15.78	3.27	34.48	0.29
0/0/0	22.33	13.91	56	0.4

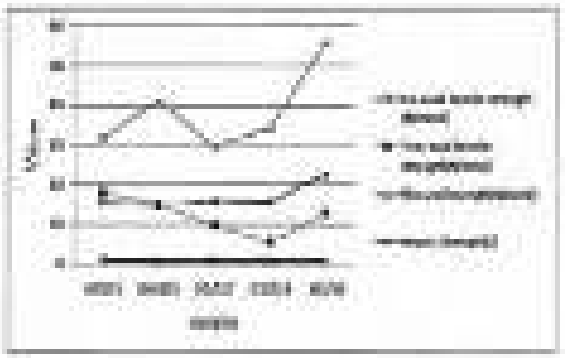

Figure 2 Mechanical properties of Jute / Sisal fiber hybrid epoxy composite

INTERNATIONAL CONFERENCE ON ADVANCES IN MECHANICAL ENGINEERING - 2018
4th & 5th May 2018

4.1.2 Tensile Strength

The effect of Jute / Steel fiber hybrid epoxy composite is presented in the tensile strength of hybrid composite at 0.25 wt% Jute and Steel fiber were 17.99 N/mm^2. As can be seen figure 3, increasing weight fraction of jute fiber resulted in negative effect on tensile properties of hybrid composites.The maximum tensile stress value of the composites was 17.99 N/mm^2.This is probably due to the loss of the integrity of the matrix and insufficient wetting between fiber and matrix as a result of high fiber loading.

The tensile strength of a composite material is mainly dependent on the strength and modulus of fibers, the strength and chemical stability of the matrix and fibers in transferring stress across the interface. When fiber reinforced composites are subjected to load, the fibers act as carrier of load and stress is transferred from the matrix along the fibers leading to effective and uniform stress distribution, which results in a composite having excellent mechanical properties.

4.2 Flexural Test

The flexural test was performed by the three-point bending method according to ASTM D 790, and a cross-head speed of 2 mm/min. 3-specimens were tested, and the averages were calculated. The maximum load was applied in the middle of the specimen, when the specimen was freely supported by a beam. The flexural modulus are evaluated from the slope of the initial portion of the load-deflection curve. The figure 2 shows that incorporation of Jute and Steel fiber at a 35/0 wt% relative weight fraction leads to hybrid composites having a superior flexural strength. The maximum flexural strength of the composite was 96.3 N/mm^2. Flexural strength is nothing but a strength combining the tensile and compressive strengths and dictates with the interfacial shear strength between the fiber and matrix. It was observed from figure 2 that the flexural strength and modulus of Jute / Steel fiberepoxy composite increased with increasing jute fiber. If adding steel fiber will reduce flexural strength.

4.3 Impact Test

The impact strength of Jute / Steel fiber hybrid epoxy composites the impact energy increasing with increasing weight fraction of steel fiber upto 35/0%.The relationship between fiber loading and impact strength is shown in Figure 2. The load which applied on fibers is transferred by shear to the fibers, may exceed the fiber/matrix interfacial bond, and debonding May occur. The frictional force along the interface may transfer the stress to the debonded fiber. If the fiber stress level exceeds the fiber strength, fibers may break. The obtained results reveals that the fiber is capable of absorbing energy due to the strong interfacial bonding between the fiber and matrix up to 30 wt% steel fiber loading. However, at higher loadings, the more fiber interaction decreases the effective stress transfer between the fiber and matrix. This contributes to a decrease in impact properties at higher fiber loadings. The high impact strength steel fiberepoxy found[8,9].

4.4 Compression Test

Compression testing of a specimen prepared according to ASTM D 3410. The effect of hybrid fiber hybrid epoxy composite is presented in figure 2. wt% Jute/andsteelfiberwas53.09 N/mm^2. The fibers act as carrier of load and stress is transferred from the matrix along the effective and uniform stress distribution. When fiber reinforced composites are subjected to load. Due to this results, it leads a good composite having excellent mechanical properties. At a low level of fiber loading, the matrix is not restrained by enough fibers paving the bond between matrix and fiber to break, leaving the matrix divided by non-reinforcing debonded fiber.

4.5 SEM Images

Figure.3 shows the different samples and images. The variation of the Mechanical properties of prepared composite specimens through phase information shown by means of the topography properties. A figure clearly shows the poor bonding capacity of the composite so that mechanical properties are reduced. Sample 3shows the jute-steel fiber bundles, which indicate that these fibers were not adequately wet by epoxy polymer resin and thus led to low stress.SEM images indicate that presence of jute fibers which indicate that medium interfacial bonding between epoxy and jute and gives excellent mechanical properties compared to composite.

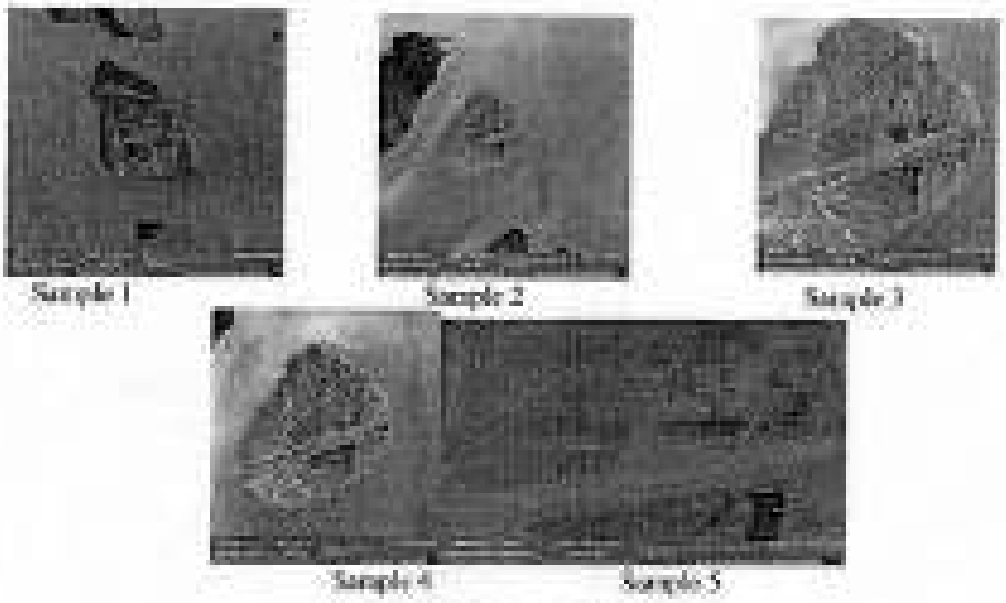

Figure 3 Different samples images

5. Conclusions

The Mechanical properties of Jute/ Sisal Fiber reinforced hybrid composites were studied, and the following conclusions are drawn.

1. The jute, sisal fibers was successfully used to fabricate natural hybrid composites with 35% fiber and 65 % resin, these fibers are biodegradable and highly crystalline with well-aligned structure. The co axial tensile strength of jute/epoxy and sisal fiber/epoxy composite having compared to sisal epoxy the result was increased 30%. Hybrid composite the tensile strength is decreased.
2. Compare to Trans axial loading and coaxial loading is a better result.
3. The flexural strength of jute/epoxy composite improved by increasing fiber loading up to 35wt.%.
4. Addition of sisal fiber decreases the tensile, flexural, compression and increases the Impact properties of composites.
5. The tensile, flexural, and compression strength of jute fiber/epoxy composites are higher than those of sisal fiber/epoxy composites at the same fiber loading.
6. Impact properties of sisal/epoxy composite are better than the jute fiber epoxy composites.
7. The west analysis of the different hybrid composite with jute composites which gives excellent mechanical properties compared to jute and sisal hybrid epoxy composite.

References

1. P.Navaneethan and M.Jayaraman, "Experimental Investigation on the Mechanical Properties of Jute/Sisal/Glass and Jute/Banana/Glass Hybrid Composite Materials" European Journal of Applied Sciences 7 (2): 2015 138-144.
2. M. Ramesh, K. Palanikumar and K. Hemachandra, "Modelly Mechanical property evaluation of sisal-jute-glass fiber reinforced polyester composites", Composites Part B, 48, 2013, pp.1-9.
3. Satyanarayana K.G,Sukumaran K. Mukherjee P.S. Pavithran. Cand Pillai S.G.K."Natural fiber-Polymer Composites" Cement and Concrete Composites,12(2),1990,pp.117-136.
4. M. Boopalan, M. J. Umapathy & T. Jayabal, "A Comparative Study on the Mechanical Properties of Jute and Sisal Fiber Reinforced Polymer Composites" Silicon,4., 2012,pp.145–149.
5. M.K.Gupta & R.K. Srivastava, "Effect of sisal fiber loading on dynamic mechanical analysis and water absorption behaviour of jute fiber epoxy composite." Materials Today: Proceedings 2 2015 Pp. 2508 – 2517.
6. M. K. Gupta and R. K. Srivastava, "Effect of Sisal Fibre Loading on Wear and Frictional Properties of Jute Fiber Reinforced Epoxy Composite". American Journal of Polymer Science & Engineering, 3, 2015, pp.198-207.
7. Hari Om Niranjan, M.K. Gupta, R.K. Srivastava and H. Singh, "Study on the mechanical properties of the epoxy composite using short sisal fiber." Materials Today: Proceedings 2, 2015,pp. 1347 – 1355.

Nano Composite Properties and its Applications: A Review

Mr. K. Sushmala[1], Dr. I. Satyanarayana[2], Dr. G. Amarendra Rao[3]
[1]Mechanical Engineering, Vignana Bharathi Institute of Technology, Hyderabad, India
[2]Mechanical Engineering, Sri Indu Institute of Engineering & Technology, Hyderabad, India
Email: kondasushmala07@gmail.com, [2]satyaprofessor@gmail.com

Abstract

The field of nanocomposite is one of the most popular areas for current research and development in basically all technical disciplines. Nanocomposites, a high performance material exhibit unusual property combinations and unique design possibilities. With an estimated annual growth rate of about 25-30% and fastest demand to be in engineering plastics and elastomers, their potential is so striking that they are useful in several areas ranging from packaging to biomedical applications. In this unified overview the three types of matrix nanocomposites are presented underlining the need for these materials, their processing methods and some recent results on structure, properties and potential applications, perspectives including need for such materials in future space mission and other interesting applications together with market and safety aspects. Possible uses of natural materials such as clay based minerals, chrysotile and lignocellulosic fibers are highlighted. Being environmentally friendly, applications of nanocomposites offer new technology and business opportunities for several sectors of the aerospace, automotive, electronics and biotechnology industries.

Keywords- nanocomposites, layered compounds, polymers, metals, ceramics

I. INTRODUCTION

Nanocomposites are composites in which at least one of the phases shows dimensions in the nanometric range (1 nm = 10^{-9} m)[1]. Nanocomposite materials have emerged as suitable alternatives to overcome limitations of microcomposites and monolithic. They are reported to be the materials of 21st century in the view of possessing design uniqueness and property combinations that are not found in conventional composites. The general understanding of these properties is yet to be reached[2], even though the first inference on them was reported as early as 1992[3]. It has been reported that changes in particle properties can be observed when the particle size is less than a particular level, called the critical size (Table 1)[3]. Additionally, as dimensions reach the nanometre level, interactions at phase interfaces become largely improved, and this is important to enhance materials properties. In this context, the surface area/volume ratio of reinforcement materials employed in the preparation of nanocomposites is crucial to the understanding of their structure-property relationships. Further, discovery of carbon nanotubes (CNTs) in 1991[6] and their subsequent use to fabricate composites exhibiting some of the unique CNT related mechanical, thermal and electrical properties[7-9] added a new and interesting dimension to this area. The possibility of spinning CNTs into composite products and textiles[10] made further inroads for the processing and applications of CNT-containing nanomaterials. Nowadays, nanocomposites offer new technology and business opportunities for all sectors of industry, in addition to being environmentally friendly[11].

As in the case of microcomposites, nanocomposite materials can be classified, according to their matrix material, in three different categories as shown in Table 2.

 ISBN 978-93-82338-80-4

Ceramic Matrix Nanocomposites (CMNC),

Metal Matrix Nanocomposites (MMNC) and

Polymer Matrix Nanocomposites (PMNC).

Finally, to the best of our knowledge, and in view of the very limited work on metal-based nanocomposites including the ones with CNT reinforcements, no review is available to-date on this system. Considering these facts and also the absence of a more general review comprising the three different kinds of nanocomposites (metal-, ceramic- and polymer-based), this paper gives an overview of them, including those with incorporation of CNTs. However, while doing so only a few relevant publications[2,4,7] are considered here. The main features, current status and recent developments in the area are provided, focussing on the preparation methods, properties and applications of these systems to avoid repetition. Also, the potential uses of nanocomposites and the opportunities they provide, along with perspectives for the future and market and safety aspects are also presented. Nanocomposite coating is not covered, in order to keep the focus of the review.

Table 1. Feature sizes for significant changes in properties reported in na-nocomposite systems [reference 5 : the Japan Society of Powder and Powder Metallurgy].

Properties	Feature size [nm] at which change might be expected
Ductile-ceramic	<5
Making hard magnetic materials soft	<20
Producing reflective index changes	<50
Producing super paramagnetism and atoms electromagnetic phenomena	<100
Producing strengthening and toughening	<100
Modifying hardness and plasticity	<100

Table 2. Different types of nanocomposites.

Class	Examples
Metal	Fe-C/Al$_2$O$_3$, Ni/Al$_2$O$_3$, Cu/Cr, Ti/MgO, Al/CNT, Mg/CNT
Ceramic	Al$_2$O$_3$/SiC$_w$, SiO$_2$/Ni, Al$_2$O$_3$/TiO$_2$, Al$_2$O$_3$/SiC, Al$_2$O$_3$/CNT
Polymer	Thermoplastic/thermoset polymer/layered silicates, polymer/TiO$_2$, polymer/CNT, polymer/layered double hydroxides

On the other hand, even after a decade of research, CNTs have not fully realized their potentials as nanoscopic reinforcements in polymer matrices. Thus great challenges and opportunities are still expected for the system. These are based on the following:

a) CNTs with small number of defects per unit length possess 500 times more surface area per gram on the basis of equivalent volume fraction of a typical carbon fiber, high aspect ratio (~1000), very high tensile properties and electrical and thermal conductivities.

b) Research on CNT-related areas has been more active, with publications doubling within six months. Even the patenting activity in this area has been impressive, with about 3,300 applications filed from 2001 to June 2006 as per the literature survey.

c) Because of their hollow nature, CNTs can be opened and filled with a variety of materials including biological generating technological opportunities. Added to this, the challenges in obtaining homogeneous dispersions and strong interfacial interactions, which can be better done by surface grafting functionalization, make the use of CNTs in composites more intriguing.

d) Various applications of CNTs in composites have been reported extensively.

e) The possibility of spinning polymers to obtain textiles[10] certainly constitutes a great promise for their extended use in a variety of applications, particularly in the electronic and thermal management sectors.

f) Nanoreinforcements with biodegradable polymers have a high potential for the design of environmentally friendly 'green materials' for future applications.

On the whole, opportunities and research appear to be great with nanocomposites and hence there is a tremendous world-wide interest in these materials.

II. PROCESSING OF NANOCOMPOSITES

A. Raw Materials

As with nanocomposites, CMNC matrix materials include Al_2O_3, SiC, Si_3N_4, etc., while metal matrices employed in MMNC are mainly Al, Mg, Pb, Sn, W and Fe, and a whole range of polymers, e.g. vinyl polymers, condensation polymers, polyolefins, specialty polymers (including a variety of biodegradable molecules) are used in PMNC. In general, it is the reinforcement that is in the nanorange size in these materials. Both synthetic and natural crystalline reinforcements have been used, such as Fe and other metal powders, clays, silica, TiO_2 and other metal oxides, although clays and layered silicates are the most common. This is so due to their availability with very low particle sizes and well-known intercalation chemistry, in addition to generating improved properties even when they are used at very low concentrations. Most of these reinforcements are prepared by known techniques: chemical, mechanical (e.g. ball milling), vapour deposition, etc.; details of these may be found in many of the references given in the following sections.

Similarly, CNTs are prepared mostly by chemical vapour deposition methods and details are available elsewhere. CNTs consist of graphene cylinders and are available in two varieties, as single walled (SWCNT) and multi-walled (MWCNT), with about 70% yield in the case of SWCNT. While SWCNTs are single graphene cylinders, MWCNTs consist of two or more concentric cylindrical sheets of graphene around a common hollow core. Both types exhibit physical characteristics of solids, either metallic or semiconducting in nature, with microcrystallinity and very high aspect ratios.

In the case of CNTs, use of surfactants, oxidation or chemical functionalization of surfaces are some of the techniques employed. Chemical methods may be more effective, particularly for polymer and ceramic matrices. Physical blending and in situ polymerization are used for improving dispersion in the case of CNT-reinforced polymer composites, while alignment of CNTs could be achieved by techniques such as co-extrusion techniques (filtration, template and plasma-enhanced chemical vapour deposition, for example), field-inducements, etc.[33].

B. Processing Methods

Ceramic Matrix Nanocomposites (CMNC)

Many methods have been described for the preparation of ceramic matrix nanocomposites. The most common methodologies, as used for microcomposites, are Conventional powder method; Polymer precursor route; Spray pyrolysis; Vapour techniques (CVD and PVD) and Chemical methods, which include the sol-gel process, colloidal and precipitation approaches and the template synthesis.

A large variety of parameters affecting the sol-gel process, such as type of solvent, strength, pH, precursor, water:metal ratio, etc., allow a versatile control of structural and chemical properties of the final oxide materials. Regarding the processing of carbon nanotubes (CNT)-reinforced ceramic nanocomposites, many approaches have been described.

Metal Matrix Nanocomposites (MMNC)

The most common techniques for the processing of metal matrix nanocomposites are Spray pyrolysis; Liquid metal infiltration; Rapid solidification; Vapour techniques (PVD, CVD); Electrodeposition and Chemical methods, which include colloidal and sol-gel processes. Only two reports are found, for example, on Fe-based nanocomposites prepared by solidification techniques. The first one, by Branagan, is called 'devitrified nanocomposite steel'. This was obtained by quenching the arc melt glass obtained from a Fe-based alloy, followed by devitrifying the glass precursor through heat treatment above its crystallization temperature. This resulted in a material showing a crystalline multi-phase microstructure. The formation of nanophases was explained by the high nucleation

frequency within the limited time for growth of grains before impingement. In order to explain the very high hardness of these Fe-based nanocomposites, Branagan and Tang studied novel nanostructures obtained in bulk Fe alloys by designing alloy compositions with different amounts of B and C to get maximum stability. Difficulties have been encountered in preparing composites with very fine particles due to their reduced agglomeration and non-homogeneous distribution. Use of ultrasound helped to improve the wettability between the matrix and the particles.

Polymer Matrix Nanocomposites (PMNC)

Many methods have been described for the preparation of polymer nanocomposites, including layered materials and those containing CNTs. The most important ones are i) Intercalation of the polymer or pre-polymer from solution; ii) In-situ intercalative polymerization; iii) Melt intercalation (Figure 1); iv) Direct mixture of polymer and particulates; v) Template synthesis; vi) In-situ polymerization; and vii) Sol-gel process. Publications dealing with various methods for the incorporation of reinforcing materials into conducting polymers are also available; the most prominent one is probably the incorporation of inorganic building blocks in organic polymers.

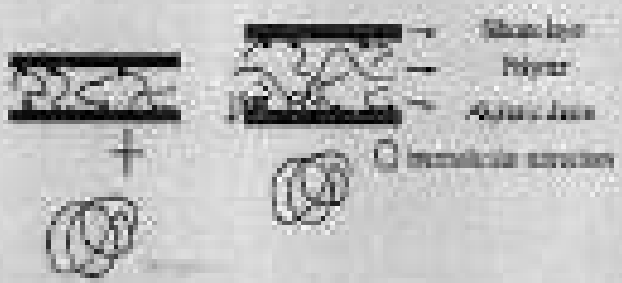

Figure 1. Melt intercalation synthesis of polymer/clay nanocomposites [the American Chemical Society, USA].

Similarly, different processing techniques, mostly chemical and electrochemical methods, have been employed for the preparation of conducting polymer nanocomposites.

When the polymer is unable to intercalate between the silicate sheets, a phase separated composite (Figure 2) is obtained, whose properties stay in the same range as that of traditional microcomposites. On the other hand, in intercalated nanocomposites, the insertion of a polymer matrix into the layered silicate structure occurs in a crystallographically regular fashion, regardless of the clay to polymer ratio. A well ordered multilayer morphology built up with alternating polymeric and inorganic layers is generated. Normally, only a few molecular layers of polymer can be intercalated in these materials.

3. PROPERTIES

It can be seen from literature that there was significant improvement in the strength of the nanocomposite compared with its micro counterpart. The fracture strength, as an example, is noticeably higher because of the higher interfacial interaction between the particles in nanocomposites. Besides, Al_2O_3 5 to 15% SiC systems exhibited superficial grooves of plastic deformation compared to the intergranular fracture observed in monolithic materials. There was no time-dependant wear transition for these composites even at loads of 20-100 N, but pre-transition wear rates of $1-2 \times 10^{-8}$ mm^3/Nm were observed for both the monolithic and composite materials. The following Tables 3,4 and 5 shows that the properties and examples of nanocomposites.

Table 3. Examples of ceramic matrix nanocomposites and their properties.

Matrix/Reinforcement	Properties
Si_3N_4/SiC	Improved strength and toughness
$Mullite/ZrO_2$	-
B_4C/TiB_2	-
Al_2O_3/SiC	-
MoSi2/SiC	-
Mullite/SiC	-
Al_2O_3/ZrO_2	-
Al_2O_3/Mo, Al_2O_3/W	-
$Al_2O_3/NiAl3$	Improved

4. APPLICATIONS OF NANOCOMPOSITES

From the foregoing, it becomes evident that nanocomposites may provide many benefits such as enhanced properties, reduction of solid wastes [lower

groups (thickness firm and lower reinforcement usage) and improved manufacturing capability, particularly for packaging applications. Tables 21 to 23 present potential applications of ceramic-, metal- and polymer-based nanocomposites, respectively. As it can be observed, the promising applications of nanocomposite systems are numerous, comprising both the generation of new materials and the performance enhancement of known devices such as fuel cells, sensors and coatings. Although the use of nanocomposites in industry is not yet large, their massive switching from research to industry has already started and is expected to be extensive in the next few years. Table 6 shows that the application of nanocomposites.

Table 4. Properties of Al2O3/SiC nano- and microcomposites[36, 37].

Properties/Material	Al_2O_3/SiC(p) composite	Al_2O_3/SiC(p) nanocomposite
Vickers Hardness [GPa]	-	22
Young's Modulus [GPa]	-	393
Fracture Strength [MPa]	350-380	500-650
Fracture Toughness [MPa$m^{1/2}$]	2.4-4.0	4.6-5.5

Table 5 . Examples of metal nanocomposites and their properties.

Matrix/reinforcement	Properties
Ag/Au	Improvement in catalytic activity
NiP/SiC and Ni/SiC	Improved hardness and strength
Cu/Nb	Improved mechanical properties
Al/AlN	Higher compressive resistance and low shear rate
Al/SiC	Improved hardness and elastic moduli
CNT/Ni and CNT/NiFe	Improvements in Li^+ intercalation properties
$Ni_3Al_2O_4$	Tribological improvement in hardness
Cu_2O/Cr_2O_3	Improved microhardness and wear resistance

Table 6. Potential applications of metal nanocomposite systems.

System/material	Application
Fe/MgO	Catalysts, magnetic devices
Ni/PTFE	Wear resistant coatings and chemically grafted coatings
Ru/TiO_2	Photo-electrochemical applications
Al/SiC	Aerospace, naval and automotive structures,
Cu/Al_2O_3	Electronic packaging
Al/MB	Microelectronic industry, High speed machinery, bearing cermet and
Ni/CNT, Ni/GNR	
Cu/GN	Magnetic storage materials
Ni/Cr	Structural materials for high temperature applications
Fe_2Ni_2/CNT/β-PVDF	Structural materials
Fe/TiN	Catalysts
	Microelectronic industry
Al_2O_3/Ag	Microelectronics, optical devices, light energy conversion

CONCLUSIONS

In conclusion, new technologies require materials showing novel properties and/or improved performance compared to conventionally processed components. In this context, nanocomposites are suitable materials to meet the emerging demands arising from scientific and technologic advances. Processing methods for different types of na-nocomposites (CMNC, MMNC and PMNC) are available, but some of these pose challenges that give opportunities for researchers to overcome the problems being encountered with various materials. They offer improved performance over monolithic and micro-composite counterparts and are consequently suitable candidates to overcome the limitations of many currently existing materials and devices. A number of applications already exists, while many potentials are possible for these materials, which open new vistas for the future. In view of their unique properties such as very high mechanical properties even at low loading of reinforcements, gas barrier and flame related properties, many potential applications and hence the market for these materials have been projected in various sectors. Thus all the these types of na-nocomposites provide opportunities and rewards creating new world-wide interest in frontiers materials

Table 7. Potential applications of polymer nanocomposite systems.

Nanocomposites	Applications
Polycaprolactone/SiO_2	Bone-biomedical for skeletal tissue repair.
Polyimide/SiO_2	Microelectronics.
PMMA/SiO_2	Dental application, optical devices.
Polyethylacrylate/SiO_2	Catalysis support, sensors, glass for chromatography.
Poly(p-phenylene vinylene)/SiO_2	Non-liner optical material for optical waveguides.
Polyamide (nylon) / TiO_2	Composite membranes for gas separation applications.
poly(1,4-ethylene-dioxythiophene)/V_2O_5	Cathode materials for rechargeable lithium batteries.
Polycarbonate/SiO	Abrasion resistant coating.
Shape memory polymer/SiC	Medical devices for guiding or releasing therapeutics within blood vessels.
Nylon-6/LS	Automotive timing belt – TOYOTA.
PBT/LS	Airplane interiors, fuel tanks, components in electrical and electronic parts, fenders and trim.
PLA/LS	Lithium battery development.
PET/clay	Food packaging applications. Specific materials include packaging for processed meats, cheese, confectionery, cereals and nuts, ready-to-eat foods, fruit juice and dairy products, beer and carbonated drinks bottles.
Thermoplastic olefin/clay	Beverage container applications.
Polyimide/clay	Automotive engine covers - GM Safari and Astro Vans.
Epoxy/SWCT	Materials for absorption.
SPEEK/Laponite	Direct methanol fuel cells.

Table 8. Advantages and limitations of processing methods for metal-based nanocomposites.

Process	Advantages	Limitations
Spray Pyrolysis	Effective preparation of ultrafine, spherical and homogeneous powders in multicomponent systems, reproducible size and stability.	High cost associated with processing large quantities of uniform nanosized particles.
Liquid Infiltration	Short reaction times between matrix and reinforcement, enabling near-net-shape manufacturing of different ceramic and reinforcement volumes, rapid solidification, both for scale and industrial scale production.	Use of high temperatures, formation of undesired products during processing. Only small-sized nanocomposites, poorest of glass-ceramic and non-homogeneous distribution of fine particles.
Rapid Solidification Process (RSP)	Simple, effective.	
RSP with ultrasonics	Good distribution without agglomeration, even with fine particles.	
High Energy Ball Milling	Homogeneous mixing and solid state diffusion.	
CVD/PVD	Capability to produce highly dense and pure nanosized materials, efficient high deposition rates, good reproducibility.	Optimization of many parameters, only relatively thin coatings.
Chemical Processes (Sol-Gel, Colloidal)	Simple, low processing temperature, high purity, chemical homogeneity, right stoichiometry, good control of particle size, controlled high purity products.	Weak bonding, low mechanical strength, high porosity, CTE, CM and difficult control of porosity.

Table 3. Advantages and limitations of polymer-based nanocomposite processing methods.

Process	Advantages	Limitations	Ref.
Intercalation	Synthesis of intercalated nanocomposites based on polymers with an inherent polarity	Industrial use of large amounts of solvents	5-18
Polymerization	Preparation of homogeneous dispersions of the filler		131-137
Solution	Easy procedure, based on the dispersion of the filler in the polymer precursor.	Difficult control of intercalative polymerization Limited application	156-164
Melt Intercalation	Environmentally benign: use of polymers not soluted for other processes compatible within industrial polymer processes	Limited applications: cannot be used for polymers with polar matrices Limited application of polyolefins, also important for the majority of used polymers.	101-109
Template Synthesis	Large scale production, easy procedure.	Limited applications: based mainly on water soluble polymers, contaminated by side products.	170-175
Sol-Gel Process	See Table 2a	See Table 2a	

References

1. Ray E, Ray EA, Ray DM. Abnormal orientation or "point crystallinity", non-uniformity and microcrystalline. Materials Letters. 1986; 4(8-9):323-328.
2. Sahoo B, Dash D, Giannelis EP. New advances in polymer layered silicate nanocomposites. Current Opinion in Solid State & Materials Science. 2002; 6(6):505-510.
3. Okada H. Materials tell: double-nanocomposites: nanocomposites and perspectives. Nanocomposite Materials. 1992; 1(1):1-19.
4. Braun T, Schubert A, Szabolcs Z. Nanocomposites and nanotechnology on the horizon. Scientometrics. 1997; 39(1):141-225.
5. Kawaguchi O. Which one to improve by nanocomposite? Journal of Japan Society of Powder Metallurgy. 1997; 45:315-321.
6. Iijima S. Helical microtubes of graphitic carbon. Nature. 1991; 354(6348):56-58.
7. Dresselhaus MS, Dresselhaus G, Saito R, Jorio A. Raman spectroscopy of carbon nanotubes. Physics Reports. 2005; 409(2):47-99.
8. Thostenson ET, Ren Z, Chou TW. Advances in the science and technology of carbon nanotubes and their composites: a review. Composites Science and Technology. 2001; 61(13):1899-1912.
9. Schadler LS, Giannaris SC, Ajayan PM. Load transfer in carbon nanotube epoxy composites. Applied Physics Letters. 1998; 73(26):3842-3844.
10. Lahiri D, Singh V, Benaduce AP, Seal S, Kos L, Agarwal A. Microstructure and tribological behavior of polymethylmethacrylate reinforced ultra high molecular weight polyethylene nanocomposites. Journal of the Mechanical Behavior of Biomedical Materials. 2011; 4(8):1844-1855.
11. Ajayan PM, Schadler LS, Giannaris C, Rubio A. Single-walled carbon nanotube-polymer composites: strength and weakness. Advanced Materials. 2000; 12(10):750-753.
12. Coleman JN, Khan U, Blau WJ, Gun'ko YK. Small but strong: a review of the mechanical properties of carbon nanotube-polymer composites. Carbon. 2006; 44(9):1624-1652.
13. Breuer O, Sundararaj U. Big returns from small fibers: a review of polymer/carbon nanotube composites. Polymer Composites. 2004; 25(6):630-645.
14. Gojny FH, Wichmann MH, Fiedler B, Kinloch IA, Bauhofer W, Windle AH, Schulte K. Evaluation and identification of electrical and thermal conduction mechanisms in carbon nanotube/epoxy composites. Polymer. 2006; 47(6):2036-2045.
15. Gojny FH, Wichmann MH, Fiedler B, Bauhofer W, Schulte K. Influence of nano-modification on the mechanical and electrical properties of conventional fibre-reinforced composites. Composites Part A: Applied Science and Manufacturing. 2005; 36(11):1525-1535.
16. Gojny FH, Wichmann MH, Köpke U, Fiedler B, Schulte K. Carbon nanotube-reinforced epoxy-composites: enhanced stiffness and fracture toughness at low nanotube content. Composites Science and Technology. 2004; 64(15):2363-2371.
17. Sandler J, Shaffer MS, Prasse T, Bauhofer W, Schulte K, Windle AH. Development of a dispersion process for carbon nanotubes in an epoxy matrix and the resulting electrical properties. Polymer. 1999; 40(21):5967-5971.
18. Sandler JK, Kirk JE, Kinloch IA, Shaffer MS, Windle AH. Ultra-low electrical percolation threshold in carbon-nanotube-epoxy composites. Polymer. 2003; 44(19):5893-5899.

NATIONAL CONFERENCE
On
RECENT TRENDS AND DEVELOPMENTS IN MECHANICAL ENGINEERING

RTDIME - 2018
1st & 2nd March -2018

Organized by

DEPARTMENT OF MECHANICAL ENGINEERING

SOUVENIR

ANAND INSTITUTE OF HIGHER TECHNOLOGY
(KOVALAM ANAND GROUP OF INSTITUTIONS)

(Approved & Accredited by AICTE and NBA
Affiliated to ANNA UNIVERSITY, CHENNAI)
Kelambakkam-Vandalur Road, Off Old Mahabalipuram Road,
Kazhipattur, Chennai-603 103, TAMIL NADU
Phone: 044-27473300/27472020
Website: www.aiht.ac.in

INFLUENCE AND EFFECT ON MECHANICAL PROPERTIES OF STITCHED AND UN-STITCHED WOVEN GLASS FIBER / EPOXY COMPOSITE LAMINATES

[1]Dr.C.Sivakandhan, [2]R.Balaji, [3]Dr.G.Murali, [4]Dr.D.Madan
[1]Professor, Department of Mechanical Engineering
Sri Indu Institute of Engineering and Technology-Hyderabad, Telangana, India
[2]Assistant Professor, Department of Mechanical Engineering
Er.Perumal Manimekalai College of Engineering- Hosur
[3]Professor, Department of Mechanical Engineering
Koneru Lakshmaiah Educational Foundation – Guntur, Andra Pradesh, India
[4]Professor, Department of Mechanical Engineering
Sri Indu College of Engineering and Technology –Hyderabad, Telangana, India

ABSTRACT

The work presented in this project investigates the effect of stitched and un-stitched woven glass fiber / Epoxy composite laminates and to investigate the ability of through thickness reinforcement to improve the de-lamination resistance of laminates. Un-stitched and Stitched specimens were prepared. The test specimens are fabricated by simple hand lay-up technique and prepared according to ASTM standards and tensile test, compression and impact tests to conduct. Under low velocity impact loading, unidirectional laminates suffer from extensive delamination damage that reduces their residual mechanical properties. To increase the resistance to delaminations; through the thickness stitching was adopted. From the experiment work to find the strength, deformation and breaking forces for both stitched and unstitched specimens. In order to distinguish the effect of fibers, a number of experiments were performed. Details of the experiments conducted along with the results were discussed in the paper and it concludes.

Keywords: Epoxy, Composite Materials, Hand lay-up, Tensile strength, flexural strength, Impact strength.

A steganographic technique for transferring source image file without stego file with high level of robustness

Publisher: IEEE

Abstract

Abstract:
Steganography is a branch of computer science where original information can be transmitted as

A novel steganographic technique for transfering image file without stego file by using shuffled absolute differential vectors of image

P. V. Balakrishnan | A. Tamilarasan | All Authors

Abstract: Cryptography and Steganography are the areas of research in the field of information security [1]. Steganography is the technique of hiding information into the cover file like text, audio, video or image without causing statistically significant modification to the cover file. The success of the steganography is to hide the existence of the information from the attacker [2] [3]. While embedding information in an image, a proper balance is required in between the increasing embedding capacity and in reducing the stego-image distortion quality. In the proposed work, secret single bit of data was embedded in the pixels of the cover file was transmitted on the channel. Only the secret image generated with the help of differential vectors is transmitted on the channel. The cover file is there with the data repository at both sender and receiver side. Hence, there is no change to identify the data embedded on the cover image. At the destination end by using differential vector image and the cover image from the repository, the whole secret image was reconstructed. As there is no single bit of data was embedded in the cover image even a powerful steganalysis technique cannot be able to detect the steganographic process.

Published in: 2012 International Conference on Wireless Communications, Signal Processing and Networking (WiSPNET)

Date of Conference: 22-24 March 2012 INSPEC Accession Number: 12826821

Date Added to IEEE Xplore: 22 February [illegible] DOI: 10.1109/ICSCET.2011.5739481
ISBN Information:
Publisher: IEEE
Conference Location: Chennai, India

Contents

Steganography is the process of embedding the data bits in the
[illegible] positions of the pixels in the carrier file. The file on which data
[illegible] will be stuffed is called as carrier file or cover file [1]. If the carrier file
used is a color image, [illegible] method as color
image steganographic technique. After embedding the data bits on the
cover image, the cover image is called as stego image. Most of the
image steganographic algorithms will be used the Least Significant Bit
(LSB) method, because it will not much affect the quality of an image.

IEEE Account | Purchase Details | Profile Information | Need Help?
» Change Username/Password | » Payment Options | » Communications Preferences | » US & Canada: +1 800 678 4333
» Update Address | » Order History | » Profession and Education | » Worldwide: +1 732 981 0060
» View Purchased Documents | » Technical Interests | » Contact & Support
About IEEE Xplore | Contact Us | Help | Accessibility | Terms of Use | Nondiscrimination Policy | Sitemap | Privacy & Opting Out of Cookies
A not-for-profit organization, IEEE is the world's largest technical professional organization dedicated to advancing technology for the benefit of humanity.
© Copyright 2011 IEEE – All rights reserved. Use of this web site signifies your agreement to the terms and conditions.

Proceedings of International Conference on Computational Intelligence and Multimedia Applications 2007 | Chapter

An Efficient and Robust Image Steganographic Technique Without Stuffing Data Bits

Author(s) Author(s) and affiliation(s)

K. B. Raja [illegible] | V. Venkatesha

Conference paper
First Online: 08 April 2017

Abstract

Steganography is the process of hiding data bits in cover or carrier file. The carrier file may be

International Conference On Emerging Trends in Science Technology Engineering and Management
09th & 10th, October 2015

Cooling and Heating of a Substance Using Vapour Compression Refrigeration Cycle

Dr.L.Rajamanikyam[1], D.S.V.S.R.A.Vamsi Raju[2], P.Chandrashekar[3]

[1]Principal&Professor of Mechanical Engineering, Hyderabad, Telangana, India
[2]PG student of Mechanical Engineering, Hyderabad, Telangana, India
[3]Associate professor of Mechanical Engineering, Hyderabad, Telangana, India

[1]rajamanikyam.lingala@gmail.com, [2]vamsiraju.dsvsra@gmail.com
[3]pavanmail.chandra@gmail.com

Abstract— the present invention relates to refrigeration and heating system based on vapour compression refrigeration cycle. Generally in vapour compression refrigeration cycle, refrigeration effect takes place in the evaporator as we can pass copper tubes in which cold refrigerant is flowing through the substance (Water) at evaporator side to produce cooling effect. During vapour compression refrigeration cycle heat rejection takes place in the condenser, at condenser side the refrigerant passing through copper tubes is hot due to compression, so we can utilize this heat to heat the substance (Water) by passing hot copper tubes through the substance before it passes through the condenser, here I am using two steel members filled with substance(water) one is fixed at evaporator side to cool the substance(water) and other one is at condenser side to heat the substance(water).

*Keywords—*Compressor, Condenser, Evaporator, Expansion Device, Heater

I. Introduction

Refrigeration is the action of cooling, and in practice this requires removal of heat and discarding it at a higher temperature. Refrigeration is therefore the science of moving heat from low temperature to high temperature. In addition to chilling and freezing applications, refrigeration technology is applied to air conditioning and heat pumps, which therefore fall within the scope of this book. The fundamental principles are those of physics and thermodynamics, and those principles, which are relevant to all applications.

Water heating is a thermodynamic process that uses an energy source to heat water above its initial temperature. Typical domestic uses of hot water include cooking, cleaning, bathing, and space heating. In industry, hot water and water heated to steam have many uses. Fossil fuels (natural gas, liquefied petroleum gas, oil, or solid fuels) are commonly used for heating water. These may be consumed directly or may produce electricity that, in turn, heats water. Electricity to heat water may also come from any other electrical source, such as nuclear power or renewable energy. Alternative energy such as solar energy, heat pumps, hot water heat recycling, and geothermal heating can also heat water, often in combination with backup systems powered by fossil fuels or electricity.

II. Vapour Compression Refrigeration cycle

A. Working of vapour compression refrigeration cycle

Vapour Compression Refrigeration cycle is widely used in refrigeration systems, including refrigerators, refrigeration air conditioning, freezers, and auto air conditioners. R22 and R12 refrigerants are the most commonly used, but are being phased out due to effects on the ozone layer. The working principle of an ideal vapour compression refrigeration cycle is shown in figure1.main parts of a vapour compression refrigeration system are compressor, condenser, expansion device and an evaporator. Here compressor and condenser are at high pressure side and expansion device and evaporator are at low pressure side.

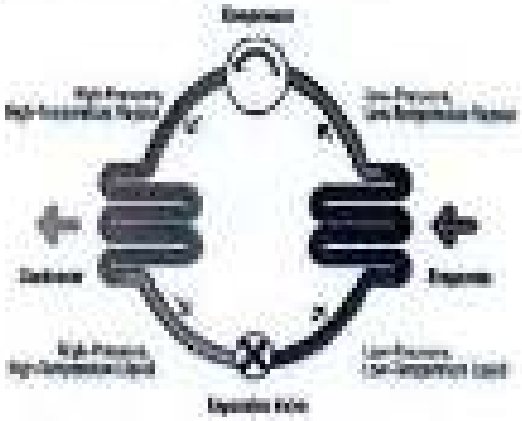

Figure 1: Schematic diagram of vapour compression refrigeration system

B. High pressure side

During compression the low pressure and low temperature vapour refrigerant enters in to compressor after compression the temperature and pressure of the refrigerant increases. This high pressure and high temperature vapour refrigerant passes through a condenser heat heat rejection takes place during this processes the temperature of refrigerant decreases and pressure remains constant, and the phase of refrigerant changes from vapour state to liquid state.

C. Low pressure side

After condensation the high pressure and low temperature liquid refrigerant goes in to expansion device which is also known as throttling device here pressure of the liquid refrigerant decreases at this point the pressure and temperature of liquid refrigerant are lower than its surrounding temperature and pressure then this low temperature and low pressure liquid refrigerant made passed through the evaporator here the refrigerant evolve the space heat it changes its phase from liquid state to vapour state then again this low pressure and low temperature vapour refrigerant goes in to compressor to repeat the cycle.

D. Thermodynamic Analysis

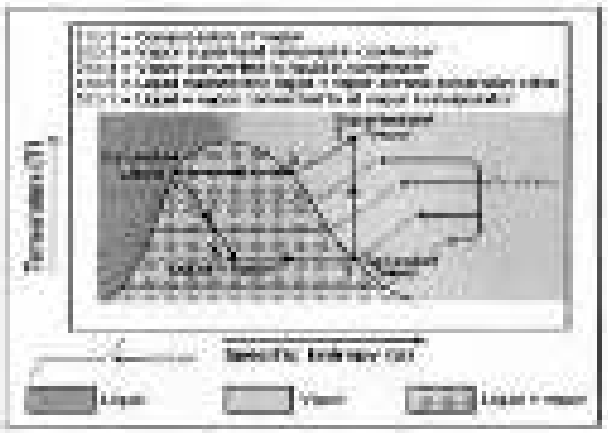

Figure 2: Temperature and Entropy diagram for vapour compression refrigeration system

The thermodynamics of the vapour compression cycle can be analyzed on a temperature versus entropy diagram as depicted in Figure 2. At point 1 in the diagram, the refrigerant is at vapour state enters the compressor there it compresses the refrigerant reversibly and adiabatically (isentropically) and exits the compressor as a superheated vapour refrigerant at point 2 during this process the pressure and temperature of refrigerant increases.

From point 2 to point 3, the superheated vapour refrigerant travels through part of the condenser which removes the heat by cooling the vapour refrigerant. Between point 3 and point 4, the vapour refrigerant travels through the remaining part of the condenser reversibly and isothermally during this process temperature of the refrigerant decreases and pressure remains constant vapour refrigerant converts in to liquid refrigerant.

Between points 4 and 5, the saturated liquid refrigerant passes through the expansion valve and undergoes an abrupt decrease of pressure. This process is known as throttling process it is an irreversible processes during this process enthalpy remains constant therefore it is also known as isenthalpic process. During isenthalpic process the pressure and temperature decreases.

Between points 5 and 1, the cold and partially vaporized refrigerant travels through the coil or tubes in the evaporator where it is totally vaporized by the warm air (from the space being refrigerated) reversibly at constant pressure. During this process the liquid refrigerant converts in to vapour refrigerant then this saturated vapour refrigerant returns to compressor to complete the cycle.

It should be noted that the above discussion is based on the ideal vapour-compression refrigeration cycle which does not take into account real world facts like frictional pressure drop in the system, slight internal irreversibility during the compression of the refrigerant vapour etc.

E. COP of Vapour Compression Refrigeration cycle

Coefficient of performance of a vapour compression refrigerator is the ratio of refrigeration effect (heat removed in the evaporator) to the amount of work done.

$$COP = \text{Refrigeration effect} / \text{Work done}$$

$$\text{Refrigeration effect} = h_1 - h_5, \text{ work done} = h_2 - h_1$$

$$COP = \frac{h_1 - h_5}{h_2 - h_1}$$

III. OUTCOMES OF (A) VAPOUR COMPRESSION REFRIGERATION CYCLE

From figure 2 we can observe that the temperature of the superheated vapour refrigerant after compression is high at point 2 and at point 3 saturated vapour refrigerant enters in to condenser after condensation at point 4 the temperature of the liquid refrigerant decreases. So we called the heat which is rejecting during process 2 to 3, to heat the substance (water) also during process 4 to 5 the temperature of the liquid refrigerant is low at point 5, during the process 5 to 1, we can see the low temperature liquid refrigerant to cool the substance (water).

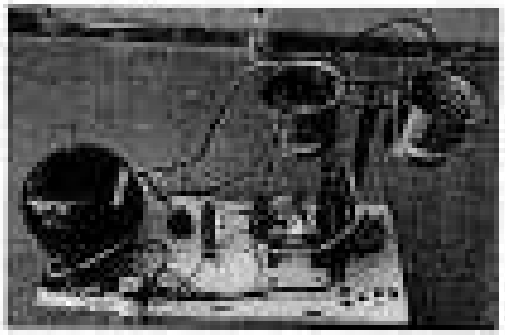

Figure 3 Diagram of cooling and heating effect using vapour compression refrigeration system

Figure 3 shows the practical vapour compression refrigeration system it consists of a compressor, condenser, expansion device, two pressure gauges & two metal tumblers, one tumbler 1) for heating the substance (water) other one (tumbler 2) for cooling the substance (water) after running this vapour compression refrigeration system for some time observed that the water in the tumbler 1 through which superheated vapour refrigerant is passing is gets heating and the water in tumbler 2 through which low temperature liquid refrigerant is passing is cooling.

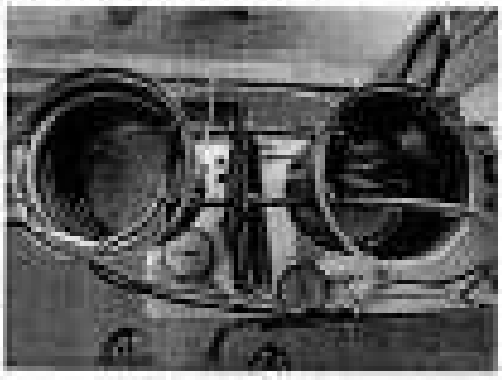

Figure 4 diagram of water cooling and water heating in test condition

From the figure 4 we can clearly observe that the water in the right tumbler gets heated and the water in the left tumbler gets cooled.

A. Refrigerant Used (R134a)

Figure 4 Diagram of Refrigerant R134a

R-134a is also known as Tetrafluoroethane (CF3CH2F) from the family of HFC refrigerant. With the discovery of the damaging effect of CFC's and HCFC's refrigerants on the ozone layer, the HFC family of refrigerants has been widely used as their replacement.

It is now being used as a replacement for R-12 CFC refrigerant in the area of centrifugal, rotary screw, scroll and reciprocating compressors. It is safe for normal handling as it is non-toxic, non-flammable and non-corrosive. The R134a is most environmental friendly refrigerant so we preferred the refrigerant R134a over R22, R12 these refrigerants cause ozone damage in ozone layer.

TABLE I

Properties Of Refrigerant R134a

Sno	Properties	R134A
1	Boiling Point	-15.9°F or -26.7°C
2	Auto-ignition Temperature	743°F or 778°C
3	Ozone Depletion Level	0
4	Solubility In Water	0.11% by weight at 77°F or 25°C
5	Critical Temperature	252°F or 122°C
6	Oil under Ozone Code	Light blue
7	Global Warming Potential (GWP)	1200

IV. Results & Discussions

Water cooling and water heating using vapour compression refrigeration cycle is successfully operated. The desired results of heating and cooling of water simultaneously is achieved and the rate of cooling and heating are as follows

TABLE I

TEMPERATURE RESULTS

S.NO	Time in minutes	Temperature of cold water in °C	Temperature of hot water in °C
1	0	20	20
2	10	9	41
3	18	6	46
4	22	4	50
5	25	-1	52

Table shows the temperature results of hot water and cold water in °C water at 20°C poured in the steel containers, and then we started the vapour compression refrigeration system after 10 minutes we have checked the temperature of hot and cold water temperatures with the help of thermometer the temperature of hot water reaches to 41°C and the temperature of cold water reaches to 9°C after 18 minutes the temperatures are 46°C & 6, after 25 minutes the temperatures of hot and cold waters are 52°C & -1°C and our final observation at 25minutes at that point of time the temperatures of hot and cold waters are 52°C & -7°C.

A COP of Vapour Compression Refrigeration System with Heater Coils

The condenser pressure we noticed in the high pressure gauge is 0.8 Mpa and evaporator pressure is 0.07Mpa from refrigerator table's and values at various points are noted down

$h_1 = 377.305$ kj/kg

$h_2 = 402.31$ kj/kg

$h_3 = 249.800$ kj/kg

$$COP = \frac{h_1 - h_3}{h_2 - h_3}$$

$$COP = \frac{377.305 - 249.800}{402.31 - 377.305}$$

$$COP = 1.228$$

V. CONCLUSION

Finally we proved that the heating and cooling of a substance (water) simultaneously is possible during a vapour compression refrigeration cycle. Now a day's every house has at least one refrigerator in some food items and water heaters to heat water both water heaters and refrigerators requires power to operate but by using this attachment of heater to the refrigerator we can refrigerator itself as a water heater to save the power.

References

[1] Roy J Dossat, "Principles of Refrigeration"

[2] C P Arora, "Refrigeration and Air Conditioning", Tata McGraw Hill Publications

[3] W F Stoecker, "Refrigeration and Air Conditioning" Tata McGraw Hill Publications

[4] Sienkiewicz S, "A Course in Heat and Mass Transfer"

[5] ASHRAE, "ASHRAE Handbook and Product directory"

[6] Manohar Prasad, "Refrigeration and Air Conditioning" Wiley Eastern Limited

[7] P L Ballaney, "Refrigeration and Air Conditioning", Khanna Publish

[8] Arora domkundwar, "Basic Refrigeration and Air Conditioning", Tata McGraw Hill Publications

[9] Wikipedia

[10] E.Rathakrishnan "Engineering Thermodynamics"

[11] R.K.Rajput "Thermal Engineering"

International Conference On Emerging Trends In Science Technology Engineering and Management
(ICETSTEM'15), October 2015

Thermal Analysis Comparisions On Natural Ventilated Open Poly Greenhouse To Closed Poly Greenhouse

Sri Saravanan[1], K Vinay[2],

K Anil Kumar[3]

[1]Principal & Professor of Mechanical Engineering
Sri Indu Institute of Engineering and Technology, Sheriguda, Ibrahimpatnam
Ranga Reddy District-501510

[2]Assistant Professor of Sri Indu Institute of Engineering and Technology, Sheriguda, Ibrahimpatnam
Ranga Reddy District-501510

[3]Associate Professor
Sri Indu Institute of Engineering and Technology, Sheriguda, Ibrahimpatnam
Ranga Reddy District-501510

[illegible]

Abstract: Poly Greenhouses create optimal climatic conditions for crop growth and protect crops from outside pests. To achieve mid bottom crop production climate, traditional tropical Poly Greenhouse designs utilize a standard fan ventilation system to decrease temperatures. The basic reasons that such fans are energy intensive and are prone to failure when faced with tropical storms. The proposed solution is natural ventilation augmented cooling Poly Greenhouse, or NVAC Poly Greenhouse. A NVAC Poly Greenhouse comprises several, open-roof shelter improved by coupling natural ventilation.

In the present thesis we are analyzing the air ventilation and temperature changes in natural ventilation to closed conditions. The structural layout is analyzed to get the maximum optimal results to cope up with practical studies in present area conditions.

In the present thesis we are analyzing the air ventilation and temperature changes in natural ventilation to closed conditions. The structural layout is analyzed to get the maximum optimal results to cope up with practical studies in present area conditions.

Variations in temperatures will observe between summers to winters. The main application to maintain the ambient temperatures thorough out the year. Such results were obtained by comparing outside temperatures to inside temperatures with the existing system functional. Two design configurations of the same Poly Greenhouse were considered, open roof and open roof. The degree of sophistication also varies from a simple poly house with polyethylene film covering to highly sophisticated, fully automated drip and fogger systems, FAN lightings, full style computerized fully automated systems. In conventional Agricultural practices the crops are being grown / cultivated in the open field under natural conditions where the crops are most susceptible to sudden changes in climate i.e. temperature, humidity, light intensity, pests, pests and other conditions due to which the quality, yield of a particular crop can get affected and may be decreased.

Key words: poly house, natural ventilation, thermal conditions, temperature analysis.

I. INTRODUCTION

A Poly Greenhouse is a structure [illegible]

A Poly Greenhouse [illegible]

2. LITERATURE SURVEY

INTRODUCTION

The first simulation by means of Computational Fluid Dynamics (CFD) for the study of the ventilation in Poly Greenhouses was carried out by Okushima et al. (1989) who compared this numerical method with the experimental results

© Sri Indu Institute of Engineering and Technology (Autonomous)

studied in a wind-tunnel close to air. (1990). Although their results showed little correlation with the experimental data, probably due to the limited power of the available computer resources at that time, they provided important information on the patterns of flow inside the Poly Greenhouses. This technique was used later the same time until the conclusions of CFD were compared to a low span Poly Greenhouse with the data obtained by means of wind tunnel measurements (Bot et al., 1995; Boulard et al., 1996). Mistriotis et al. (1997) studied Mediterranean type Poly Greenhouses using CFD in a two-dimensional grid and they concluded that CFD is a powerful tool to develop improvements in the design of Poly Greenhouses for different conditions.

2.1. Types of Poly Greenhouse

Keeping in view the Indian climatic conditions, two types of Poly Greenhouse have been taken into consideration under the Govt. of India schemes (National Horticulture Mission (NHM)& Horticulture Mission for North East and Himalayan States(HMNEH)) for subsidy, and they are Naturally Ventilated Poly Greenhouse and Poly Greenhouse with Fan & Pad Cooling System.

1. Open type Poly Greenhouse System
2. Closed Type Of Poly Greenhouse System

2.2. Open type of Poly Greenhouse System

One of the main advantages of a naturally ventilated system is that the size of the structure is not limited by the pumping capacity of mechanical ventilation systems. This allows the wind powering zone to have fewer "edges," resulting in a more uniform growing temperature from one end to other.

2.2.1 Naturally ventilated Poly Greenhouse

Fig 2.2.1 naturally ventilated Poly Greenhouse

In accordance climate the design of the naturally ventilated Poly Greenhouse is popular for the level of protection and control it provides. Particularly when where the natural conditions outside make ventilation impossible or inadequate. An extra level of control helps ensure an ideal growing climate inside at all times.

While growing in Poly Greenhouse one can use the dependence on climate a resilience specialty plant land is a call duplication as an open is complete set of screens or roller constructions inside. The key to sustained quality, quantity and profitability lies in managing all these variables and their impact, and maximizing control of them.

Growing inside Poly Greenhouse allows plants to grow in temperatures typically between 12-28 °C and relative humidity of around 65-85%. The reason these conditions are ideal is because the plants' rate of photosynthesis is optimized at this point.

Features

- Maximum natural ventilation
- Environment controlled Poly Nets ridge and sidewall venting
- Available with either double poly film or polycarbonate covering
- Economical grow gable economical
- Produce an economically yield in complex stability operation
- Wide range of options to fit your needs

2.2.2 Siting for Natural Ventilation Systems

For some Poly Greenhouses, like a hoop house, simply rolling up a portion of the wall is all the ventilation it takes to provide for natural ventilation. However, Poly Greenhouses that are built from more rigid materials need to follow a few guidelines to ensure proper ventilation. The most important aspect of natural ventilation for these Poly Greenhouses is the size of the ridge (roof) vent and sidewall vents. It is recommended that the total combined ridge vent area should be equivalent to the total combined area of the sidewall vent and each should equal approximately 20% of the floor area.

2.2.3 Temperature Control Poly Greenhouse

The Natural Ventilated Poly Greenhouse regulate indirectly by using the temperature in the environment of a Poly Greenhouse (PG). If the heat is not required from the environment, it can cause unfavorable conditions for plant growth.

2.2.4 Air Circulation

Air circulation, or air movement, within a Poly Greenhouse serves many purposes. Proper air circulation creates uniformity in temperature, humidity, CO2, and oxygen within the environment. Plants respond better to consistent conditions, and proper air circulation can help each plant within the Poly Greenhouse to receive the same advantages as others.

2.3 Closed types Poly Greenhouse

Modern Poly Greenhouse production requires a high level of environmental control. In this context, it has been suggested that fully closing a Poly Greenhouse, i.e. without any exchange with the outside environment, would have a number of advantages. A fully closed Poly Greenhouse could be a significant improvement in water handling. The main challenge of closing the Poly Greenhouse is to be able to continuously control temperature (T) and relative humidity (RH) under

varying outside and outside conditions the environmental Control and management objectives are achieved are:

- Climate control system
- Temperature distribution (horizontal and vertical)
- Energy use

2.3.1 Poly Greenhouse with fan and pad cooling system (Mechanical Poly Greenhouse)

This type is also suited for hot dry climatic conditions and in Northern plains where temperature goes above 30°C. The system is working on the principle that when water evaporates and heat is absorbed from surroundings. This is possible by drawing over air into Poly Greenhouse through wet pad located at one end of the wall, where hot air is replaced by cool air blown through the opposite end of wall. The decrease in temperature causes various changes in the morphology and physiological processes of plants such as flower shedding, bad smell, poor fruit quality, excessive transpiration, shortened life span of the plants and low net photosynthesis. Due to excessive respiration etc. Hence, it is important to maintain air temperature inside the Poly Greenhouse ranging between 21°C to 24°C for better crop growth.

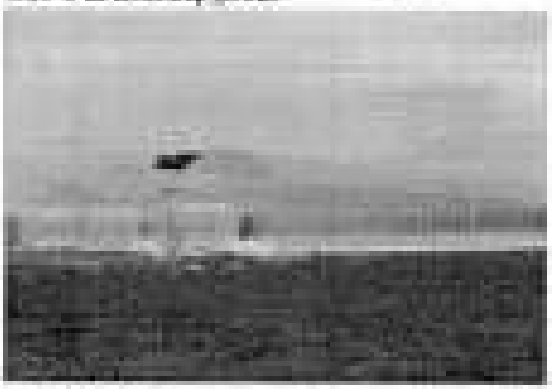

Fig: 2.3.1 Poly Greenhouse with fan and pad cooling system

2.3.2 Orientation criteria for mounting fan & pad

The orientation of the model upon Poly Greenhouse with fan & pad cooling system should be made in such a way to take an advantage of prevailing wind direction. Wet pad should be mounted on the wall of Poly Greenhouse facing winds and fan on the leeward side. The temperature gradient inside the Poly Greenhouse fitted with cool fan & Pad system. The cool room should be on the leeward side to prevent structural damage to the Poly Greenhouse.

2.3.3 Factors to reduce canopy temperature are as follows:

- Shading area and fan in the structure
- Limit the maximum distance between fan & pad to 25 m.
- Decrease the distance of fans for efficient air flow.
- Provide additional cooling facility in all parts/ways.
- In case of saline/brackish water, continuous flow of pad as water flows downwards it supplies the pads has a self-cleaning effect.
- The water used for cooling the pad should be stored from underground tank and provision to be made for recirculation.
- Uniform water pressure of the system needs to maintained to keep the pad completely wet.
- The cooling efficiency of Poly Greenhouse can be increased by using double row of fan to 95%.

2.3.4 MATERIALS AND METHODS

To control the inside climate, air will be circulated and conditioned by means of fan and cooling pads. These pads are corrugated to cool, dehumidify and heat the air. After treatment, the air is distributed through the greenhouse. Apart this air is used for ventilation and dehumidification. The inputs of crop tests are designed to realize optimal control and technical implementation processes. Then, a growth will be able to control the temperature, relative humidity, and CO2 concentration.

3. Designs and Materials are structure of Poly Greenhouse

Poly Greenhouses are houses of radiant enjoyment covered with a transparent material in which crops are grown under controlled environmental conditions. Poly Greenhouse cultivation as well as other modes of controlled environment cultivation has been evolved to ensure favourable microclimates, which favours the crop production could be possible at through the year or part of the year as required. Poly Greenhouses and other technologies for controlled environment plant production are associated with the efficient production of ornamentals and fruits of high value in cold climates where outdoor production is not possible. The primary environmental parameter practically controlled is temperature, usually providing heat in temperate environmental conditions. However, environmental control can also include cooling in tropical countries. Transparencies, light control and other shading or diffusing applications, CO2 control, humidity levels, relative humidity, water, plant nutrition and pest control.

3.1 Types of Glazing Materials

The most common Poly Greenhouse glazing materials are glass, rigid plastics and plastic films.

Glass

Glass has the highest light transmission, but is the heaviest. Poly glass is used in the most expensive. Tempered or laminated glass is recommended because it is stronger allowing the fewer supporting bars, and it increases the safety for people working.

Plastic Films

Plastic films (e.g., polyethylene) are the cheapest Poly Greenhouse cladding material. An inflated Poly Greenhouse film is constructed with a double layer of plastic film. It is important to inflate the outside to inflate the two layers of film because this will significantly reduce potential sag between the layers.

3.2 Design

The structure has to carry the following loads and is to be designed accordingly.

a) Dead loads: weight of all permanent construction, including roofing and siding, equipment, water pipes and all other construction against it can be borne.

b) Wind load: The structure should be able to withstand winds of 110 kilometer per hour and or load 50 kg per square meter of wind pressure.

c) Snow load: These are to be taken as per the average snowfall of the location.

D) Wind effect

If the Poly Greenhouse is naturally ventilated, the advantage of natural wind direction has to be taken to the maximum possible. The maximum dimension (height or Poly Greenhouse should be perpendicular to the wind direction especially in summer. For fan and pad Poly Greenhouse the natural wind direction should be taken as this air blown by fan.

4. MODELS AND METHODS

CFD application in Poly Greenhouse development. Computational fluid dynamics is a sophisticated design and analysis tool that uses computers to simulate fluid flow, heat and mass transfer, phase change, chemical reaction, mechanical movement, and solid and fluid interaction. The advantage and the sophisticated model of a physical system to be studied in the many different design circumstances. CFD had the ability to efficiently develop optimal and improved fluid situations of fluid pressure, temperature and velocity, and has proved its effectiveness in system design and performance within many industries. The application of CFD in the agricultural industry is however more uncommon due to the above mentioned factor. The versatility, accuracy and cost-effectiveness offered by CFD has led to increased take-up in the agricultural engineering community to identify and analyze the problem domains of the Poly Greenhouse. This is supported by Norton et al. (2007) by the increase in peer reviewed papers of CFD applications in agriculture buildings.

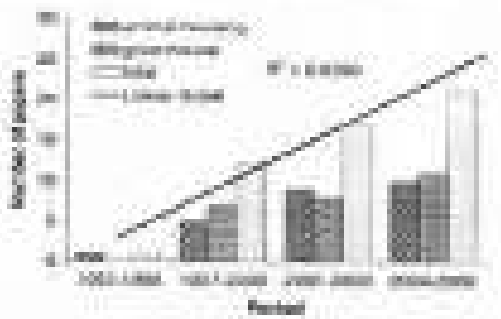

Figure 4.1: The number of published peer-reviewed publications of CFD applied to the ventilation of agricultural buildings. (Norton et al., 2007).

The values of the aerodynamic properties of the greenhouse shape and its boundary conditions were calculated using wind tunnel tests (Fidaros et al., 2004). The study may also conducted using the porous media approach for the validation of a computational wind tunnel, where the drag effects of the crop, in the simulated fluid flow equations.

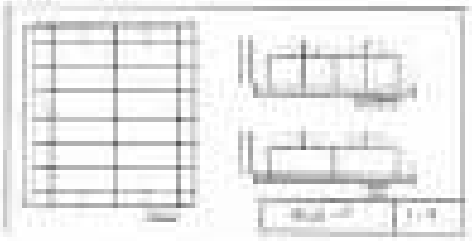

Fig: 4.1.1 Poly house structure layout

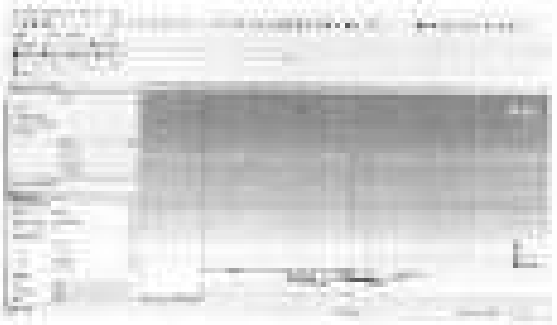

Fig: 4.1.2 3d Layout of green House

4.2 Heat Loss Calculations

Heat loss by conduction may be evaluated with the following equation:

$$Q = A(U) \cdot \Delta T$$

Where, Q = Heat Loss, BTU/hr

A = Area of Poly Greenhouse surface, sq ft

U = Heat transfer coefficient

ΔT = Air temperature difference between inside and outside

Heat different materials commonly used in Poly Greenhouse construction and their associated R-values.

After heat energy (Q value) the various components are assembled. Note that high R- values indicate less heat flow, but drag materials that absorb sunshine will conduct heat even they are not. Use vapor barriers to protect materials that are permeable to water vapor.

Heat is also lost to the ground underneath and beside a Poly Greenhouse. The perimeter heat loss may be added to other heating and the equation.

$Q = P(L)(T_i - T_o)$

P = Perimeter heat loss coefficient, BTU/hr °F ft

L = Distance around perimeter

Add additional heat losses in the construction heat losses. This equation the ventilation heat consists

Fig 5.1.1 Velocity contours for open ventilation greenhouse structure

Fig 5.1.2 Velocity vectors for open ventilation greenhouse structure

Fig 5.1.3 Temperature contours for open ventilation greenhouse structure

Fig 5.1.4 Pressure contours for open ventilation greenhouse structure

5.2 Closed Type Analysis results

Fig 5.2.1 Velocity contours for closed type ventilation greenhouse structure

5. RESULTS AND DISCUSSIONS

5.1 OPEN TYPE GREEN HOUSE

Fig

5.1.2Velocity vectors for closed type ventilation greenhouse structure

Fig 5.1.3Temperature contours for closed type ventilation greenhouse structure

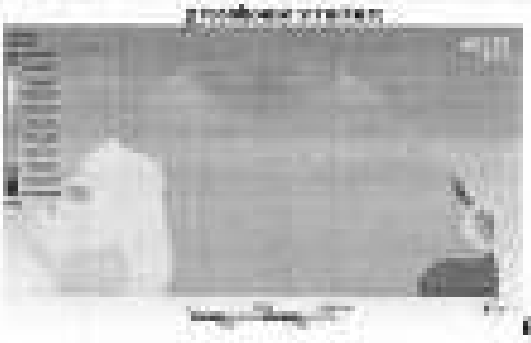

Fig

5.1.4Pressure contours for closed type ventilation greenhouse structure

5. CONCLUSIONS

1. For each case, the distribution of temperature inside the Poly Greenhouse was quite different and the resultant temperature profile was greatly affected by airflow. When the inlet velocity was 1 m/s and a temperature equal to 5°C, the temperature inside the Poly Greenhouse decrease significantly (from 18°C to 10°C). This dangerous aspect deeply and only on the inlet velocity and its temperature but also on its direction, as studied.

This paper describes and evaluates the computational facilities using the finite element method to study the effects of natural ventilation on Polyethylene indoor air properties especially during the days.

2. The influence of the inlet velocity on airflow and temperature patterns was successfully investigated for a closed Poly Greenhouse with continuous side openings by means of a CFD package. The simulation results indicated that the system had a considerable effect on Poly Greenhouse climate. A system through natural air velocity inside the Poly Greenhouse is impossible, inside the crop areas and airflow rate (with reference velocity of 1 m/s) from temperature increase. With respect to outside temperature (27 °C), maximum temperature augmentation was 3 °C higher for the Poly Greenhouse without screen and up to 7 °C higher for the Poly Greenhouse with screen.

Reference:

1. Bot, G.P.A., 1983. Poly Greenhouse climate: Basic physical processes in a dynamic model. PhD Thesis, Agricultural University of Wageningen.
2. Bouhoot, T., Hadlle, A., 1999. A simple Poly Greenhouse climate control model incorporating effects of outside wind and evaporative cooling. Agric For Meteorol. 95, 145–157.
3. Boulard, T., Roy, J.C., Lamrani, M.A., Fatnassi, N., 1995a. Characterizing and modelling the air flow and temperature profiles in a closed Poly Greenhouse during summer days. Mathematical and Control Applications in Agriculture and Horticulture. IFAC Workshop, Hannover, Germany.
4. Boulard, T., Papadakis, G., Kittas, C., Mermier, M., 1997a. Air flow and associated sensible heat exchanges in a naturally ventilated Poly Greenhouse. Agric. For. Meteorol. 86, 111–118.
5. Boulard, T., Haxaire, R., Lamrani, M.A., Roy, J.C., Jaffrin, A., 1995b. Characterization and modelling of Climate Poly Greenhouse induced by natural ventilation in a Poly Greenhouse. J. Agric. Eng. Res. 61, 181–189. CFD2000(5.7)UM v.1.0, 1998. Computational Fluid Dynamics Practice, Pacific Sierra Corp., USA.
6. Fatnassi, H.E., Bailey, B.J., 1992. Measurement and prediction of Poly Greenhouse ventilation rates. Agric. For. Meteorol. 58, 229–245.
7. Fidaros, D.K., Baxevanou, C.A., 2006. The influence of flow on environmental conditions in Poly Greenhouses. J. Agric. Eng. Res. 58, 301–315. Fröhlich, J., 1913. Wasserbewegung durch
8. Soulos, S. Ver. Deutsch. 45, 1782–1788. Hendry, R., 1999. Caractérisation et modélisation des écoulements d'air dans une serve. PhD Thesis, University of Nice Sophia Antipolis, Nancy (in), F.E., 1985. Solution of the sudden downward fluid flow equations by operator. J. Comput. Phys. 62, 36–54.
9. Jones, P.J., Wilcox, G.E., 1992. Computational fluid dynamics for building airflow prediction. Build. Env. 27, 321–338.
10. Kacira, S.M., Radzevsky, G.E., Christianson, L.L., 1992. Tests and model parameter studies for Poly Greenhouse ventilation. Trans. ASAE, 35, 1807–1823. Lamrani, M.A., 1997. Characterization and modelling of the natural ventilation of Mediterranean Poly Greenhouses. Ph.D. thesis, University of Agadir, Morocco.

DESIGN AND ANALYSIS OF TORSEN DIFFERENTIAL

D.J Satyanarayana[1], A. Sampath Kumar[2],
C.S.S. Kumar[3]
[1]Principal & Professor of Mechanical Engineering,
Sri Sai Institute of Engineering and Technology, Garugubilli, Parvathipuram,
Parvathipuram Manyam District, 535518
[2]Assistant Professor & Head of the Department of Mechanical Engineering,
Sri Sai Institute of Engineering and Technology, Garugubilli, Parvathipuram,
Parvathipuram Manyam District, 535518
[3]Research Engineer,
Sri Sai Institute of Engineering and Technology, Garugubilli, Parvathipuram,
Parvathipuram Manyam District, 535518
[1]satyanarayanadoora@gmail.com, [2]sampathkolam@gmail.com, [3]sridharan7133@gmail.com

Abstract— The Torsen differential is a purely mechanical device; it has no electronics, clutches or viscous fluids. The Torsen (from Torque Sensing) works as an open differential when the amount of torque going to each wheel is equal. As soon as one wheel starts to lose traction, the difference in torque causes the gears in the Torsen differential to load together. This paper presents an automotive differential in that if one wheel is held stationary, the counterpart wheel turns at twice its normal speed as was to save by example the complete scheme of automobile differential. The wheel without traction will spin without providing traction and the opposite wheel will stay still so that the car does not move. Torsen Differential is designed in CREO 2 and the fabrication of the gears in the differential is done, with 3D modeling and analysis is done in ANSYS 14 comparison with other differential, by this the traction vehicle is produced will be reduced and slipper's of vehicle in mud and wet roads will be completely avoided. Instead of going with All Wheel drive which is expensive in the market. Here design of worm and worm wheel gear shaft, key and helical gear is done in CREO 2 and analysis is done in a gear tooth of spur gear to find the efficiency in comparison with the standard worm wheel gear. By the use of Torsen Differential in an Automotive Vehicles the torque which is produced will be equally distributed even when the vehicle is moving in hilly areas or in mud or in wet areas instead of going with AWD which is expensive this also maintains the most used efficiency of worm and worm wheel increases with the new method we obtain 84 percent more.

Keywords—Torsen Differential, Worm and Worm Wheel gear, Ansys 14, CREO 2

INTRODUCTION

At the Automotive Vehicles moves with the differential, without the differential a vehicle cannot make a turn and cannot adjust its speed accordingly so wide differentials are used in all vehicles. In present day life some vehicles run with Front wheel drive and few vehicles run with rear wheel drive and few with all wheel drive, generally all wheel drive is used in all SUV's which can run everywhere in hilly areas, mud, wet areas with all wheel working but it is quite expensive vehicle is not affordable to all. This is the reason for a device known as a limited slip differential or traction control. The Solution to the above problem is to have a Torsen Differential. This Torsen Differential works as an open differential when the amount of torque going to each wheel is equal. As soon as one wheel starts to lose traction, the difference torque causes the gears in the Torsen differential to bind together. The design of gears in differential determines the torque bias ratio. When the left wheel is spinning faster than the right wheel which is used transfers the torque which is available in the left wheel to right wheel by this torque will be equally distributed to both the wheels known in India normally the most common vehicles used are Hatch Backs and present days Cross-over's are used but these vehicles when moving in slushy places and hilly areas the kind of open differentials which is used right now cannot equally distribute the torque to wheels, in order to avoid this problem a new kind of differential has to used to avoid such affordable cars as Cross-over's. This will reduce the skidding in such areas as well as such cars also be affordable.

LITERATURE SURVEY

Jesus Rajal [1], has performed the two Primary function of a differential system is to allow the driven wheels to rotate at different angular velocities relative to each other and also to transfer power to them from transmission. The first function is important to allow smooth turning as can be seen in the following Fig.1 which illustrates a left hand run.

Shih, Y. and Benevenuto, [2], has performed W Open differentials make use of a planetary gear set mechanism which distributes torque equally between the drive axles while allowing the wheels to rotate at different rates. The input shaft transmits torque from the driveline to a large ring gear within the differential carrier. When the vehicle is travelling in straight line the mechanism rotates changing and the differential casing rotates at same rate as the drive axles. As the vehicle enters the turn the gear set engages and the meshing of the pinion gears allows the drive axle to rotate at different speeds [3].

Hartvik Jill [4], has done an experiment in a model of the forces on the base of the driving wheel for loads presented by [6]. The forces transmitted by a tire to the ground are separated into longitudinal and lateral components. The longitudinal force is responsible for forward motion. When torque applied to the wheel exceeds the maximum longitudinal force the tire can transmit, slippage results, the maximum force transmittable by the tire is a function of the normal force acting against the footprint surface of the tire and that also is a function of the amount of load above the tire. During high speed cornering, the weight of a vehicle shifts away from the turning direction due to inertia creating a higher load on the outer wheel and a smaller load on the inner.

H. B. Pacejka, [7], has performed the analysis on the outer wheel ought to receive a progressively larger amount of torque over rides as the load shifts. Several dynamic solutions have been developed to mitigate the problems experienced by open differentials during the negotiation of turns at high speed. The maximum transmittable longitudinal force is therefore reduced for the inner tire and increased for the outer tire, thus the outer tire becomes capable of handling more torque and the inner tire, less. As torque is divided equally between both drive axles in an open differential, the inner wheel most experiences more torque than its tire can tolerate causing a spin and loss of control. In high performance conditions, this instability can pose a significant risk to the occupants safety.

DESIGN

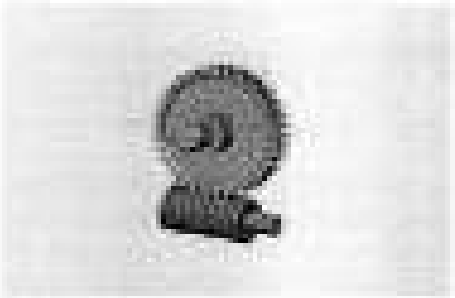

Fig 1 Worm and worm wheel is shown in one parametric 3-D software

Worm gear drives are used to transmit power between two non-intersecting shafts, which are, in general, at right angles to each other. The worm is a threaded screw, while the worm wheel is a toothed gear. The teeth on the worm wheel envelope the threads on the worm and give line contact between mating parts.

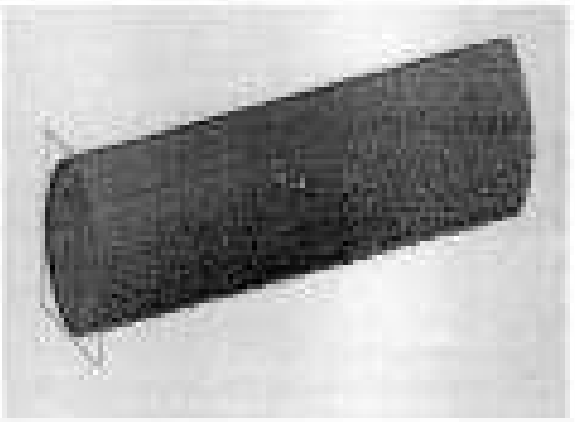

Fig 2 Shaft is shown in one parametric 3-D software

In order to transfer the power from one shaft to another, the various members such as pulley,gears etc., are mounted on it. These members along with the forces exerted upon them cause the shaft to bending in other words, we may say that a shaft is used for the transmission of torque and bending moment.

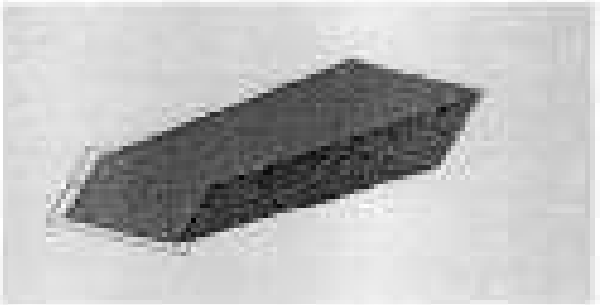

Fig 3 Key is shown in one parametric 3-D software

Key is a piece of mild steel inserted between the shaft and hub or boss of the pulley to connect these together in order to

power relative motion between them. It is always mounted parallel to the axis of the shaft. Keys are used as temporary fastenings and are subjected to considerable crushing and shearing stresses. A keyway is a slot or recess in a shaft and hub of the pulley to accommodate a key.

Fig 4 Propeller spline shaft gear

The propeller shaft transmits power from the gear box to the rear axle. The splines on the axle of the propeller shaft fit perfectly into the splines in the sleeve. This allows a length variation between the driving and the driven axle as very slightly without disrupting the drive and input bearings.

Fig.5 Differential gear assembly with worm gears

With a single start worm, for each 360° turn of the worm, the worm gear advances only one tooth of the gear. Therefore, regardless of the worm's size, the gear ratio is the size of the worm gear to 1. Given a single start worm, a 50 tooth worm gear will reduce the speed by the ratio of 50:1. With spur gears, a gear of 12 teeth (the smallest size permissible). If designed to good engineering practice would have to be matched with a 240 tooth gear to achieve the same ratio of 20:1.

Fig 6 Shaft gear for rear wheel

ANALYSIS

Static structure

Fig 7 shows the worm and worm wheel single tooth is considered for the analysis here is where load is applied and fixed with all the forces acts on it simultaneously and failure of that tooth in different stages is calculated.

Static Structure Failure

Fig 8 shows the failure analysis are known in different stages plastic intensity and at what load it could fail maximum strength at what load it can with stand maximum is known here in this analysis. And the efficiencies are known by the loads in relation to power and torque.

Thermal analysis

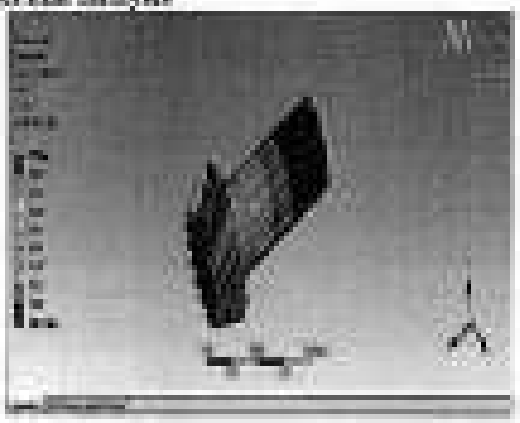

Figure 9 shows the temperature distribution on the gear tooth, maximum of 180°c was found The initial temperature of the was specified as 100K which was due to preheating. The analysis the maximum temperature of 480K which was applied temperature.

Direction Heat flux along X axis

Figure 10 shows the thermal stress of the tooth, maximum of 220 was observed and The maximum thermal stress obtained in the analysis was found to be below the permissible stress and this shows that the above analysis has been successfully carried under with the loads.

Heat flux along y Axis

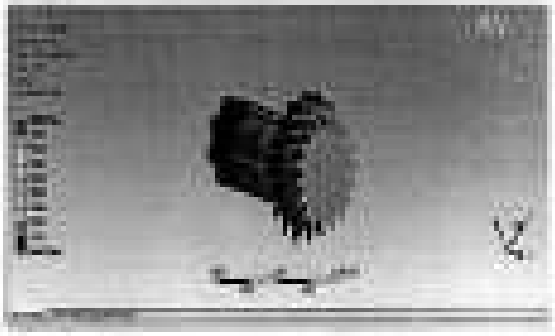

Figure 11 shows the Heat flux variation across the die in X-axis. The maximum heat flux was found to be 1.0950e5 W/m² at the end of the tooth. The total heat flux was maximum at the tip due to thermal load specified. Heat flux is quantity of heat flowing per unit area.

Heat flux along X Axis

The Figure 12 shows the variation of heat flux in X direction along the tooth.

The heat flux along X direction is very minimum at the opening face of the tooth this shows the non uniformity of temperature distribution on the gear tooth for the thermal load of 150°C

Temperature distribution

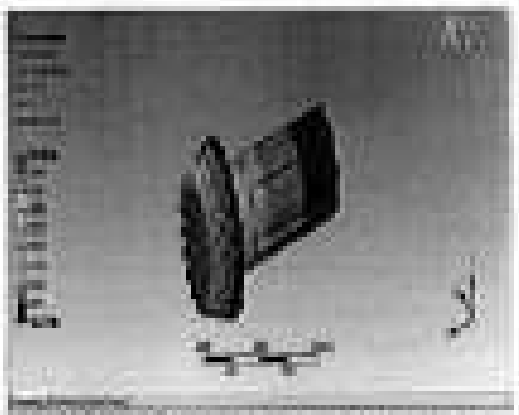

Figure 13 shows the thermal error of the tooth, maximum of 200 was observed and The maximum thermal error obtained in the analysis was found to be below the permissible error and this shows that static analysis has been successfully carried under with the loads

Temperature distribution along XYZ axis

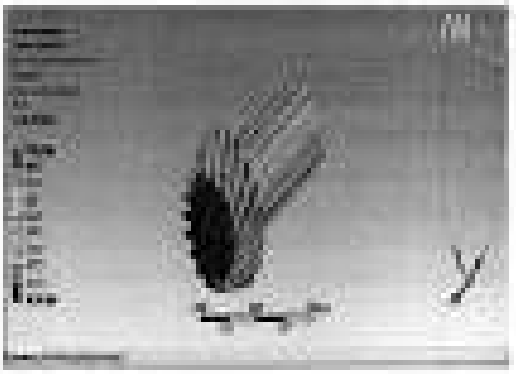

Figure 14 shows the temperature distribution on the teeth, and a maximum of 84°C was found. The tooth has the minimum temperature of 30°C which was applied temperature

Temperature distribution along XY Plane

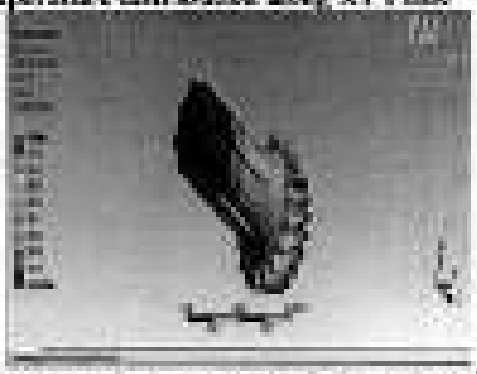

Figure 15 shows the temperature distribution on the teeth, a) point maximum of 147°C was found. The tooth has the minimum temperature of 30°C which was applied temperature

Temperature distribution along YZ Plane

Figure 16 shows the temperature distribution on the teeth, a maximum of 216°C was found. The tooth has the minimum temperature of 30°C which was applied temperature

Temperature gradient

Figure 7 shows the temperature distribution on the teeth in one plane. The initial temperature of the gear specified as 34°C which was due to preheating. The tooth has the maximum temperature of 98°C which was applied to operation.

RESULTS & DISCUSSIONS

TABLE 1 Shows the observation of conventional system efficiency by comparison of load with effort. Increasing the load simultaneously on helical gear the effort and efficiency of these gear are calculated with the conventional gears which gives an average value of about 85 percent approximately.

Observation Table for conventional system

Sl. No.	Load (N)	Effort (N)	Efficiency	Avg. Efficiency
1	1471	1.338	51.828	83.78%
2	1962	1.810	50.684	
3	2452	1.275	51.779	
4	2943	1.368	50.484	
5	3434	2.060	51.286	
6	4414	2.305	51.558	
7	4905	2.402	50.850	

Table 2 shows the comparing the above results from the conventional system to the actual system so called efficiency of the running worm pair is increased increasing the load simultaneously on helical gear the speed,Torque,Power and efficiency of the worm and worm wheel gear are calculated with the conventional gears which gives an average value of about 84 percent approximately which is more than the conventional.

Result table for running worm pair system

Sl. No	No. of gear	Speed (Nm)	Torque (Tw)	Power (Pw)	Efficiency (η)	Avg. Efficiency (%)
1	100	9.68	0.85	0.10	50.78	84.00
2	200	8.20	0.81	0.20	53.01	
3	300	7.68	1.26	0.47	73.38	
4	400	7.28	1.15	0.84	82.71	
5	500	6.86	1.17	0.96	83.73	
6	600	6.78	0.93	0.83	93.02	
7	700	6.50	1.20	1.08	94.05	
8	800	6.30	1.20	1.20	94.05	
9	900	6.40	1.00	1.14	93.11	
10	1000	6.00	1.00	1.20	94.05	

Worm Gear And Sliding Worm Pair System

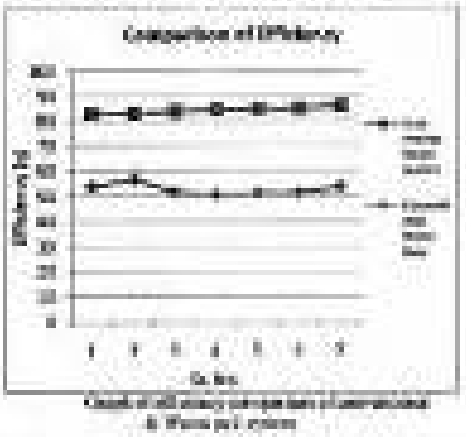

Comparison of efficiency between conventional & Worm pair system

Fig 6 show the efficiency of worm pair system in comparison with the conventional to standard experiment values, by using worm gear pair we are achieving 84% efficiency. By increasing the load on the worm and worm wheel gear gradually the effort is also become from conventional gears is compared with the practical gear values which is higher than the previous one.

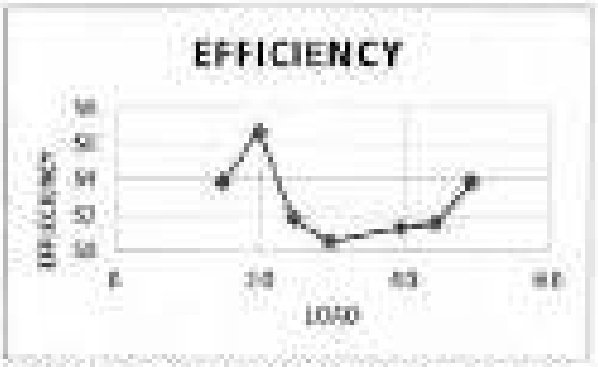

Fig 5 show the efficiency of worm pair system in comparison with the load to standard experiment values, by using worm gear pair. As the load is increasing the efficiency first increases and then decreases slowly and then increases finally by reaching the maximum load.

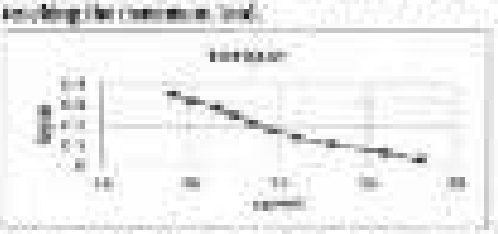

Fig 10 show the torque variation of worm pair system in comparison with the speed to standard experiment values, by using worm gear pair. As the speed of the vehicle is increased initially the torque produced should be high initially and then when it reaches to the maximum speed it has to be minimum here in this figure shows the same where initially it is high and then finally reached to the optimum value.

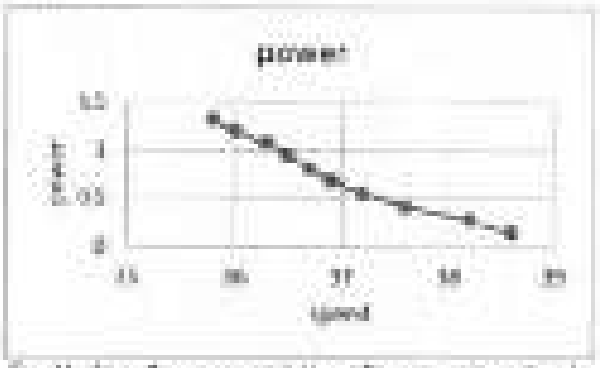

Fig 11 show the power variation of worm gear system in comparison with the speed to standard experiment values by using worm gear pair. Here by increasing the speed of the vehicle the power loss to be increased as when the vehicle is turning or moving in the slippery areas the power produced has to shared equally by the wheels so it should be reliably low and it should increase by increasing the speed this is achieved here.

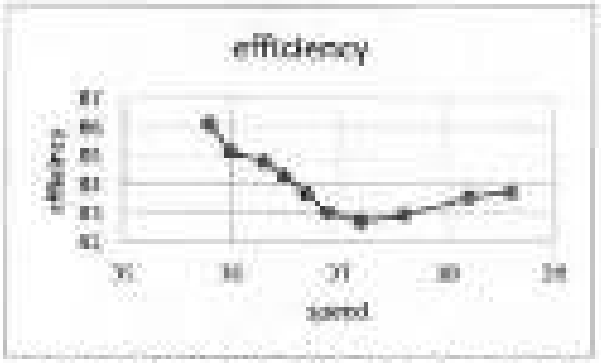

Fig 12 show the power variation of worm gear system in comparison with the speed to standard experiment values by using worm gear pair. By likely increasing the speed of the vehicle initially which has the minimum efficiency for the worm wheel has to be increased and then slowly it decreases and then reaches to the maximum value which is achieved 84 more than the conventional one.

CONCLUSIONS

This work would help for realizing a complete system with FWD or RWD. A more logical and realistic method is proposed considering simulations as well as further real-time implementation of Torsen differential in different type of analysis. An established and a promising outcome a real-time for all vehicles in all future works.

The presented work was aimed at reducing the sliding and pits to noisy issues in all vehicles without all wheel drive. The drive shaft of a standard values of a car was chosen for determining the dimensions which were then used for creating a model in CREO 2. Being a complex availability for a number of parts it has to be analyzed in ANSYS 14 work bench. Despites the improvements made in design there is of course still room for improvement.

The finite element analysis is performed to analyze the efficiency of worm and worm wheel gear. It is seen that the efficiency is approx. 84% which is more than conventional worm gear. Therefore from it would also that design is safe. In concluding the words since the torsen differential is very much useful in reducing a considerable amount of loss due to the transmission through a differential in all FWD, RWD vehicles from pits to noisy issues and in the longer runs this could be a reason for the above said solutions.

References

[1] Comparative Study of Torsen Differential Ishan Bagul Dept. of Mechanical Engineering, R.K.G.I.T. Ghaziabad, Uttar Pradesh, India, ISSN : 2249-9962 (Online) | ISSN : 2249-9970, IJEMET Vol. 5, Issue 1, November 2014 - April 2015

[2] Blocking Coefficient of a Differential, 12th WSEAS International Conference on AUTOMATIC CONTROL, MODELLING & SIMULATION

[3] The development of a differential for the improvement of traction control by E F CRICHTON JR, BSME Gleason Corporation, Rochester, New York, United States of America

[4] Comparative Study of Torsen Differential IJEMET Vol 5, Issue 1, November 2014 - April 2015 ISSN : 2249-9962 (Online)

[5] The Analysis of the Geometrical Features Influence of the Helical Gears on the Blocking Coefficient of a Differential 12th WSEAS International Conference on AUTOMATIC CONTROL, MODELLING & SIMULATION

[6] Simulation of Differentials in Four-Wheel Drive Vehicles Using Multibody Dynamics ASME 2011 International Design Engineering Technical Conferences and Computers and Information in Engineering Conference

[7] The Automotive chassis: Engineering principles, SAE International.

[8] Driveline Systems of Ground Vehicles: Theory and Design

[9] Gopal singh vol. 1st Edition 12th -2011 ISBN 978-81-7814-417

[10] http://www.sae.org/

International Conference on Emerging Trends in Science Technology Engineering and Management
26th & 27th October 2015

CFD ANALYSIS ON TURBULENT CONVECTION HEAT TRANSFER WITH Fe3O4 NANOPARTICLES IN WATER

L.Ramakrishnan, D.L.Satyanarayana, J. Prasanth Rao

Department Of Mechanical Engineering, Sri Indian Institute of Science and Technology

Abstract— A theoretical study of single phase through a pipe will be carried out. The CFD simulation of heat transfer characteristics of a nanofluid in a circular tube under constant heat flux will be considered using CFX solver (version 13.0) in the turbulent flow. Fe3O4nanoparticles in water with concentrations of 0.02%, 0.1%, 0.3%, and 0.6% will use in this simulation. All of the thermo-physical properties of nanofluids are assumed to be temperature independent. The average particle sizes of 36 nm will be used in this research. The goal is to find out the change in heat transfer coefficient with changing the Reynolds number and the concentration of nano-particles. The maximum convective heat transfer coefficient will be observed with the change in concentration of nano-particles in water. The computational fluid dynamics (CFD) model equations will be solved to predict the hydrodynamic and thermal behaviour of the pipe. The geometry of the problem and meshing of it will be done in ANSYS Workbench.

Keywords – Nano Technology, Heat Transfer, CFD Analysis

I. INTRODUCTION

Thermal conductivity of Fe3O4 nanofluids is explained by many researchers Most of the experimental work is undertaken for the estimation of heat transfer coefficient of Al2O3 and Cu nanofluids in plain tube and some researchers have concentrated for the estimation of heat transfer coefficient of Al2O3 nanofluid in plain tube with twisted and wire coiled inserts.

Thermal conductivity of magnetic Fe3O4 nanofluids literature is available, experimental turbulent convective heat transfer and friction factor of Fe3O4 magnetic nanofluid for tube flow and with twisted tape inserts data is not available. The advantage with this fluid is separation of magnetic nanoparticles (Fe3O4) from the base fluid is possible, which is not possible with non magnetic (Al2O3,Cu and TiO2 type nano particles. The present investigation is carried out to estimate turbulent forced convective heat transfer and friction factor at different volume concentrations of Fe3O4nanofluid in a plain tube under turbulent flow conditions. Based on the experimental data generalized regression equations are developed for Nusselt number and friction factor.

PREPARATION OF NANOFLUID

There are two primary methods to prepare nanofluids: A two-step process in which nanoparticles or nanotubes are first produced as a dry powder. The resulting nanoparticles are then dispersed into a fluid in a second step. Single-step nanofluid processing methods have also been developed. Several studies, including the earliest investigations of nanofluids, used a two-step process in which nanoparticles are first produced as a dry powder. This method is most extensively used to produce nanofluids because nanopowders are commercially available nowadays.

The nanoparticles may agglomerate during the drying, storage, and transportation process, leading to difficulties in the following dispersion steps of two-

way method. Consequently, the stability and thermal conductivity of nanofluid are not ideal. In addition, the production cost is high.

OBJECTIVES:

A theoretical study of single phase through a pipe will be carried out. The CFD simulation of heat transfer characteristics of a nanofluid in a circular tube under constant heat flux will be considered using CFX solver (version 13.0) in the turbulent flow. $FeIO_4$nanoparticles in water with concentrations of 0.02%, 0.1%, 0.2%, and 0.6% will used in the simulation. All of the thermo-physical properties of nanofluids are assumed to be temperature independent. The average particle sizes of 36 nm will be used in this research. The goal is to find out the change in heat transfer coefficient with changing the Reynolds number and the concentration of nanoparticles. The maximum convective heat transfer coefficient will be observed with the change in concentration of nano-particles in water. The computational fluid dynamics (CFD) model equations will be solved to predict the hydrodynamic and thermal behavior of the pipe. The geometry of the problem and meshing of it will be done in ANSYS Workbench. The models will get solved by ANSYS CFX 13.0 solver.

Enhancement Mechanisms:

There are many studies in the literature regarding the effect of Brownian motion on the thermal conductivity of nanofluids. Bhattacharya et al. [04] used Brownian dynamics simulation to determine the effective thermal conductivity of nanofluids, by considering the Brownian motion of the nanoparticles. Effective thermal conductivity of the nanofluid was defined as:

$$k_{nf} = \phi k_p + (1-\phi)k_f ,$$

where k_p is not simply the bulk thermal conductivity of the nanoparticles, but it also includes the effect of the Brownian motion of the nanoparticles on the thermal conductivity. A method called the Brownian dynamics simulation was developed, the expressions were provided to calculate k_p, then the effective thermal conductivity of Ethylene glycol and Al_2O_3/ethylene glycol nanofluids were calculated for different particle volume fractions. The results were compared with previous experimental data [43, 63] and they were found to be in agreement. The prediction of the Hamilton and Crosser [44] model (Eq. 2, 1) for these two nanofluids was also included in the comparison. It was found that conduction-based Hamilton and Crosser model underpredicted the effective thermal conductivity of the nanofluid, since it does not take into account the Brownian motion of the particles within the base fluid.

Importance of numerical simulations:

Numerical simulations of fluids, often known as CFD (computational fluid dynamics), has become one of the three basic approaches that can be employed to solve problems in fluid dynamics and heat transfer, the other two approaches being experimental and analytical methods. CFD not only employs disciplines of fluid mechanics with mathematics, but it also uses the knowledge of computer science. With the rapid advancement of digital computers, the numerical approaches emerged as another viable approach in

studying fluid and heat transfer problems. Density of nanofluids can be determined by using the following expression

$$\rho_{nf} = \phi\rho_p + (1-\phi)\rho_f \quad (1)$$

Here, ϕ is particle volume fraction and subscripts nf, p, and f correspond to nanofluid, particle, and base fluid, respectively. Pak and Cho [13] experimentally showed that Eq. (1) is an accurate expression for determining the density of nanofluids.

Specific Heat

There are two expressions for determining the specific heat of nanofluids

$$c_{p,nf} = \phi c_{p,p} + (1-\phi)c_{p,f}$$

$$(\rho c_p)_{nf} = \phi(\rho c_p)_p + (1-\phi)(\rho c_p)_f$$

It is thought that above Eq is theoretically more consistent since specific heat is a mass specific quantity whose effect depends on the density of the components of a mixture.

SIMULATION OF SINGLE PHASE FLUID FLOW:

SPECIFICATION OF PROBLEM :

Consider a steady state fluid flowing through a circular pipe of constant cross section as shown in Fig. 3. The diameter and length of circular channel are 0.014 m and 1.5 m respectively. The inlet velocity is a (m/s), which is constant over the inlet cross-section. The fluid exhausts into the ambient atmosphere which is at a pressure of 1 atm.

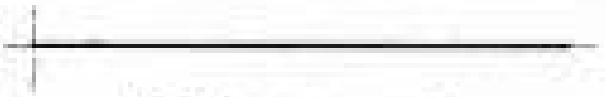

Fig 3 circular pipe geometry

As fluid flows through in a pipe at both hydraulic and thermally fully developed condition, the Nusselt number is constant for laminar flow and it follows the Dittus-Boelter equation for turbulent flow.

MESHING OF GEOMETRY:

Structured meshing method done in ANSYS Workbench was used for meshing the geometry. Nodes were created. The 2D geometry of circular channel with structured mesh is shown in Fig. 4.

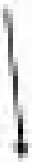

Fig 4 Meshed model of pipe with nanofluid

MATERIAL PROPERTIES

Pure water is used as base working fluid andnaparticle Fe3O4nanofluid is taken as nanoparticles.The density, heat capacity and thermal conductivity of Fe3O4are5180kg/m3,670J/KgK and 9.34W/mK respectively. The properties of nanofluids (nf) are given inTable 4.2 at 30°C temperature and 100 kPa pressure

Table 1 Water base fluid properties with different concentration of Fe3O4 nanoparticles

Volume fraction (%)	Density (kg/m3)	Specific heat (J/kgK)	Thermal conductivity	Viscosity
0.02	999.33	4312.10	0.609337	0.0008018
0.1	999.88	4044.82	0.610165	0.0008250
0.3	1000.25	4136.49	0.611713	0.0008668
0.6	1001.804	4111.60	0.61978	0.0008864

BOUNDARY CONDITIONS: A no slip boundary condition was assigned for the tube pipes wall

surfaces, where both velocity components were set to zero at that boundary. A constant heat flux (13359 W/m2) is applied on the channel wall. A uniform mass flow inlet and a constant inlet temperature were assigned at the channel inlet. At the exit, pressure was

Boundary conditions

METHOD OF SOLUTIONS

There are two ways to solve the problem stated above: (i) analytical method and (ii) CFD method. Lee and Mudawar, 2007 have used analytical method. The method consists of calculation of heat transfer coefficient (h) from either of Eq. 4.5 or Eq. 4.6 depending on whether flow is laminar or turbulent, calculation of bulk mean temperature of fluid using Eq. 4.32 followed by the calculation of wall temperature using eq. 4.11. The results given by Lee and Mudwar, 2007 are having errors in wall temperature and mean temperature calculation at the pipe inlet. [illegible] flow in the present study, the analytical values of heat [illegible] coefficient are calculated using Eq. 4.5 or Eq. 4.6. The heat transfer coefficient are also obtained using CFD method and then both the values are compared. The CFD method follows the use of commercial software ANSYS CFX 15.0 to solve the problem. The specified solver uses a pressure correction based iterative SIMPLE algorithm with 1st order upwind

scheme for discretizing the convective transport terms. The convergence criteria for all the dependent

variables are specified at 0.8. The default values of under-relaxation factor as shown in Table 4.3 are used in the simulation work.

Results and discussion

Pure water

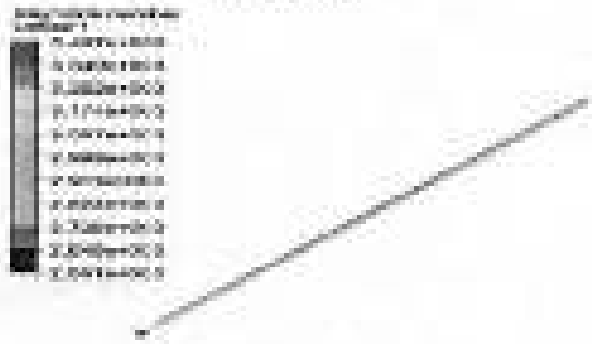

0.02% nanofluid

0.1% nanofluid

0.5% nanofluid

0.05% nanofluid

Fig : Friction factor plot

Pure water

0.05% nanofluid

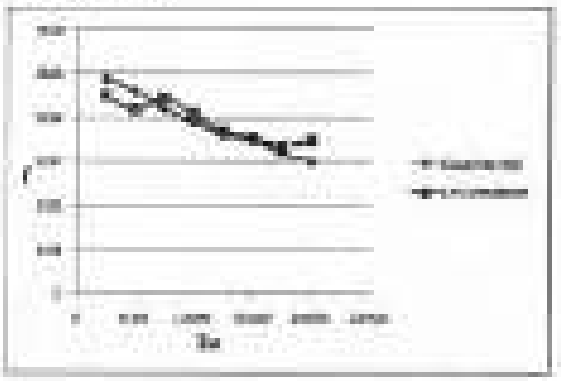

Fig : Reynolds num Vs Nusselt Number Graph

In the figure, it is seen that the local Nusselt number is larger for nanofluids throughout the tube. This is

mainly due to the thermal dispersion in the flow. Thermal dispersion results in a higher effective thermal conductivity at the center of the tube which Nusselt number becomes higher when compared to the flow of pure water. Figure above also shows that increasing particle volume fraction increases Nusselt number. This is due to the fact that the effect of thermal dispersion becomes more pronounced with increasing particle volume fraction.

It should be noted that the fully developed nanofluid Nusselt number values are also higher than pure water case. Associated values for different particle volume fractions of the Fe_3O_4/water nanofluid are presented in above figures. It is seen that increasing particle volume fraction increases the fully developed Nusselt number.

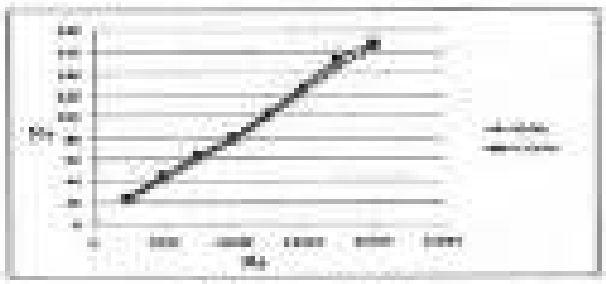

0.1% nanofluid

0.6% nanofluid

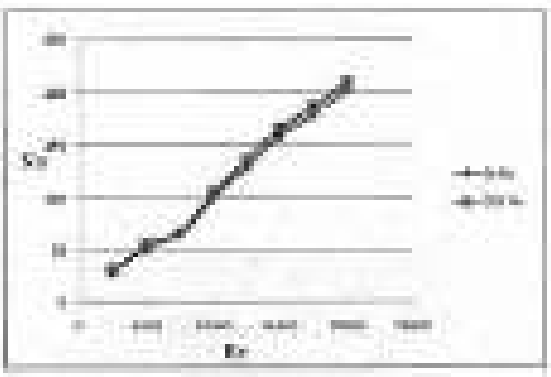

Fig 13: Reynolds Number Vs friction Factor graph.

CONCLUSION

The heat transfer coefficient in the developed region of pipe flow containing Fe_3O_4 water nanofluid during the constant heat flux was simulated using CFD. The focal point of investigation was to evaluate the effect of particle volume concentration on convective heat transfer characteristics in the developed region of the tube flow containing water-Fe_3O_4 nanofluid. It was observed that 0.6% of nanofluids showed higher heat transfer characteristics than that of the base fluid (water).

- The computational results successfully validated the analytical data for circular pipe channel.
- Heat transfer coefficient is constant throughout the circular channel due to its fully developed conditions
- As the concentration of nanoparticle increases heat transfer coefficient also increases, with the increase in Nusselt number
- Wall temperature increase within the flow direction of circular channel at very low Re simulation of Single Phase Fluid Flow in a Circular channel

FUTURE SCOPE

- In the present thesis Fe_3O_4 is used with the base fluid, it can be counted by using other nano fluids such as Al$_2$O$_3$ or CuO.
- The analysis can be extended for flow through radiator tubes and heat exchanger tubes instead considering single tube.

- Sedimentation aspects of nano fluids should be studied.
- Analysis can be done for different volume fractions of nano fluids which are not considered in the present thesis

REFERENCES

[1] J. Buongiorno, Convective transport in nanofluids, J Heat Transfer 128 (3) (2006) 240–250.

[2] S.K. Das, S.U.S. Choi, W. Yu, T. Pradeep, Nanofluids: Science and Technology, Wiley-Inter Science (2007) 397

[3] S. Kakac, A. Pramuanjaroenkij, Review of convective heat transfer enhancement with nanofluids, Int. J. Heat Mass Transfer 52 (2009) 3187–3196

[4] R. Parish, R.S. Lee, Magnetic field induced enhancement in thermal conductivity of magnetite nanofluid, Journal of Applied Physics 107 (2010)094321.

[5] V.K. Pershin, E.B. Gorbenkov, N.F. Moskovich, Thermal conductivity of magnetic magnetic fluids, J. Magnet. Magnet. Mater. 85 (1987) 231–234.

[6] J. Philip, P.D. Shima, B. Raj, Enhancement of thermal conductivity in magnetite based flux no chainlike structures, Appl. Phys. Lett. 91 (2007)203108-203108-3.

[7] W. Yu, H. Xie, L. Chen, Y. Li, Enhancement of thermal conductivity of kerosene-based Fe3O4 nanofluids prepared via phase-transfer method, Coll. Surf. A: Physicochem. Eng. Aspects 355 (2010) 109–113.

[8] D. Wen, Y. Ding, Experimental investigation into convective heat transfer of nanofluid at the entrance region under laminar flow conditions, Int. J. Heat Mass Transfer 47 (24) (2004) 5181–5188.

[9] S.Z. Heris, M.N. Esfahany, S.Gh. Etemad, Experimental investigation of convective heat transfer of Al2O3/water nanofluid in circular tube, Int. J. Heat Fluid Flow 28 (2007) 203–210.

[10] Y. Xuan, Q. Li, Investigation on convective heat transfer and flow features of nanofluids, J. Heat Transfer 125 (2003) 151–155.

[11] B.C. Pak, Y.I. Cho, Hydrodynamic and heat transfer study of dispersed fluids with submicron metallic oxide particles, Exper. Heat Transfer 11 (1998) 151–170.

[12] E. Smithberg, F. Landis, Friction and forced convective heat transfer characteristics in tube with helical-tape swirl generators, J. Heat Transfer108 (1986) 39–49.

[13] R.P. Lopina, A.E. Bergles, Heat transfer and pressure drop in tape-generated swirl flow of single phase water, J. Heat Transfer 91 (1969) 434–442.

[14] R.M. Manglik, A.E. Bergles, Heat transfer and pressure drop correlations for twisted-tape inserts in isothermal tubes: part II-transition and turbulent flows, J. Heat Transfer 115 (1993) 890–896.

[15] P.K. Sarma, P.S. Kishore, V. Sharma Rao, T. Subrahmanyam, A combined approach to predict coefficients and convective heat transfer characteristics for tube with twisted tape inserts for a wide range of Re and Pr, Int. J. Thermal Sci. 44 (2005) 393–398.

ADVANCED FUEL OPERATED INTERNAL COMBUSTION ENGINES

Dr.I.Satyanarayana[1], Y Srikanth Reddy[2], Anil Kumar[3]

[1]Principal & Professor of Mechanical Engineering
Sri Sai Institute of Engineering and Technology, Aleripalli, Nandyalapuram,
Ranga Reddy District- 501510

[2]M.Tech Sri Sai Institute of Engineering and Technology, Aleripalli, Nandyalapuram,
Ranga Reddy District- 501510

[3]Associate Professor, Sri Sai Institute of Engineering and Technology, Aleripalli, Nandyalapuram,
Ranga Reddy District- 501510

[1]satyaprofessor@gmail.com, [2]srikanthreddy7193@gmail.com
[3]anilkumar71.k@gmail.co

Abstract—Fossil fuels (i.e., petroleum, natural gas and coal), which meet most of the world's energy demand today, are being depleted rapidly. Also, their combustion products are causing global problems, such as the greenhouse effect, ozone layer depletion, and more and pollution, which are posing great danger for our environment, and eventually, for the total life on our planet. Many engineers and scientists agree that the solution to all of these global problems would be to replace the existing fossil fuel system with the clean hydrogen energy system.

Hydrogen is a very efficient and clean fuel. Its combustion will produce no greenhouse gases, no ozone layer depleting chemicals, and little or no acid rain ingredients and pollution. Hydrogen, produced from renewable energy (solar, wind, etc.) sources, would result in a permanent energy system which would never have to be changed.

However, at the present time, hydrogen is not competitive with other energy carriers. Global utilization of fossil fuels for energy needs is rapidly resulting in critical environmental problems throughout the world. There is an urgent need of implementing the hydrogen technology. A worldwide conversion from fossil fuels to hydrogen would eliminate many of the problems and their consequences. The production of hydrogen from non-polluting sources is the ideal way.

Solar hydrogen is a clean energy carrier. Hydrogen obtained from solar energy is ecologically responsible along its entire energy conversion chain. Energy stored in hydrogen would be available at any time and at any place on Earth, regardless of when or where the solar irradiance, the hydropower, or other renewable sources such as biomass, ocean energy or wind energy was converted. Solar hydrogen is a clean energy carrier.

Solar hydrogen combines the advantages of hydrocarbons (storability and transportability) with the advantages of solar energy (ecological acceptability, renewability and low risk). Solar hydrogen has no need for the carbon atom, which makes the hydrocarbons almost infinitely storable at room temperature, but is also the reason for their negative ecological impact.

Keywords—Electrolysis of water, Photolysis, thermal decomposition of water and finally produced the HHO gas for IC Engines.

INTRODUCTION

Fossil fuels possess very useful properties not shared by non-conventional energy sources that have made them popular during the last century. Unfortunately, fossil fuels are not renewable. In addition, the pollutants emitted by fossil energy systems (e.g. CO, CO_2, Dalfin, SOx, NOx, radioactivity, heavy metals, ashes, etc.) are greater and more damaging than those that might be produced by a renewable based hydrogen energy system (Winter CJ. 1989).

Solar hydrogen is a clean energy carrier. Hydrogen obtained from solar energy is ecologically responsible along its entire energy conversion chain. Energy stored in hydrogen would be available at any time and at any place on Earth, regardless of when or where the solar irradiance, the hydropower, or other renewable sources such as biomass, ocean energy or wind energy was converted. Solar hydrogen is a clean energy carrier. It makes solar energy as storable and transportable as oil and natural gas are by nature, but without the burden of their negative environmental impact. Solar hydrogen combines the advantages of hydrocarbons (storability and transportability) with the advantages of solar energy (ecological acceptability, renewability and low risk). Solar hydrogen has no need for the carbon atom, which makes the hydrocarbons almost infinitely storable at room temperature, but is also the source for their negative ecological impact.

Hydrogen has long been recognized as a fuel having some unique and highly desirable properties for application as a fuel in engines. It is the only fuel that can be produced entirely from the plentiful renewable resource water, though through the expenditure of relatively much energy. Its combustion in oxygen produces uniquely only water but in air it also produces some oxides of nitrogen. These features make hydrogen an excellent fuel to potentially meet the ever increasingly strict environmental controls of exhaust emissions from combustion devices, including the reduction of greenhouse gas emissions.

The use of hydrogen as an engine fuel has been attempted on very limited basis with varying degrees of success by numerous investigators over many decades, and much information about their findings is available in the open literature. However, these reported performance data do not display consistent agreement between various investigators. There is also a tendency to focus on results obtained in specific engines and over narrowly charged operating conditions. Moreover, the increasingly greater emphasis being placed on the nature of emissions and efficiency considerations often makes much of the very early work fragmentary and mainly of historical value. Obviously, there is a need to be aware of what has been achieved in this field while focusing both on the attractive features as well as the potential limitations and associated drawbacks that need to be overcome for hydrogen to become a widely accepted and used fuel for engine applications. Also, there is a need to indicate practical steps for operating and design measures to be developed and incorporated for hydrogen to achieve its full potential as an attractive and superior engine fuel.

LITERATURE OF SURVEY

1.1 Use of H_2 as IC engine fuel

In the early years of the development of internal combustion engines hydrogen was not the "exotic" fuel that it is today. Water splitting by electrolysis was a well known laboratory phenomenon. Otto, in the early 1870s, considered a variety of fuels for his internal combustion engine, including hydrogen. He rejected gasoline as being too dangerous. Later developments in combustion technology made gasoline safe.

Most early engine experiments were designed for burning a variety of gases, including natural gas and propane. When hydrogen was used in these engines it would backfire. Since hydrogen burns faster than other fuels, the fuel-air mixture would ignite in the intake manifold before the intake valve could close. Injected water controlled the backfiring. Hydrogen gave less power than gasoline with or without the water.

1.2 HHO Gas

The HHO gas is nothing but the electrolyte form of water. It is also called as oxy hydrogen or brown gas. It is produced by electrolysis process, where an electrical power source is connected to two electrodes and which are placed in a mixture of water and electrolyte. Oxyhydrogen appears to be a favorable alternative fuel on account of its high specific energy per unit weight, its all-time availability as a component of water, good combustion characteristics and eco-friendly, fast burning and higher flame propagation rates are the attractive features of HHO gas. HHO gas is a mixture of hydrogen and oxygen gases, typically in a 2:1 atomic ratio, the same proportion as water. At normal temperature and pressure, oxyhydrogen can burn when it is between about 4% and 94%

hydrogen by volume, with a flame temperature around 2000°C. Oxyhydrogen will combust (turning into water vapor) and releasing energy which sustains the reaction) when brought to its auto-ignition temperature. For a stoichiometric mixture at normal atmospheric pressure, this is about 570°C(1065°F). The minimum energy required to ignite such a mixture with a spark is about 0.02mJ. The quantity of heat evolved, according to Julius Thomson, is 34,180 calories for each gram of hydrogen burned. This heat-disturbance is quite independent of the mode in which the process is conducted, but the temperature of the flame is dependent on the circumstances under which the process takes place. It obviously attains its maximum in the case of the firing of pure "oxyhydrogen" gas (a mixture of hydrogen with exactly half its volume of oxygen, the quantity it combines with in becoming water, Gerson Kaufmann). It becomes less when the "oxyhydrogen" is mixed with excess of one or the other of the two reacting gases, or an inert gas such as nitrogen, because in any such case the same amount of heat spreads over a larger quantity of matter.

1.3 Performance characteristics of petrol and HHO gas when used as a fuel

The performance of petrol engine with HHO up to 30% of full load, brake thermal efficiency will remain same for both the case (petrol and blended). Beyond this point brake thermal efficiency increase linearly for the mixture of petrol and HHO gas. And also up to 30% of full load for both cases the brake thermal fuel consumption increases linearly and reaches maximum value. BSFC decreases more rapidly for fuel mixture of petrol and HHO gas than petrol as a fuel.

By comparing the results of above two cases the mixture of petrol and HHO gas gives better result for higher loads. Since HHO is highly combustible fuel, it ensures the complete combustion of the fuel mixture. Thus it results in the increased speed of the engine and in turn increases the power output.

1.4 PROPERTIES OF HHO GAS

There are many unique and unusual properties that HHO Gas possesses. Below is a list of some of the properties.Gas proves to be odorless, colorless and lighter than air. In the production of HHO Gas, there is no evaporation process at all, the electric energy used being insufficient for evaporation.

The variable character of the energy content of HHO Gas is evidence that the gas has a unique structure with a chemical composition including bonds beyond base of valence type.

HHO Gas does not follow the fundamental PVT Law for gases.

- HHO Gas demonstrates an anomalous adhesion to gases, liquids and solids. HHO Gas bonds to gaseous fluids (such as natural gas, propane fuel, and others) and also to liquid fuels (such as diesel, gasoline, liquid petroleum, and others).
- Santilli describes the creation of the gaseous and combustible HHO from distilled water at atmospheric temperature and pressure via a process structurally different than evaporation or separation, which suggests the existence of a new form of water.

HHO is described to have the structure H-O-H where represents the new magnecular bond and the conventional molecular bond. The transition from the conventional H-O-H configuration to the new H-O-E species is explained as being a change of the atomic polarization of water caused by the electrolysis.

1.5 Design consideration for kit:

The following are the design consideration for a HHO generating kit

- Compact in size
- Suitable for long operation
- Energy efficient
- Safe
- Easy to operate and maintenance free
- Leak proof
- Affordable Price

1.6 BASIC DETAILS OF KIT

The HHO generator (kit) is basically an electrolytic cell. Here the kit used is of simple in construction, whose base (container) is made of PVC

pipe and the electrodes are made from copper plate of length 500mm and thickness 1 mm.The 500mm length copper plate is cut into pieces such that two equal lengths plate are of 250mm respectively. The lengths of both plates are of 250mm respectively and the plates are separated from each other by means of an insulator. Now these arrangements are placed inside a cane (container) of diameter 150mm and it's both sides are sealed with end caps (PVC). The upper end cap houses the electrode terminals and also a hole for HHO gas outflow. The lower end cap has a hole for inlet of electrolyte solution. The electrode connections are made in such a way that the small part of the electrode is projected outwards so the wiring of the connection between the electrode and the connection is eliminated.

In the electrolysis process the oxygen is generated at anode & hydrogen is generated at cathode. A small free space at the top of the cylinder will allow the gases to mix together. The HHO gas generated from the kit is supplied to the engine. A hole at 30degrees is drilled at the engine manifold to supply the gas. Since HHO gas is highly inflammable, the gas is passed through the water. The container of water acts as a Back Fire Arrestor. This is for safety reasons. Then the gas is passed through the carburetor to run the engine.

Figure 5.1 Supply of HHO gas to the engine

Design calculation

Some of the important design calculations are as mentioned below,

2.1 Length and diameter of the coils

The length and diameter of the coils depend on the production capacity of kit. We have decided to design this system for 12 Amps current. Following are the design calculation for determining the length and diameter of coils.

Design current - 12 Amp
Design voltage - 15 Volts

However in our design, the length and diameter of the copper wire are 250mm and 1mm respectively. The length of coils (i.e. both electrodes) is 300mm. The dimensions are selected such that to get the optimum results based on both power consumption as well as HHO gas liberation.

2.2 Features of kit

Some of the features of kit are as given below,

2.2.1 Water temperature

The output voltage of battery or an alternator of a vehicle depends on the engine speed i.e. between 12 volts and 13.8 volts. If the source of power supply to the kit is car battery, the voltage and the current to the kit will always be fluctuating due to the varying engine speed. The amount of gas produced in the kit depends on the voltage applied to the system i.e. at 12 volt the Hydroxyl production will be less however at 13.8 volts the Hydroxy production will be at peak.Similarly when the water is cold the voltage required to break the water molecules is around 3 volts. The voltage required to break the water molecules decreases as the water temperature of water increases, as this reduces the resistance. In the kit i.e. reduction in the voltage drop due to lower of resistance. At this point of time there is an additional voltage available at set of electrodes, which further heats up the water.

2.2.3 Efficiency of kit

As per the Faradays law thumb rule around 3.2M watts energy is required to produce 1 lit of gas per hour. The kit is producing 1 lpm at 15.6 volts and 12 amps i.e. 168 watts.

As per our experiment the most efficient water temperature to operate a kit is between 40-45 deg centigrade. At this stage the production of the Hydroxy is at peak.

2.2.4 NaOH Concentration

In most of the cells, it is required to increase the concentration of the solution in time to time basis. However in this kit, a mesh is fixed just above the coils to hold the KOH fluids coming out with the Hydroxy

produced in the system. Cost of KOH is also high (nearly ten times of NaOH).
Due to these problems we started to use NaOH solution. This NaOH produces fewer fumes. So there is no problem of reduction in concentration.

2.2.5 Water level indicator
The water level indicator is made using transparent 10mm diameter tube. These components are joined to leak proof joint on the outer side. This indicator also provides the provision for water topping up.

2.2.6 Fire arrestor
HHO gas is a highly combustible fuel. In order to protect the kit from the back fire produced from the engine the fire arrestors are used. It is a simple method in which, instead of directly supplying HHO gas to the engine it is made to flow through a container containing water. Such that even though the gas catches fire it won't reach the kit.

PRODUCTION OF HYDROGEN

Hydrogen is not a fuel that occurs free in nature like fossil fuel. Primary source of energy like solar, nuclear or hydro-electric is necessary to separate it from original combined state. The following methods are considered suitable for hydrogen production:

3.1 Electrolysis of water

In this method, electrical energy is used to break water into H_2 and O_2. In principle, an electrolysis cell consists of two electrodes, commonly flat metal or carbon plates, immersed in an aqueous conducting solution called the electrolyte.

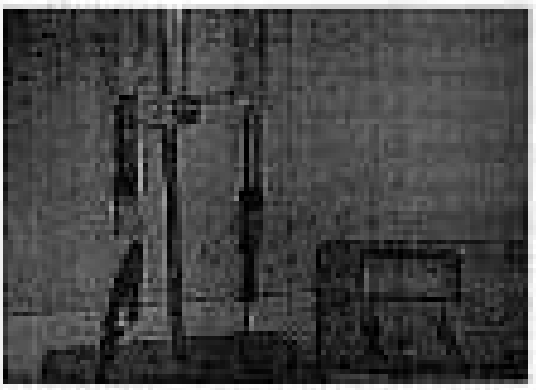

Figure 4.1 Electrolysis Process

A source of DC voltage connected to the electrodes so that an electric current flows through the electrolyte from anode to cathode. As a result, water in the electrolyte solution is decomposed into H_2 which is released at the cathode and oxygen at the anode. Since water itself is the poor conductor of electricity an electrolyte like KOH is used increase the electric conduction.

3.2 Thermochemical method

This method is considered potentially most promising. It depends on complex series of interactions between the primary energy, water and some specific chemicals to produce hydrogen at temperatures substantially lower than thermal decomposition. The chemicals used are recyclable. A variety of compounds of iron, iodine, lithium and cadmium are used for the purpose.

3.3 Photolysis:

In this process, action of certain catalyst to produce H_2 from water by use of direct sunlight at ambient temperature. Though, it appears attractive, the present efficiency of production is only 1%.

3.4 Thermal decomposition of water

In this method, heat at high temperature (2000°C) is used to thermally decompose water into H_2 and O_2.

3.5 Advantages of HHO gas as a fuel in Diesel engine

- HHO gas mixture burns nearly 10 times faster compared to gasoline air mixture.
- HHO ignition limits are much wider than gasoline's. So it can burn easily and give considerably higher efficiency.
- High self ignition temperature but very little energy is required to ignite it.
- Its clean exhaust is the most attractive feature of all.
- No greenhouse effect.

3.6 Disadvantages of HHO gas as a fuel in Diesel engine

- Produces toxic emission of NO.

- One of the major practical difficulties using HHO as car fuel is its very low density either in gas or liquid form.
- The handling of HHO gas is more difficult and storage requires high capital and running cost.

- Weight of hanger W_2: 1kg
- Co-efficient of discharge: 0.62
- Specific gravity of diesel: 0.8275
- Calorific value of diesel: 45357KJ/Kg K
- Specific heat of exhaust gases: 1.005KJ/Kg K
- Specific heat of cooling water: 4.187KJ/Kg K

3.7 Engine

The engine used in this project is 4-stroke single cylinder diesel engine (kirloskar)

Engine specification:

- Type: 4-stroke water cooled.
- Cylinder: single
- BHP: 5HP
- RPM: 1500RPM
- Fuel: diesel
- Bore: 80mm
- Stroke length: 110mm
- Orifice diameter: 32.2mm
- Compression ratio: 16:1
- Brake drum diameter: 0.32m

3.8 Dynamometer (mechanical type)

It is a simple device used for measuring brake power of an engine. It consists of a flat belt of 5mm thickness and 100mm width wound around the rotating drum of 350mm of diameter, attached to the shaft of 30mm diameter, which is connected to the engine out put through chain drive. The both ends of the flat belt is

DESIGN CALCULATION

4.1 Brake dimensions

Intake Drum Diameter =32cm

Radius R=16cm

BHP= (2πNT)/4500

DESCRIPTION OF TEST RIG

connected to the spring gauge. It consists of 0 to 100 kg of graduations. The load is applied on the drum by using nut and bolt arrangement.

3.9 Manometer (U-tube)

It consists of a U tube filled partially with water. One end of the tube is connected to air drum to measure inside the drum and another leg to measure atmospheric pressure.

3.10 Burette

It is a glass tube with graduation. This is used to measure the fuel consumption by the engine. It is connected in between fuel tank and injector.

3.11 Digital RPM indicator

It consists of a digital display with a sensor, which measures the revolution of the output shaft.

3.12 Air drum

It is a cylindrical drum of 590mm length and 300mm diameter, with two openings. One end is connected to the engine through intake manifold other end is free to absorb atmospheric air. The intake air from atmosphere is purified using filter present in the intake passage.

3.13 C-frame

The base of the test rig is made of C-section steel frames. The width of the frame is 80mm and the height is 50mm. Thickness of frame is 5mm.

Where N= speed in rpm

$T = W_{max} R$

Where T=torque

W_{max}= maximum load carrying capacity of engine

R= brake drum radius

4.1.1To find Maximum Load

W_{max}=4500*BHP/(2π*N*R)

=4500*5/(2π*1500*0.16)

=14.93Kg

∴Maximum Load for the engine, W_{max}=14.93Kg

4.2 CALCULATIONS

Referring to table 6.1

For load, W =13kg

Brake Power: BP = (2π60WR*9.81) kW
60000

Where,
N is speed in RPM
W is load in kg
R is radius of brake drum in meter

BP = (2π*1500*13*0.16*9.81)
60000

= 3.2051 kW

Total Fuel consumption, TFC= 10* Specific gravity*3600, kg/hr
1000*t

Where,
Specific gravity of Diesel= 0.8275
T is time for 10cc of fuel consumption in seconds

TFC =10*0.8275*3600
1000*25

= 1.1916 kg/hr

Friction power, FP= 4.5KW
Indicated power, IP= FP+BP
=4.5+3.2051=7705

Brake specific fuel consumption, BSFC = TFC, kg/kWhr
BP =1.1916/ 1.235665 =0.3717kg/kWhr
Brake mean effective pressure, BMEP = BP*0.6 , bar
L*A*(N/2)
Where,
L is the stroke length = 80mm = 0.08 m
A is the piston area,A = πr^2
=0.0804m^2
BMEP = 3.2051*0.6
0.08*0.0804*(1500/2) =0.28985 bar

Brake thermal efficiency, η_{bth}= BP*3600*100 %
TFC*CV Where,
CV is the calorific value of fuel = 45357 kJ/kgK
η_{bth} =3.2051*3600
1.1916*45357

= 21.3 %

Mechanical efficiency, η_{mech}= BP*100 IP Where, BP is the brake power IP is the indicated power

=3.2051/7.5051*100 =42.718%

Indicated thermal efficiency, ηind.th= IP*3600
TFC*CV
=(7.505*3600)/(1.1916*45357) =49.08%

CONCLUSION

5.1 Optimum method of HHO generation

By comparing the reading from table 6.1 and table 6.2 the discharge of HHO gas is 34.4LPH for KOH and NaOH, which is almost same for both the cases. KOH solution produces lot of fumes which leads to loss of concentration of electrolyte and in turn decreases the generation of HHO gas. Therefore comparing the production, rate of change of electrolyte concentration and cost of KOH and NaOH, NaOH electrolyte solution is best suited for the generation of HHO gas.

5.2 Performance characteristics of Diesel and HHO gas when used as a fuel

From graph 1up to 50% of full load, brake thermal efficiency will remain same for both the case. Beyond this point brake thermal efficiency increase linearly for fuel mixtures of diesel and HHO gas. From graph 2up to 50% of full load for both cases the total

fuel consumption increases linearly and reaches maximum value. TPC decreases more rapidly for fuel mixture of diesel and HHO gas than diesel as a fuel

Result

By comparing the results of above three graphs we can conclude that The mixture of diesel and HHO gas gives better result for higher loads. Since HHO is highly combustible fuel, it ensures the complete combustion of the fuel mixture. Thus it results in the increased speed of the engine and in turn increases the power output.

Future scope

It was found that the HHO engines saves as much power and at the same time cost also less compared to normal diesel operated engines. However, such results should be interpreted with caution and the finding should be supported by a larger body of statistical data. In future efforts, it so helpful for researching of HHO gas operated IC Engines up to 100% than 50% efficiency results.

References

[1]. Verdegiu TN. 1987, International Journal of Hydrogen Energy 12:99 INSPEC Compendex.

[2]. Winter CJ. 1987, International Journal of Hydrogen Energy 12:521 INSPEC Compendex.

[3]. Serpone N, Lawless D, Terenin R. 1992, Solar Energy 49:331 INSPEC Compendex.

[4]. Zweig RM. 1992, Proceedings of the Ninth World Hydrogen Energy Conference. Paris (France):1995.

[5]. Bayer H. 2000, Renewable Energy World, Review Issue 2001–2002 ed. by James jana, vol.4, no 4, p177.Grutz J. 1992, Proceedings of the Second World Renewable Energy Congress. Reading (England) 2038.

[6]. Block DL, Veziroglu TN. 1994, Hydrogen energy progress X, Proceedings of the Tenth World Hydrogen Energy Conference. Cocoa Beach (Florida, U.S.A.), Foreword.

[7]. King RO, Reid M. 1968, "The Andrajeen engine" Canadian Journal Technology50:445-60.

[8]. Erren RA, Campbell WE. 1933, "*Hydrogen a Commercial fuel for internal combustion engines and other purposes*" J Inst Fuel 1933; 6:277-90.

[9]. Stewart, W. F., 1986, "Hydrogen as a 'molecular fuel'" In Recent Developments in Hydrogen Technology, Vol 2, Eds K. D. Williamson Jr. and F. J. Edeskuty. CRC Press, Cleveland, OH.

[10]. Block DL, Veziroglu TN. 1994, Hydrogen energy progress X, Proceedings of the Tenth World Hydrogen Energy Conference. Cocoa Beach (Florida, U.S.A.), Foreword. King RO, Reid M. 1968, "The hydrogen engine" Canadian Journal Technology 22:445–60.

[11]. Cox KE, Williamson KD. 1977, "*Hydrogen: its technology and applications*" Vols. I–V Boca Raton, FL: CRC Press.

International Conference On Emerging Trends in Science Technology Engineering and Management

(ICE) & 18th, October 2015

Performance test on single cylinder four stroke diesel engines by using convergent divergent inlet manifold

Dr.I.Satyanarayana[1], G.Lakshmi[2], K.Anil Kumar[3]

[1]Professor of Mechanical Engineering, Sri Indu Institute of Engineering and Tech., Sheriguda(V), Ibrahimpatnam(M), Rangareddy, Telangana, India

[2]PG student of Mechanical Engineering, Hyderabad, Telangana, India

[3]Associate professor of Mechanical Engineering, Hyderabad, Telangana, India

[1]satyanarayana.iit@gmail.com, [2]lakshmi.g1990@gmail.com, [3]k.anilkumar@gmail.com

ABSTRACT

Growing demands on reduction of Internal Combustion Engine fuel consumption with increase of its performance new designs and optimization of existing ones are introduced. Air motion in CI Engine influences the atomization and distribution of fuel injected in the air charge. Better atomization of injected fuel allows for a more complete burn and helps to reduce the engine Knock.A four stroke compression ignition engine with power 8 H.P and rated speeds 1400,1500,1600 rpm is selected for the present work to investigate the performance test. The swirl motion of the air is an important parameter in optimizing the performance of the engine.In order to increase the air velocity in the inlet manifold a convergent-divergent nozzle is used. The rise in velocity with the use of nozzle generates turbulence at the exit of the manifold which facilitates for better combustion of injected fuel. The Performance test is calculated without nozzle and without nozzle in the inlet manifold and compared.

Keywords: I-C manifold, Diesel engine, Performance Characteristics, Speed, Velocity

I INTRODUCTION

Thermal energy (heat) is one of the oldest forms of energy known to mankind. Thermal energy is usually evolved from energies such as chemical energy and electrical energy. The device for converting one form of energy to another is termed as engine. In an energy conversion process the conversion efficiency plays a vital role and it determines the efficient use of the supplied energy. Heat engine is the device that can transform chemical energy of a fuel into thermal energy and utilizes this thermal energy to perform useful work.Here, in this work we have implemented the helical threaded manifold by varying pitches for generating the swirl while entering the cylinder. The turbulence was achieved in the inlet manifold by threading the inlet manifold of size 4mm width and 3mm depth with different pitches to direct the air flow.The tests are carried with different configurations by varying the pitch of the helical threads from 10 mm to 25 mm in steps of 5mm inside the intake manifold. The measurements were taken at constant speed of 1400,1500,1600 rpm. The results are compared among normal manifold.

1.1 Analysis of gas flow in De Laval nozzles.

The analysis of gas flow through de Laval nozzles involves a number of concepts and assumptions:

1. For simplicity, the gas is assumed to be an ideal gas. The gas flow is isentropic (i.e., at constant entropy). As a result the flow is reversible (frictionless and no dissipative losses), and adiabatic (i.e., there are no heat gained or lost).
2. The gas flow is constant (i.e., steady) during the period of the propellant burn.
3. The gas flow is along a straight line from gas inlet to exhaust gas exit (i.e., along the nozzle's axis of symmetry).
4. The gas flow behavior is compressible since the flow is at very high velocities (Mach number > 0.3).

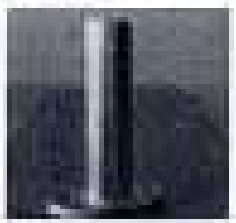

Fig.1 Convergent Divergent manifold

Fig. 2 Preparation of Convergent-Divergent manifold

Fig.3 Projection of Connecting Rod and Crank Shaft

II. BASIC ENGINE TERMINOLOGY

A number of basic terms are used to describe and compare engines. A few commonly used terms are explained here.

1) Top dead centre (T.D.C):

This refers to the position of the crank shaft when the piston is at top most position i.e., the position closest to the cylinder head (position 1 in fig)

2) Bottom Dead Center (B.D.C):

This refers to the position of the crankshaft when the piston is in its lowest position, i.e., the position farthest from the cylinder head (position 3) in Figure.

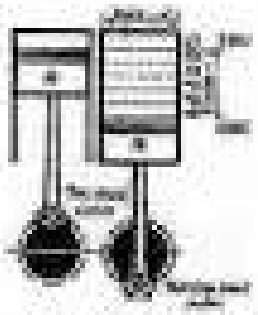

Fig.4 Top and Bottom Dead Centres

3) Bore: Diameter of the engine cylinder is referred to as the Bore.

4) Stroke: Distance travelled by the piston in moving from T.D.C to the B.D.C. is called 'stroke' Obviously as the piston strokes the volume in the cylinder changes.

Volume: The volume of cylinder (including combustion chamber) above the piston when it is in T.D.C position (volume between '1' and '2' in fig) is called as 'clearance volume'

5) **Piston displacement:** This is the volume swept by the piston in moving from T.D.C to B.D.C this is also called 'swept volume'. If 'd' is the cylinder bore and 's' the stroke, the piston displacement Vs, is given by

$$Vs = \frac{\pi}{4} \times d^2 s$$

6) **Engine Capacity:** This is a total piston displacement or the swept volume of all the cylinders. If 'n' is the number of cylinders and Vs is the piston displacement, then 'Engine displacement' or engine capacity Vd is given by

$$Vd = Vs \times n$$

7) **Compression ratio:** This indicates the extent to which the charge in the engine is compressed. This is calculated as the ratio of the volume above the piston at B.D.C to the volume above the piston at T.D.C. If 'r' is the compression ratio, then

$$r = \frac{Vs + Vc}{Vc}$$

For petrol engines compression ratios are about 8 to 10, where for diesel engines, these vary from 15 to 24.

8) **Mean effective pressure:** This is the average effective pressure throughout the whole power stroke. In fact the cylinder pressure varies considerably during the power stroke. Thus it is more helpful to refer to the mean pressure formed. It is expressed in bars or kilo Pascals (1 bar=100kpa).

10) **Power:** It is the work done in a given period of time. Obviously the same amount of work in a lower time would require more power.

11) **Indicated power (I.P):** The power developed within the engine cylinder is called indicated power. This is calculated from the area of the engine indicator diagram. It is usually expressed in kilowatts (K.W).

12) **Brake Power (B.P):** This is the actual power delivered at the crank shaft. It

obtained by deducting various power losses in the engine from the indicated power. It is measured with a dynamometer and is expressed in kilowatts. It is always less than the indicated power, due to frictional and pumping losses in the cylinder and the reciprocating mechanism.

13) **Engine Torque:** It is the force of rotation acting about the crank shaft axis at any given instant of time.

It is given by

$$T = F \times r$$

T - Engine torque (nm)

F - Force Applied to crank (n)

R - Effective crank radius (m)

Obviously the engine manufacturers always quote the average value of torque throughout the engine cycle. Engine torque goes through the vehicle transmission system to the road wheel and is responsible for creation of the force and hence the pulling of the vehicle.

2. EXPERIMENTAL SETUP & PROCEDURE

2.1 Introduction: The details of the experimental set up are presented in this chapter the alterations made to the instrumentation are also described. The experimental setup is fabricated to fulfill the objective of the present work. The various

components of the experimental set up including modification are presented in this chapter.

2.2 Experimental set up: The experimental set up consists of engine, air chamber, test tank system, fuel tank along with manometer, exhaust gas measuring digital device and manometer.

Engine:

The engine which is supplied by M/s Kirloskar Company. The engine is single cylinder vertical type four stroke, Air-cooled, compression ignition engine. The engine is self governed type whose specifications are given in Appendix I is used in the present work.

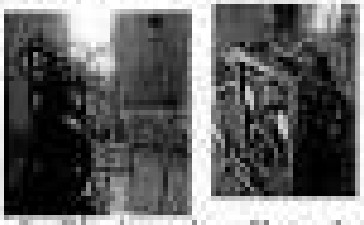

Fig. 4. Diesel engine Photo look normal&CD manifold

Fuel injector (BOSCH)

A cross sectional view of a typical BOSCH fuel injector

The injector assembly consists of

i. A needed valve
ii. A compression spring
iii. A nozzle
iv. An injector body

U-tube manometer

The one of end of the U-tube manometer is connected to the orifice of the air tank and the other end is exposed to the atmosphere, the manometer liquid used is water.

Digital thermometer

It consists of a temperature sensing element connected to the electronic digital display which is operated by battery.

2.3 VARIOUS PARTS OF EXPERIMENTAL SET UP

1. KIRLOSKAR ENGINE
2. ALTERNATOR 3. DIESEL TANK
4. AIR FILTER
5. THREE WAY VALVE
6. EXHAUST PIPE
7. PROBE
8. EXHAUST GAS ANALYSER
9. ALTERNATIVE FUEL TANK
10. BURETTE
11. THREE WAY VALVE
12. CONTROL PANEL

2.5 Instructions

1. Measurement of brake power:

The power developed by the engine is measured by using electrical dynamometer. The pump is run by using the power developed by the engine. The total power is obtained by adding pump power to the product of voltage and current.

2. Measurement of fuel:

The fuel flow is measured by volume through a burette tube which is fixed between fuel tank and fuel pump. A T-joint prepared and one side of it is connected to the fuel measuring tube. The remaining two sides of the joints are connected to the fuel tank and the fuel pump respectively. Fuel flow is measured by noting the time taken for 10cc of fuel consumption by stop watch.

3. Measurement of air flow:

Air flow is measured by using a viscous flow air meter. A paper element filter is an integral part of the meter .The meter consists of an orifice, the pressure drop across the orifice is measured by manometer, to ensured that there are no leakages in the connecting tubing.

4. Load on engine:

Initially fuel tank and auxiliary fuel tanks are filled with right amount of required fuel. The instruments such as NDir meter and GOTEC analyzers are connected to the exhaust pipe. The engine is started and allowed to run for 20 minutes to attain steady state condition.

5. Measurement of emissions:

Engine emissions are measured by using exhaust gas analyzers.

6. Measurement of exhaust gas temperature:

The temperature of exhaust gas is measured by using digital thermocouple devices. It gives the exhaust gas temperature directly.

2.6 Experimental Procedure

Before starting the engine, the fuel injector is separated from the fuel system, it is clamped on the fuel injection pressure tested and operated for tester pump. Observe the pressure reading from the dial. At which the injector starts spraying. In order to achieve the required pressure by adjusting the screw provided at the top of the injector.

This procedure is repeated for obtaining the various required pressures.

As first said, diesel alone is allowed to run the engine for about 30 min, so that it gets warmed up and steady running conditions are attained. Before starting the engine, the lubricating oil level in the engine is checked and it is also ensured that all moving and rotating parts are lubricated.

The various steps involved in the setting of the experiments are explained below

1. The Experiments were carried out after installation of the engine.
2. The injection pressure is set at 200 bar for the entire test.
3. Precautions were taken, before starting the

experiment.

4. Always the engine was started with no load condition.

5. The engine was started at no load condition and allowed to work for at least 10 minutes to stabilize.

6. The readings such as fuel consumption, spring balance reading, cooling water flow rate, manometer reading etc., were taken as per the observation table.

7. The load on the engine was increased by 20% of FHLL Load using the engine controls and the readings were taken as shown in the tables.

8. Step 7 was repeated for different loads from no load to full load.

9. After completion of test, the load on the engine was completely relieved and then the engine was stopped.

10. The results were calculated as follows

The above experiment is repeated for various loads on the engine. The experimental procedure is similar as formed. While starting the engine, the fuel tank is filled to required fuel proportions up to its capacity. The engine is allowed to run for 30 min, for steady state conditions, before load is performed.

We have not been observed any separation in the blend of 20% Fish oil & 20%diesel. We have heated the blend about 70°C in order to reduce the viscosity for easy flowing in the tubes, better injection and atomization in the cylinder the viscosity is nearly equal to the viscosity of diesel.

Finally, the engine is run by blend (200ml) at various injection pressure the corresponding observations are noted.

Fig.7. Raw material

Proposed manifold

4. TABLES AND GRAPHS

Table3.1 Performance test Results on normal manifold at 1400rpm

Fig.8. Load against Mechanical efficiency

Fig. 9. Load against Brake Thermal Efficiency

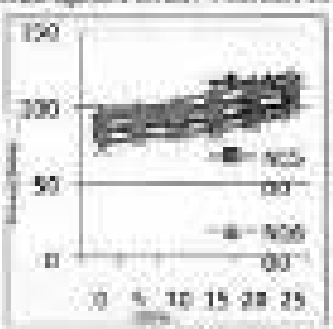

5. RESULTS AND DISCUSSION:

5.1 Brake specific fuel consumption:

The result for the variations in the brake specific fuel consumption (BSFC) is presented in the fig4.3. For all the fuels the BSFC falls with increasing load. The differences of BSFC are very small when using different speeds. The maximum BSFC values are 0.91 kg/kW hr for diesel, 0.77 kg/kW hr for N1500, 0.975 kg/kW hr for N1400, 1.029 kg/kW hr for N1600, 1.113kg/kW hr and for CD1500, 1.095 kg/kW hr. The higher

5.2 Brake thermal efficiency:

The variation of brake thermal efficiency with load is shown in Fig. 4.3 Brake thermal efficiency gives an idea of the output generated by the engine with respect to heat supplied in the form of fuel. For all the fuels the brake thermal efficiency increases with load. The brake thermal efficiency values at full load are 18.84% for diesel, 16.12%

5.3 Volumetric efficiency:

The fig.4.14 shows the variation of volumetric efficiency with load for various speeds Volumetric efficiency is a measure of success with which the air supply is, and thus the charge, is inducted in to the engine.

it indicates the breathing capacity of the engine. From the figure it is evident that the volumetric efficiency values of N1500 and CD1500 are exceeding the volumetric efficiency values of diesel at all loads.

5.4 Brake mean Effective Pressure:

The variation of Brake Mean effective pressure with load. Mean effective Pressure is the average Pressure inside the cylinders of an internal combustion engine based on the measured output. From the figure it can be seen that, Brake mean effective values of neem oil and its diesel blends are slightly less than diesel.

5.5 Indicated Mean Effective Pressure:

Fig.6.6 shows the variation of Indicated Mean effective pressure with load. Mean effective Pressure is the average Pressure inside the cylinders of an internal combustion engine based on the measured output. From the figure it can be seen that, Brake mean effective values of neem oil and its diesel blends of N1500 and CD1500 are slightly less.

5.6 Exhaust gas Temperature:

Fig.6.6 shows the variation of exhaust gas temperature with load for various test fuels. It is observed that the exhaust gas temperature increases with load because more fuel is burnt at higher loads to meet the power requirement. It is also observed that the exhaust temperature increases for N1400 and CD1400 and at all loads. This may be due to the oxygen content of the neem oil, which improves combustion and that may increase the exhaust gas temperature.

5.7 Mechanical Efficiency:

Mechanical efficiency indicates how good an engine is inverting the indicated power to useful power. Fig.6.2 shows the mechanical efficiency for N1400 is less than 420-500 for pure diesel. Because higher fuel injection pressure increases the sharpness of the reactions. The friction of piston rotates engine bearing.

CONCLUSION

The Performance characteristics of an engine without nozzle and with nozzle in the intake manifold were compared in the present work. A Convergent Divergent Nozzle of different speeds N1400,N1500,N1600, CD1400,CD1500 &CD1600rpm.

1) Brake power is increased by 2.28%.
2) Total fuel consumption is reduced by 2.93%
3) Specific fuel consumption is reduced by 5.55%
4) Indicated power is increased by 4.27%
5) Mechanical efficiency is reduced by 1.81%
6) Heat input is reduced by 2.59%
7) Brake thermal efficiency is increased by 5.15%
8) Indicated thermal efficiency is increased by 7.16%
9) Volumetric efficiency is reduced by 11.3%
10) Brake mean effective pressure is increased by 2.58%.

BIBLIOGRAPHY

[1] A.K. Agarwal, L.M. Das, "Biodiesel development and characterization for use as a fuel in CI engine", Journal of Engineering, Gas turbine and power (ASME), Vol. 123,2001,440-447.

[2] A.S.Ramadhas, S.Jayaraj, C.Muraleedharan, "Use of vegetable oils as IC engine fuels: A Review", Renewable Energy, Vol.29, 2004, 727-742.

[3] A.Srivastava, R.Prasad, "Triglycerides- based diesel fuels" Renewable Energy Reviews Vol.24, 2004, 111-133.

[4] B.K.Barnwal, M.P. Sharma, "Prospects of bio-diesel production from vegetable oils in India," Renewable and sustainable energy reviews, Vol. 9, 2005, 363-378.

[5] F. Karaosmanoglu, "Vegetable oil fuels: A review", Energy sources, Vol.20, 1999, 221-231.

[6] M.A. Fangrui, M.A.Hanna, "Biodiesel production: A review", Bio source Technology, Vol.7

[7] H.S. Chiu, H.M. El-mashad, R.L. Avena-Bustillos, R.G. Dunn, P.J. Bechtel, " Biodiesel fuel from waste salmon oil" American society of Agricultural and Biological Engineers, Vol. 51(5), 2008,797-807

[8] El-mashad, H.M., R. Zhang, and R.L Avena-Bustillos, "A two-step process for biodiesel production from salmon oil" Biosystems Eng. Vol.99(2), 2008:220-227.

[9] G.Y. Liu, R.F. Li, Engine performance and emission characteristics of waste fried Food Processing Technology 90 (2009) 860–868 UIK. (Turkish Statistical Institute, http://www.turkstat.gov.tr/.

[10] WWW. indian_fuel.com

[11] J.F. Torres, M.A. Sepulveda, PM-10 emissions and power of a diesel engine fueled with crude and refined biodiesel from salmon oil, Fuel

DESIGN AND THERMAL ANALYSIS OF WARM (COLD) FORGING PROCESS AND DIES

Dr.I.Satyanarayana[1], M.Vedula Bharath Kalyan[2],
K.Anil Kumar[3]

[1]Principal & Professor of Mechanical Engineering
Sri Indu Institute of Engineering and Technology, Sheriguda, Ibrahimpatnam,
Ranga Reddy District- 501510
[2]Sri Indu Institute of Engineering and Technology, Sheriguda, Ibrahimpatnam,
Ranga Reddy District- 501510
[3]Associate Professor
Sri Indu Institute of Engineering and Technology, Sheriguda, Ibrahimpatnam,
Ranga Reddy District- 501510
[illegible] [illegible] [illegible]

Abstract— Forging temperature is one of the basic considerations in forging process. In warm forging, the metals are forged at temperatures above the recrystallization temperature and below the conventional hot forging temperatures. Warm forging has many advantages when compared when compared to cold forging. In this study, forging process of a part which is currently produced in the hot forging temperature range and which needs some improvements in accuracy, material usage and energy concepts, is analyzed. The proposed process is simulated using Finite Element Method and Ansys. Experimental study is also carried out in SRL Center Forging Research and Application Laboratory and it has been observed that experimental result are in good agreement.

Wastage is reduced by proposing using of energy saving and better accuracy in dimensions is achieved by reducing the forging temperature from the hot forging to the warm forging temperature range.

Keywords : Warm Forging, Finite Element Analysis, Die stress Analysis, Material Processing, Closed-die Forging.

INTRODUCTION

The term "forging" is applied to processes in which a piece of metal is worked in a machine to the desired shape by plastic deformation of the starting stock. The energy that produces deformation is applied by a hammer, press, upsetter or ring mill, alone, even or in combination. A forging is produced in three distinct plastic flow processes in the form of blows, hits, or a static plastic deformation of the metal components in single, close sequence of set steps in one of the forging processes, and appropriate secondary operations.

In this study, forging process of a part which is currently produced in the hot forging temperature range and which needs some improvements in accuracy, material usage and energy concepts, is analyzed. The forging process sequence design with a new preform design for the particular part is proposed to warm forging temperature range and the proposed process is simulated using Finite Element Method. In the simulation, coupled thermal mechanical analysis are performed and the dies are modeled as deformable bodies to consider die stress analysis.

OBJECTIVES OF PROJECT

- A forging die designed and manufactured as per the terms of interest and its design
- Process will be selected
- Material properties of the material as well as FEA material are observed
- Per forged load of raw materials in the forging and steps are as well as values for Cold
- Final results which has strong for components in the material are to be optimized with the cost involved
- The cost, availability and per forging load considerations analysis is carried out for the economic production of the component efficiency

- (iii) material properties of the elements present in the assembly for factor calculations to perform theoretical analysis

LITERATURE SURVEY

Cora et al., the forging process was simulated coupled with thermal analysis in order to determine effects of the pressure on the tooling die for the open preform stages in some forging processes. For different cases the stress distribution in the handle die had been presented. The obtained stress distributions were also used for the fatigue analysis of the die.

Kota Vaga Yamamoto et al., a history of practical use of FE simulations in forging was briefly reviewed. Then, practical use and benefits of FE simulations in forging were discussed with examples. Finally, key points for successful and effective use of FE simulations were explained. It is said by current issues for better use of the FE simulation as a practical tool in the forging industry.

III HAND TOOLS

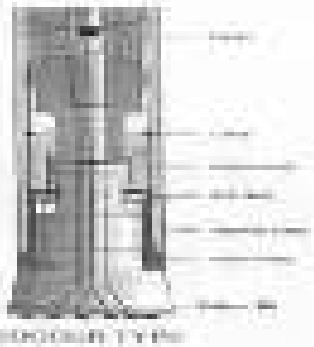

Fig2 The forging axe used in ICE wing and axe is available

I. METHODS FOR DESIGNING AND ANALYSIS TO DEVELOP THE WORK

Design and fixing the standard procedure

LE DESIGNING PROCEDURE

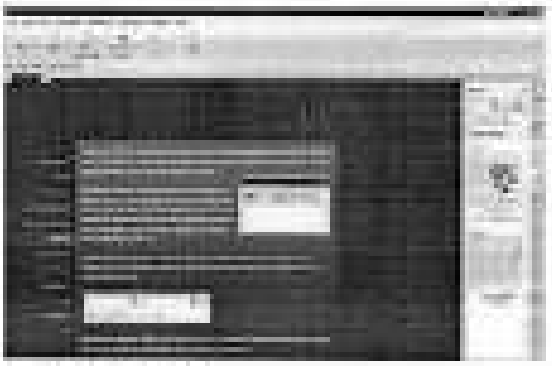

Fig 1.1.1 Starting 3D

Tool Room and tools

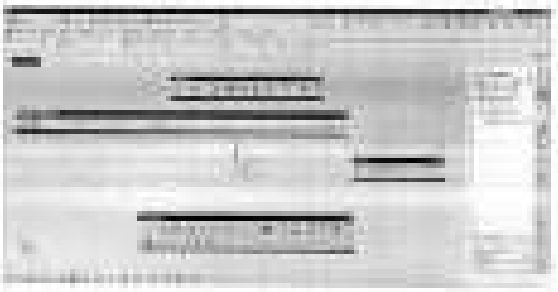

Fig 1.1.2 Shows the Screen Tool bar tools for design

1.2 Component 3D drawing with PRO/E design

Fig 1.2.1 Shows the assembly view of axe (Incorporation of rotating part in the design)

Fig 1.2.2 Shows the features creating which is used to perform the experimental analysis. Material can be added to the present domain for the creating the new features

Fig 1.2.3 Shows the design of rectified burr to die with actual [illegible] design image of The used as process for die capacity and analysis

Fig 1.2.4 Shows the machining of burr to die [illegible] proper strength. Die can be work efficient in CNC machine for precise machining.

Fig 1.2.5 Shows the polishing preparation of [illegible] as both is the material which we are going to forging so die is protected by using plastic materials. To good result of die component.

2. MATERIAL USED- D6

AISI (American Iron and Steel Institute) D6 are used as a high carbon, high chromium tool steel alloyed with tungsten that is characterized by high compressive strength, high wear resistance, high surface hardness and good hardening stability.

3.1 Thermal Properties of the material used

The thermal properties of D6 tool steels are given in the following table.

[illegible]	[illegible]
Thermal expansion coefficient (at 21-400°C (68-752°F))	13.9 µm/m°C
Thermal conductivity (@50°C/68°F)	20.1 W/m·K

3.2 Boundary conditions

Fixed support at the [illegible] as shown in fig (1.0.0.0). The stresses after flash formation is represented

$$\sigma_{yy} = 2\zeta_1 \theta_{yy}(t-1) + \sigma_{yy}$$
$$\sigma_{xy} = (E_1' / E_1)\ln\Gamma \cdot E_1 + E_2\zeta_1 + \sigma_{xy}$$
$$\sigma_{xx} = (2\alpha\theta_{yy}\zeta_1)\cdot(t-1) + \sigma_{xx}$$

Where,

$$E_1' = -2\alpha\mu\beta$$
$$E_2' = -\sigma_{yy}E_1 + 2\alpha_1\theta_{yy}(1+\ln\Gamma\cdot\beta)$$
$$E_1 = \Gamma - \Gamma_1 E_1$$
$$\text{Where } \beta = \beta - (\beta^{-1}(t-1) - \beta^{-1}(t-1)\beta_{old}\Gamma^{-1}(t-1))\Gamma^{-1}$$

3.3 Thermal Analysis of Boundary conditions

[illegible] pressure is used in the simulation analysis, [illegible] temperature 150°C, Temperature of the environment 30°C, Convection on the surface with convection coefficient of [illegible]

Fig 3.3.1 Shows the boundary conditions used for thermal analysis, convection and temperature was given as shown.

3. RESULTS & DISCUSSION

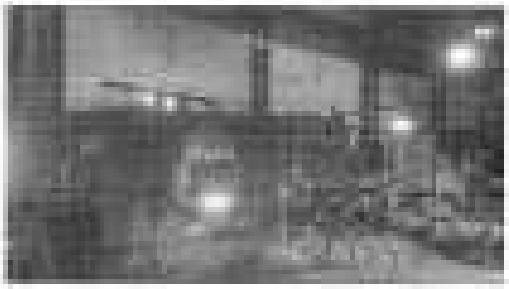

Fig 3.1 Shows the fabricated model of gravel project

Fig 3.1.1 Shows the fabricated model of gravel project

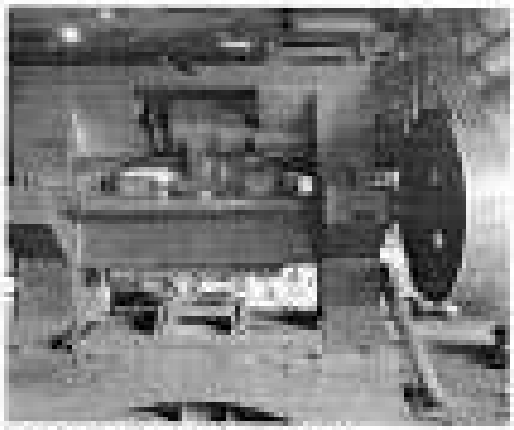

Fig 3.1.2 Shows the Static testing model

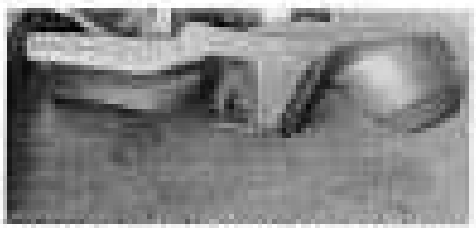

Fig 3.1.3 shows the output comparison of gravel project

4.8 Analysis in Ansys 15.0 for gravel project

4.1 STATIC STRUCTURAL ANALYSIS OF THE DIE

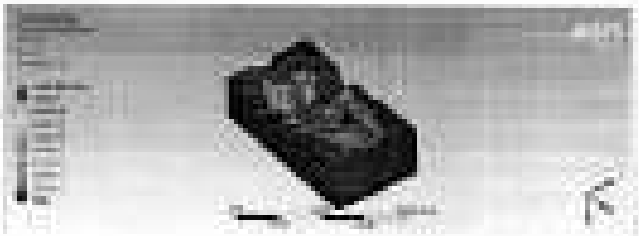

Fig 4.1.1 Shows the total deformation of the bottom die the load applied, the maximum deformation was found to be 1.0093 shown in the contours color bar

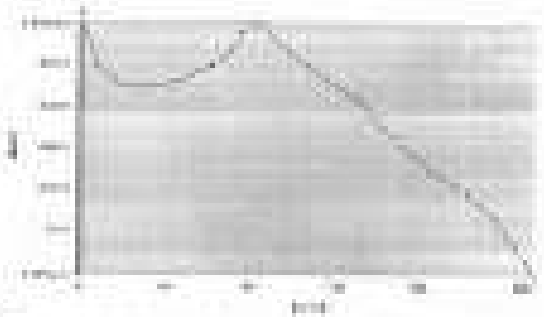

Fig 4. Total deformation in static analysis Axis and Length of the curve is taken along X axis

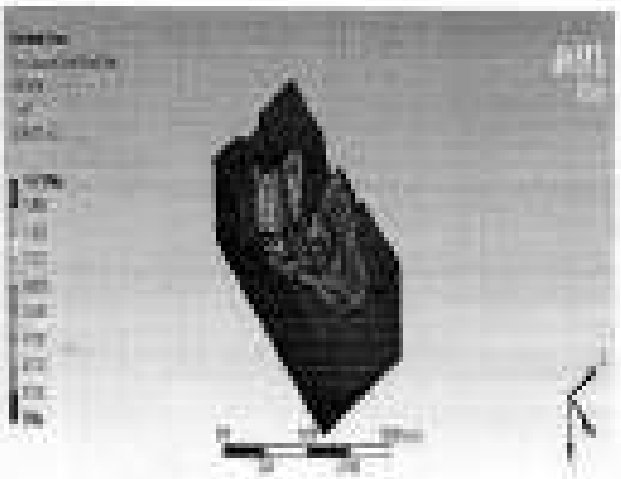

Fig.6.5(a) Shows the equivalent stress variation across the diametral cross section of 160 MPa steel billet

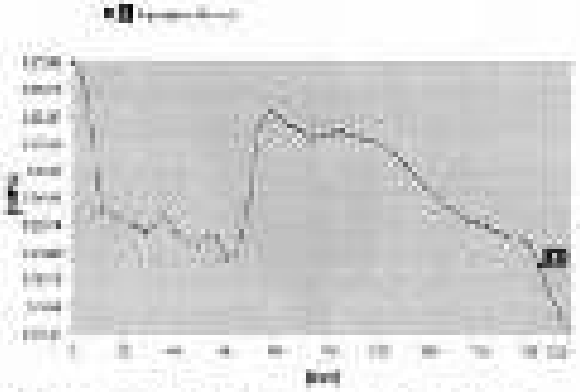

Fig.6.6 Shows equivalent stress variation in the axial direction of the billet

Table 6.1 Hot forging temperatures of different metals and alloys

Metal or alloy	Approximate range of forging temperature, °C (°F)
Aluminum alloys (wrought)	400–500 (750–930)
Magnesium alloys	250–350 (480–660)
Copper alloys	600–950 (1100–1750)
Carbon and low-alloy steels	850–1150 (1550–2100)
Austenitic stainless steels	1100–1250 (2000–2300)
Titanium alloys	750–950 (1400–1750)
Superalloys	1050–1200 (1920–2200)
Refractory alloys	1200–1500 (2200–2700)
Tool steels	900–1200 (1650–2200)
Molybdenum alloys	1150–1350 (2100–2450)

Metal or alloy	Approximate range of forging temperature, °C (°F)
Aluminum alloys	400–500 (750–930)
Magnesium alloys	250–350 (480–660)
Copper alloys	600–950 (1100–1750)
Carbon and low-alloy steels	850–1150 (1550–2100)
Austenitic stainless steels	1100–1250 (2000–2300)
Titanium alloys	750–950 (1400–1750)
Superalloys	1050–1200 (1920–2200)

Preform dimensions for carbon or low-alloy steels

Dimensions of the finish forging	Preform dimensions
Depth	No change
Diameter or width (B_f)	$B_p = B_f + C$ or $B_p = B_f + B_f/8$
Fillet radii (R_f)	$R_p = 1.5\,R_f$ (but not less than 10 mm (0.375 in.))
Depth of cavity (H_p), minus web and flash of all dimensions (H, mm (in.))	When H_p is less than 10 mm (0.4 in.), draft C = 2 mm (0.08 in.)
	When H_p is between 10 mm and 25 mm (1 in.), draft C = 3 mm (0.12 in.)
	When H_p is between 25 mm and 50 mm (2 in.), draft C = 4 mm (0.16 in.)
	When H_p is greater than 50 mm, draft C = 5 mm (0.2 in.)

B_p Maximum width of preform, B_f Width of preform, R_p corner radius, C allowance for draft, Source: Ref.[7]

6.THERMAL ANALYSES

Fig.6.7 Shows the temperature distribution on the die, calculated at 200 sec time period. It shows that the temperature variation

Temperature gradient

Fig. 6.8 Shows the normal view of the die, variation of the temperature and the change of temperature gradient

Total Heat Flux
Fig 3 Shows the Total flux variation across the die in ANSYS 15.0 version

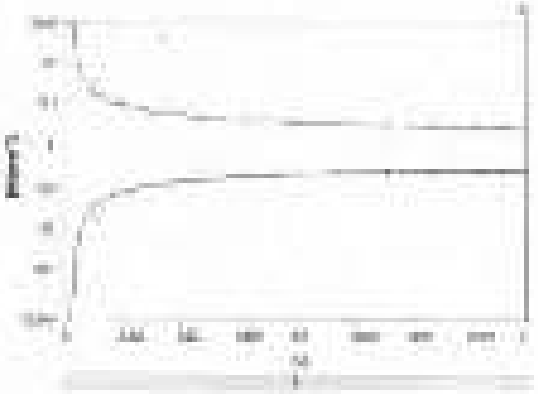

> Directional Heat Flux
Fig 4 Increasing and Decreasing direction of heat flux along the Direction

CONCLUSION

1 The simulation method based on finite element is a powerful tool that can provide information about the variables that are difficult to measure or observe in the shop floor such as stresses, strains for particular points of the forged part.

2 The knowledge of these values is the key to optimizing the existing processes and developing more productive and economic ones. This is, however, impossible without verified models, as proved by a reliable analysis of the process.

3 The present work is concerned with the application of a FEM simulation code using rigid-viscoplastic material model to the hot forging.

4 The first application of the numerical model is a novel real case including many aspects (multi-stage deformation, heat generation, changes in the shape of the forging during the loading to the workpiece, lubrication, heat exchange with the environment, the heating of the workpiece, wear of the forging die in the furnace can be minimized, the optimum shape of the forging can be found and by means of various types of problems solved.

Scope of the Future work

- It was found that the new mechanical treatment can produce practically identical properties of a work piece as conventional forging.
- However, such results should be interpreted with caution and their finding should be supported by a larger body of experimental data.
- In future studies, the FEM simulation of forging processes will be refined, e.g., the plastic behaviour of a forged part instead of the more plastic material will be.
- In a future work, different die and workpiece materials can be analysed, perform preforms and forging of the part at lower temperatures can be analysed.
- By using the results of the study, forging dies can be more good. Numerical analysis may be performed by different Finite Element programs.

References

1. V. Vazquez and T. Altan, New Concepts in Die Design-Physical and Computer Modeling Applications, J. Mater. Process. Technol., Vol. 98, 2000, p.232-239.

2. A.M. Sabroff et al., Forging Materials and Practices, Reinhold, 1968.

3. Uner, M., "Elastic Thermal Analysis of Hot Upset Forging Dies", MS. Thesis, Middle East Technical University, Ankara, Turkey, 2002.

4. Daud, Y., Lucas, M., Huang, Y., "Influence of design and process parameters on service life of cold forging die", Journal of Materials Processing Technology, 147 (2004) 339-345.

5. Kim, D.H., Lee, H.C., Kim, H.M., Kim, K.H., "Estimation of Die Service Life Against Plastic Deformation And Wear During Hot Forging Processes", Journal of Materials Processing Technology, 146(2) (2004) 273-280.

6. Ebrahimi, R., Jafarian, A., "Modelling the Service Life Behavior of Hot Forging Dies", Journal of Materials Processing Technology, 87 (1998) 237-240.

7. Jeong, K.S., Kim, H.K., Kim, J.H., Kim, H.M., Hwang, T.S., "Effects of Surface Treatments And Lubricants

For Warm Forging Die Life", Journal of Materials Processing Technology, 177 (2006), 344-350

8. Lee, K.S., Im, Y.T., "Application of Numerical Simulation for Wear Analysis Of Warm Forging Die", Journal of Materials Processing Technology, 103 (2001), 69-78.

9. Kim H., Yag, T., Yamazaki M., "Die wear behavior and shape error in multi-station forging process and tool design", Journal of Materials Processing Technology, 98 (2000), 143-149.

10. Kadir, A. R., "Analysis and Design of Preforms for Non-Axisymmetric Parts", M. Sc. Thesis, Middle East Technical University, Ankara, Turkey, 2001.

11. Kazancioğlu, A. R., "Analysis and Preform Design for Long Flash Forgings with Non-Planar Parting Surfaces", M. Sc. Thesis, Middle East Technical University, Ankara, Turkey, 2003.

12. Gökalan, S., "Preform Design for Heavy Vehicle Steering Arm", M. Sc. Thesis, Middle East Technical University, Ankara, Turkey, 2003.

13. Çiçekoğlu, O., "Analysis of Forging for Three Dimensional Alloy Steels", M. Sc. Thesis, Middle East Technical University, Ankara, Turkey, 2000.

14. Altınbalık, T., Baday, Ş., Ece, S., Recent Advances in Cold and Warm Forging Process Modelling Techniques: Selected Examples, Journal of Materials Processing Technology, vol 98, pp 253-261, 1999.

15. Behrens, A., Ji-li, H., Verification of the damage model of plastic strains in cold and warm forging operations by experimental testing and FE simulations, Journal of Materials Processing Technology, vol 125-126, pp 260-265, 2002.

16. Jeong, H.T., Kim, H.S., Kim, J.H., Kim, B.M., Choi, J. C., Effects of Surface Treatment and Lubricants for Warm Forging Die Life, Journal of Materials Processing Technology, vol 113, pp 548-553, 2001.

17. Tomov Ivanov, Vlastimir Nikolovski, Die Life and Lubrication in Warm Forging, Journal of Materials Processing Technology, vol 71, pp 47-68, 1997.

18. S. Shirgaokar, Cold Lubricating Systems in Warm Forging, Journal of Materials Processing Technology, vol 113, pp 69-73, 2001.

19. Xinbo, L., Lihua, Z., Jiuhua, F., Zhiliang, Z., Research on the Flow Stress Characteristics of AISI 1080 and AISI 1140 in the Temperature Range of Warm Forging by Means of Thermo-Mechanical Experiments, Journal of Materials Processing Technology, vol 112, pp 38-44, 2001.

20. Xinbo, L., Hongchang, X., Zhiliang, Z., Flow Stress of Carbon Steel C38 at Temperature Ranges of Warm Forging, Journal of Materials Processing Technology, vol 124, pp 385-388, 2002. 70

21. Lee, K.S., Im, Y.T., Application of Numerical Simulation for Wear Analysis of Warm Forging Die, Journal of Materials Processing Technology, vol 103, pp 69-78, 2001.

22. http://www.forging.org/

23. http://www.arc.ohio-state.edu/~tmg/research/research/forging.htm

24. http://www.moderncasting.com/Moreinfo/1104/More1104p0102.pdf

DESIGN AND THERMAL ANALYSIS OF WARM (COLD) FORGING PROCESS AND DIES

Dr.I.Satyanarayana[1], M.Vamsee Bharath Kalyan[2],
K.Anil Kumar[3]

[1]Principal & Professor of Mechanical Engineering,
Sri Indu Institute of Engineering and Technology, Sheriguda, Ibrahimpatnam,
Ranga Reddy District- 501510

[2]M.Tech Sri Indu Institute of Engineering and Technology, Sheriguda, Ibrahimpatnam,
Ranga Reddy District- 501510

[3]Associate Professor
Sri Indu Institute of Engineering and Technology, Sheriguda, Ibrahimpatnam,
Ranga Reddy District- 501510

[illegible]

Abstract— Forging temperature is one of the basic considerations in forging process. In warm forging, the metals are forged at temperatures above the recrystallization temperature and below the traditional hot forging temperature. Warm forging has many advantages when compared when compared to cold forging. In this study, forging process of a part which is currently produced at the hot forging, Temperature range and which needs some improvements in accuracy, Material usage and energy concepts, is analyzed. The proposed process is simulated using Finite Element Method and Ansys. Experimental study is also carried out in SRL Center Forging Research and Application Laboratory and it has been observed that experimental results are in good agreement.

Wastage is reduced by proposing using of energy saving and better accuracy in dimensions is achieved by reducing the forging temperature from the hot forging to the warm forging temperature range.

Keywords : Warm Forging, Finite Element Analysis, Die stress Analysis, Metal Forming, Closed-die Forging.

INTRODUCTION

The term "forging" is applied to processes in which a piece of metal is worked in a machine to the desired shape by plastic deformation of the starting stock. The energy that produces deformation is applied by a hammer, press, or other forging rolling, either alone or in combination. A forging is produced in three distinct phases: stock preparation in the form of blooms, billets, bar or ingots, plastic deformation of the metal component to rough, close tolerance or net shape in one of the forging processes and appropriate secondary operations.

In this study, forging process of a part which is currently produced at the hot forging temperature range and which needs some improvements in accuracy, material usage and energy concepts, is analyzed. The forging process sequence design with a new pre-form design for the particular part is proposed in warm forging temperature range and the proposed process is simulated using Finite Element Method in the CAE/Ansys, coupled thermal mechanical analysis are performed and the dies are analyzed at critical locations to execute die stress analysis.

OBJECTIVES OF PROJECT

- A forging die designed and manufactured as per the norms of hammer and die design.
- Forging will be carried out.
- Thermal properties of die material as well as work materials are observed.
- The forged part of the materials in the furnace and temperature will be studied by DSC.
- How much die life increasing the component from component to the material will be experienced with the use of product.
- Die with sensitivity and per forging how much cost an analysis is carried out for the mass/semi production of the component [illegible]

- How material formation will be observed practically for better conclusion compare to theoretical analysis.

LITERATURE SURVEY

Guoa et al., hot forging process was simulated coupled with thermal analysis, in order to determine effects of the process on the bracket die for the taper portion stages in spiral forging process. For different cases, the stress distribution in the bracket die had been presented. The obtained stress distributions were also used for the fatigue analysis of the die.

Kim, Engr., Yamamoto et al., a history of practical use of FE simulations in forging area was briefly reviewed. Then, practical use and benefits of FE simulations in forging area were discussed with examples. Finally, key points for successful and effective use of FE simulations were explained followed by current issues for better use of the FE simulations as a must tool in the forging industry.

DTH HAMMERS

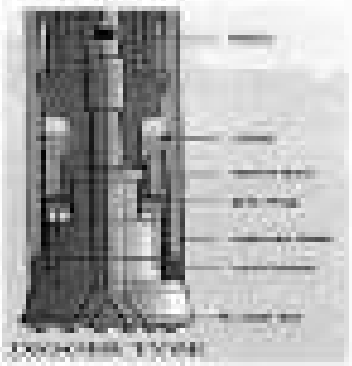

Fig1 The legs are used in R.R ring and acts as rubber

1. METHODS FOR DESIGNING AND ANALYERS TO DEVELOP THE WORK

Design and Experimental procedure

1.1 DESIGNING PROCEDURE

Fig 1.1.1 bearing 53

Toolbars and tools

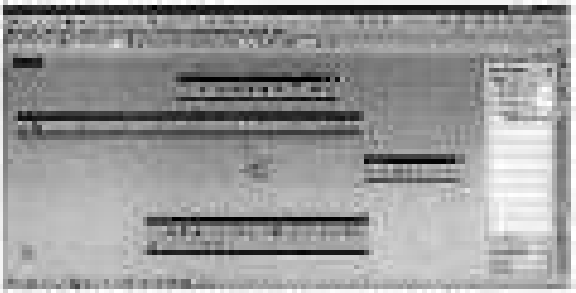

Fig 1.1.2 Shows the Siemens tool bar tabs for design

1.2 Component 3D drawing with NX8.0 design

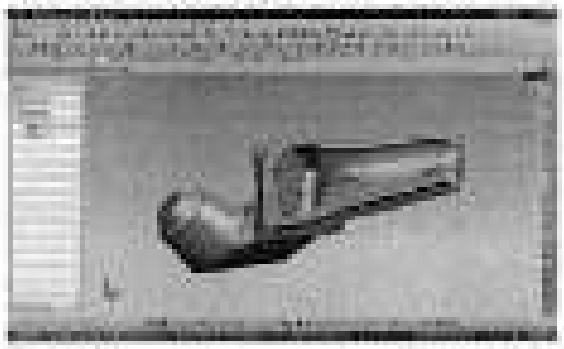

Fig 1.2.1 Shows the component taken to step file conversion of existing part for die design.

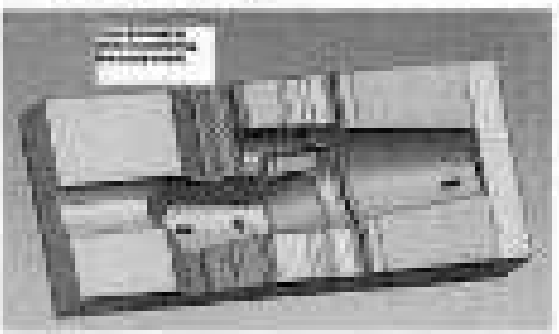

Fig 1.2.2 Shows the bottom die cutting which is used at present for this experimental analysis. Material can be added to the present surface due to indicate measuring issues.

Fig 1.2.3 Shows the design of wire EDM between die with metal flow patrol for manufacturing with model toy. It is the 2D design image of Die used as present for this experimental analysis.

Fig 1.2.4 Shows the machining of bottom die By generating the programming by Dot.net the work allowed to CNC machine for practical machining.

Fig 1.2.5 Shows the process preparation of bottom die because before the material which we are going to forging the die is machine by using plastic materials for good result of the components.

2. MATERIAL USED- D6

AISI (American Iron and Steel Institute) D6 steel unit is a high-carbon, high-chromium tool steel alloyed with molybdenum that is characterized by high compressive strength, high wear resistance, high surface hardness and good hardening stability.

2.1 Thermal Properties of the material used

The thermal properties of D6 tool steels are given in the following table

Thermal expansion coefficient (20°C-400°C/68-752°F)	10.8 µm/m°C
Thermal Conductivity (400°C/752°F)	33.5 W/mK

2.2 Boundary conditions:

Fixed support at the 40mm and 80mm of 0.005M on the cavity. The stresses after finite formation as represented

$$\sigma_{xx} = 2\mu(\varepsilon_x(w/\bar{r}) + \varepsilon_y)$$
$$\sigma_{yy} = (K_1 / K_2)\ln(\bar{r}/K_3 + K_4\gamma(3) + \varepsilon_{yy}$$
$$\tau_{xy} = (\bar{r}/\varepsilon\gamma_{yy}(1/\bar{r})) + \varepsilon_{xy}$$

Where,

$$K_1 = \tan\beta$$
$$K_2 = -\sigma_{yy}K_4 + \lambda(\varepsilon_{yy}(2 + \tan^2\beta))$$
$$K_3 = \bar{k} - \varepsilon_y K_4$$
$$\tan\beta = [1 - \bar{k}(\bar{r}/\bar{r}) - 1](\bar{r}/\bar{r})\ln(\bar{r}/\bar{r})]^{0.5}$$

2.3.Thermal Analysis of Boundary conditions

Input parameters used in the numerical simulation, Initial temperature-180°c, Temperature on the die cavity 400°c, Convection on the surfaces with convective coefficient of $10e^{-12}w/m^2$

Fig2.3.2 Shows the boundary conditions used for thermal analysis, convection radiation parameters are given as shown.

3. RESULTS & DISCUSSION

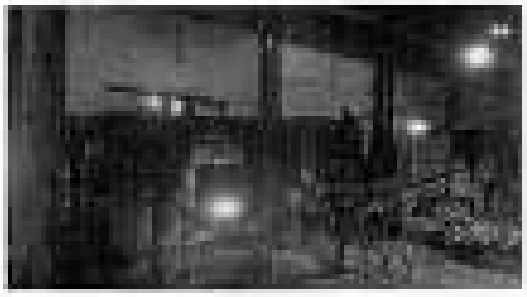

Fig 3.0 Shows the furnace with practical approach of 1200°c

Fig 3.1.2 Shows the [illegible] with pin holding arrangements

Fig 3.1.3 Shows the [illegible]

Fig 3.1.4 Shows the cut pin arrangement of proposed project

4.0 Analysis in Ansys 15.0 for present project

4.1 STATIC STRUCTURAL ANALYSIS OF THE DIE

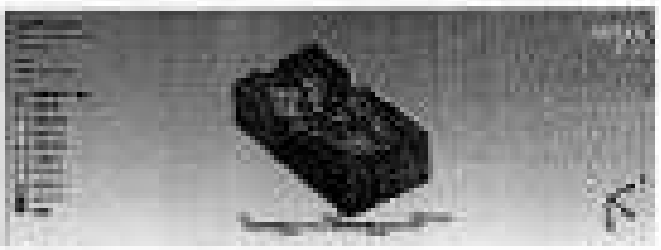

Fig 4.1.1 Shows the total deformation of the bottom die for load applied, the maximum deformation was found to be 0.038158 mm at the corners of the die.

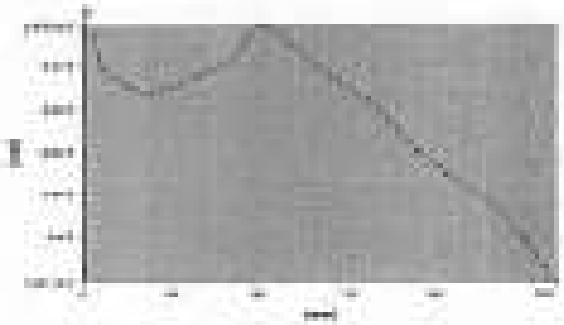

Fig 4. Total deformation in non-dialog x axis and Length of the cavity in mm along X axis

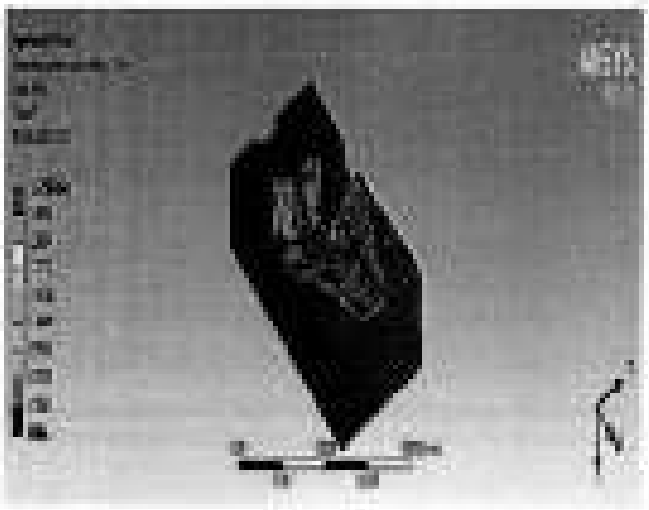

Fig4.3 Shows the equivalent stress variation across the die and maximum of 1.61N/Pa was found

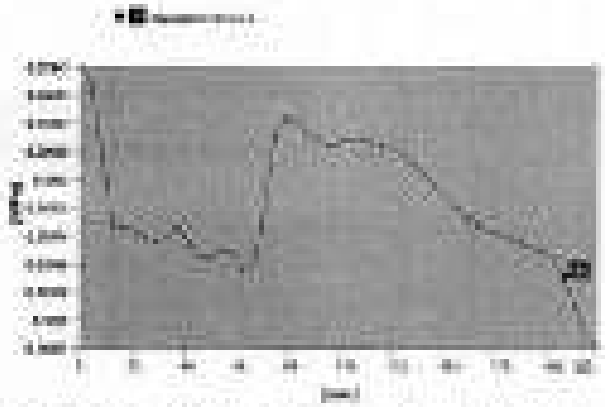

Fig4.4 Shows equivalent of die stress across the distance point & and changes of the stress points

5.0 Hot forging temperatures of different metals and alloys

Metal or alloy	Approximate range of forging temperature, °C (°F)
Aluminum alloys (hot difficult)	430–500 (750–930)
Magnesium alloys	250–350 (480–660)
Copper alloys	600–950 (1110–1650)
Carbon and low-alloy steels	950–1250 (1750–2300)
Martensitic stainless steels	1100–1250 (2000–2300)
Martensitic steels	1100–1250 (2010–2250)
Austenitic stainless steels	1100–1250 (2100–2300)
Nickel alloys	1000–1150 (1850–2100)
Semiaustenitic PH stainless steels	1000–1250 (2010–2280)
Titanium alloys	700–900 (1300–1650)
Iron-base superalloys	1000–1180 (1850–2160)
Cobalt-base superalloys	1100–1200 (2050–2200)
Niobium alloys	950–1150 (1700–2100)
Tantalum alloys	1100–1350 (2000–2460)
Molybdenum alloys	1150–1350 (2100–2460)
Nickel-base superalloys	1050–1200 (1920–2200)
Tungsten alloys (powder forging)	1300–1500 (2400–2750)

Preform dimensions for carbon or low-alloy steels

Dimensions of the finish forgings	Preform dimensions
Flash Bend-in radii (R_F)	No flash $R_P = R_F + C$ or $R_P/R < R_F < R_P/4$
Fillet radii (R_{PF})	$R_{PF} = 1.5\ R_{PF} + 3.18$ mm (0.125 in.)
Depth of cavity (H_P), mm (in.) and depth of adjacent cavity (C), mm (in.)	When H_P is less than 19 mm (0.4 in.), then $C = 2$ mm (0.08 in.) When H_P is between 19 mm and 25 mm (1 in.), then $C = 3$ mm (0.12 in.) When H_P is between 25 mm and 50 mm (2 in.), then $C = 4$ mm (0.16 in.) When H_P is greater than 50 mm, then $C = 5$ mm (0.2 in.)

R_F, bend-in radii of preform; R_{PF}, fillet radii of preform; H_P, cavity depth; C, adjacent cavity depth. Source: Ref 7

6.THERMAL ANALYSIS

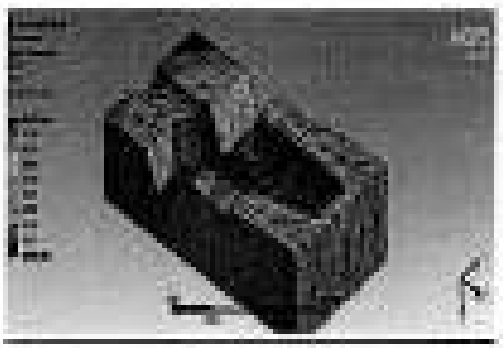

Fig5.1 Shows the temperature distribution on the die, maximum of 393°C was found. It also we see that the temperature variations

Temperature gradient

Fig6.1 It shows the thermal error of the die , maximum of 23 was observed and the change of temperature gradient

Fig6.3 Shows the Heat flux variation across the die in
With in all XYZ directions.

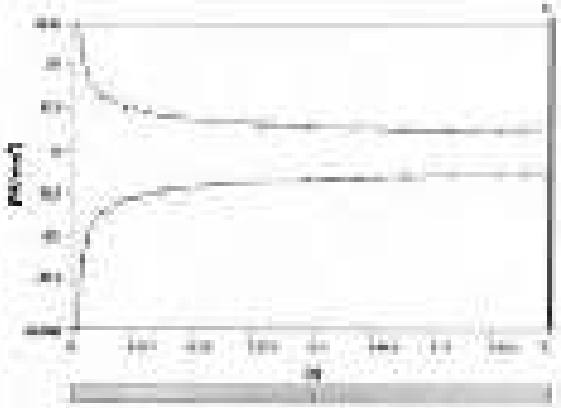

> Directional Heat Flux
Fig 6.4 Increasing and Decreasing correlated with
heat flux along the Direction

CONCLUSION

1. Finite-element method based simulation is a powerful tool that can provide information about the variables that are difficult to measure otherwise such as strain and temperature across the particular points of a forged part.
2. The knowledge of these values in the key in optimizing the existing processes and developing new processes and materials. This is, however, impossible without verified models, only then the methods as whole can be of the process.
3. The present work deals with two applications of a FEM simulation to analyzing the cause of cracking process in closed-die forging.
4. The first application of the numerical simulation involved simulating a compression model. It described the temperature changes in the metallic forging during the heating to the austenitizing temperature before the quenching. Using this model, the heating and cooling times of the forgings in the furnace can be determined, the optimum layout of the forgings in the furnace can be found and various types of problems solved.

Scope of the Future work

- It was found that thermo-mechanical treatment can produce predictable identical properties of a work piece as conventional hardening.
- However, such results should be interpreted with caution and this finding should be supported by a larger body of controlled data.
- In future efforts, the FEM simulation of heating processes will be utilized, e.g., the plastic behavior of a forged part instead of the curve plots employed so far.
- As a future work, different die and workpiece materials can be selected, preform geometries and forging of the part at lower temperatures can be analyzed.
- By using the results of this study, finish dies can be redesigned. Structural analysis may be performed by different finite element programs.

References

1. S. Vazquez and T. Altan, New Concepts in Die Design—Physical and Computer Modeling Applications, J. Mater. Process. Technol., Vol 86, 2000, p 212–225
2. A.M. Sabroff et al., Forging Materials and Practices, Reinhold, 1968
3. Ceren M., "Finite Element Analysis of Hot Upset Forging Dies", M.S. Thesis, Middle East Technical University, Ankara, Turkey, 2002.
4. Gural V., Bouchard G., Harvey L., "Influence of design and process parameters on service life of cast hot forging dies", Journal of Materials Processing Technology, 147 (2004) 389-396.
5. Kim H.H., Lee H.C., Kim H.M., Kim K.H., "Estimation of Die Service Life Against Plastic Deformation And Wear During Hot Forging Processes", Journal of Materials Processing Technology, 146 (2004) 372-388.
6. Bernicki G., Bonthier C., "Methodology for Service Life Estimation of Hot Forging Tools", Journal of Materials Processing Technology, 97 (1999) 207-216.
7. Jeong D.S., Kim D.E., Kim J.H., Kim B.M., Hans T.C., "Effects of Surface Treatments And Lubricants

Hot Warm Forging Die Life", Journal of Materials Processing Technology, 133 (2003) 344-350.

8. Lee K.S., Im I.C., "Application of Numerical Simulation For Wear Analysis Of Warm Forging Die", Journal of Materials Processing Technology, 107 (2000), 43-48.

9. Kim H., Yagi T., Yamanaka M., "FE simulation as a must tool in cold/warm forging process and tool design", Journal of Materials Processing Technology, 98 (2000), 140-149.

10. Kutlu, A. E., "Analysis and Design of Preforms for Non-Axisymmetric Parts", M. Sc. Thesis, Middle East Technical University, Ankara, Turkey, 2001.

11. Kanapcher, A. B., "Analysis and Preform Design for Long Thin Forgings with Non-Planar Parting Surfaces", M. Sc. Thesis, Middle East Technical University, Ankara, Turkey, 2002.

12. Gülbahar S., "Preform Design for Heavy Vehicle Steering Joint", M. Sc. Thesis, Middle East Technical University, Ankara, Turkey, 2004.

13. Üreyüloğlu B., "Analysis of Forging for Three Different Alloy Steels", M. Sc. Thesis, Middle East Technical University, Ankara, Turkey, 2004.

14. Shirgaon, R., Kim, S., Im, S., Hawkyard, P., Bridgwater, A., Recent Advances in Cold and Warm Forging Process Modelling Techniques for Gear Forgings, Journal of Materials Processing Technology, vol 86, pp 210-219, 1999.

15. Behrens, A., Jun, H., Verification of the damage model of effective stresses in cold and warm forging operations by experimental testing and FE simulations, Journal of Materials Processing Technology, vol 125-126, pp 299-301, 2002.

16. Jeong, D.J., Kim, D.E., Kim, J.H., Kim, B.M., Choi, T.A., Effects of Surface Treatments and Lubricants for Warm Forging Die Life, Journal of Materials Processing Technology, vol 111, pp 249-253, 2001.

17. Tamaki Inoma, Yuichiro Morimoto, Die Life and Lubrication in Warm Forging, Journal of Materials Processing Technology, vol 71, pp 41-48, 1997.

18. S. Shirgaokar, Tool Lubricating Systems in Warm Forging, Journal of Materials Processing Technology, vol 111, pp 16-21, 2001

19. Kocan, L., Palasa, Z., Jambor, P., Balling, J., Research on the Flow Stress Characteristics of ABS 1006 and AISI 5140 in the Temperature Range of Warm Forging by Means of Thermo-Mechanical Experiments, Journal of Materials Processing Technology, vol 113, pp 58-64, 2002

20. Xiaoa, L., Hongbing, X., Zhilong, Z., Flow Stress of Carbon Steel 35# in Temperature Range of Warm Forging, Journal of Materials Processing Technology, vol 130, pp 249-256, 2002.

21. Lee, K.S., Im, I.C., Application of Numerical Simulation for Wear Analysis of Warm Forging Die, Journal of Materials Processing Technology, vol 140, pp 43-48, 2003.

22. http://www.forging.org/

23. http://www.me.mtu.edu/~rajub/manufacturing/cam.htm

24. http://www.moderncasting.com/MoreInfo/1104/MoreInfo1104.pdf